

---

# Understanding the In-stream Eco-morphodynamics of Large Braided River Systems

---

*Thesis submitted in partial fulfilment of the requirements for the award of the degree of*

**Doctor of Philosophy**

*in*

Civil Engineering

*by*

**KETAN KUMAR NANDI**

*with the supervision of*

Prof. Subashisa Dutta

Prof. Kishanjit Kumar Khatua



---

Department of Civil Engineering  
Indian Institute of Technology Guwahati  
Guwahati – 781039, Assam, India

August, 2023



# Understanding the In-stream Eco-morphodynamics of Large Braided River Systems

**KETAN KUMAR NANDI**



Indian Institute of Technology Guwahati

Department of Civil Engineering, Guwahati, Assam 781039





Dedicated To  
My Family and Friends



# ACKNOWLEDGEMENTS

Acknowledgments are always special because they provide an opportunity to express gratitude towards those who have played an instrumental role in achieving a milestone. For me, completing my Ph.D. is nothing short of a miracle, and I am immensely grateful to all those who have been a part of my journey. This journey has been beautiful, remarkable at the same time lonely and depressing, but I have been fortunate to have had the support of many people who have made this journey a cheerful and lovely learning process.

First and foremost, I would like to express my deepest gratitude to my supervisor, Prof. Subashisa Dutta. Your intellectual and emotional support has been invaluable for me. You have been more than just an academic mentor, always there to provide guidance, support, and encouragement whenever I needed it. Your belief in me when I was unsure of myself, your unwavering trust when I faltered, and your fatherly care throughout this journey have been invaluable. I have learned so much from you, and I am confident that any success I achieve in the future will be rooted in the valuable lessons you have taught me. I would also like to extend my sincere thanks to my co-supervisor, Prof. Kishanjit Kumar Khatua. Your steadfast faith in my abilities, love, and support have been instrumental in my success. I am blessed to have a co-supervisor like you.

I am humbled to extend my utmost gratitude and admiration to the distinguished members of my doctoral committee, led by the visionary and accomplished Prof. Arup Kumar Sharma. The invaluable insights, suggestions, and feedback provided by committee members, Prof. Bimlesh Kumar and Prof. Niranjana Sahoo have been instrumental in shaping my thesis work at every juncture. Their timely inputs have been nothing short of a guiding light in my Ph.D. journey, and for that, I will forever be indebted to them.

My deepest appreciation goes out to my caring seniors, who have played a pivotal role in my Ph.D. journey. Suman Bhai, your inspiration has been invaluable, and your guidance have given me a profound understanding of the research process. Chandan Bhai, I cannot thank you enough for your support throughout my Ph.D., from problem

formulation to manuscript preparation and presentation. I would also like to extend my gratitude to Bighna Bhai, Anju Bhai, Satish Bhai, Suresh Bhai, Vinay Bhai, Aparimita, and Amrutha, for their constant motivation and assistance. Your contributions have been truly exceptional, and I feel incredibly fortunate to have had such amazing mentors. I express my gratitude to my wonderful lab mates, Riddick, Abhishek, Lasya, Smarak, Mridupawan, Saikat, Avinash, Manish, Om, Ajay, Nishant, Ajit and Somesh, for creating an inviting and congenial environment that makes work feel like fun. I would like to thank Bazal Da from the bottom of my heart for all of the time and effort he put into helping me setup the lab, conduct the experiments, and coordinate the field trips.

I would like to express my sincere thankfulness to a delightful group of people who have made a significant impact during this journey. Firstly, my dear school friends Jyoti, Pulin, Suwendu, Motilal, and my B.Tech mates Sritam, Muna, Papu, Gourab Goswami, Sanjeet, Nilgrib, Abhishek, Subhashrita as well as my M.Tech mates Raj, Tanmaya, Monty, Abhisek, Avinash, Somnath, Archana, Serly, and Ph.D. mates Chandrasekhar, Priyabrata, Sunil, Asesh, Sujit, Swagata, Namrita, Priyanka, Hamedari, and Nicola. I also extend my heartfelt appreciation to my Utkalika IITG family, cricket and badminton team mates, whose steadfast camaraderie has been a rejuvenating break for me. You are the ones who alleviate the stress of my Ph.D. journey, and nothing less than a second family here at IIT Guwahati. My heartfelt appreciation goes out to my dear neighbours, Manoj and Abhishek, who have been my pillars of strength during the toughest of times. Their continuous support and uplifting words of encouragement have been instrumental in keeping me motivated and focused on my goals.

Last but not the least, without my family's love, care, and support, this journey would have been impossible. From my childhood, my family have been my steadfast pillars, providing me with their unwavering prayers, emotional support, and encouragement, without which I couldn't have reached this point in my career. I am forever grateful for their endless support, and this success is not only mine, but it is theirs as well.

Ketan Kumar Nandi

# DECLARATION

I, **Ketan Kumar Nandi**, author of the Ph. D. thesis “**Understanding the In-stream Eco-morphodynamics of Large Braided River Systems**” would like to certify that

- The work presented in this thesis is original research work carried out by me.
- The research work has not been submitted for any degree or diploma or any other qualification either in this institute or in any other university.
- Whenever I have used resources [theory, concepts, texts, data, graphs, figures or any other similar nature] from other sources, a due credit by citing in the text of the thesis is clearly made.
- The work presented here is free from plagiarism to the best of my knowledge, and I take the responsibility for any issues.
- I also affirm that thesis supervisor is not responsible for any possible instance of plagiarism within this submitted work.

Date: 28.08.2023

Place: IIT Guwahati

Ketan Kumar Nandi

(186104017)





# Indian Institute of Technology Guwahati

Department of Civil Engineering, Guwahati, Assam 781039

---

## Certificate

This is to certify that thesis entitled “**Understanding the In-stream Eco-morphodynamics of Large Braided River Systems**” submitted by **Ketan Kumar Nandi**, in partial fulfilment of the requirements for the award of degree of Doctor of Philosophy, to Indian Institute of Technology Guwahati, Assam, India, is a record of the bonafide research work carried out by him under our guidance and supervision at the Department of Civil Engineering, Indian Institute of Technology Guwahati, Assam, India. To the best of my knowledge, no part of the work reported in this thesis has been presented for the award of any degree at any other institution.

**Prof. Subashisa Dutta**

Department of Civil Engineering,  
Indian Institute of Technology Guwahati,  
Assam, India-781039  
Email: [Subashisa@iitg.ac.in](mailto:Subashisa@iitg.ac.in)

**Prof. Kishanjit Kumar Khatua**

Department of Civil Engineering,  
National Institute of Technology Rourkela,  
Odisha, India- 769008  
Email: [kkkhatua@nitrkl.ac.in](mailto:kkkhatua@nitrkl.ac.in)



# ABSTRACT

Large braided river systems are complex natural phenomena that have fascinated researchers for many years. Despite the significant progress made in fluvial geomorphology, understanding the morphological erraticism of these rivers remains a major challenge. Braided rivers are characterized by intricate, unstable networks of river channels formed by the interaction of flow energy and sediment transport. These rivers are constantly changing in response to variations in flow and sediment supply, leading to complex morphological adjustments over time. To better comprehend the behaviour of braided rivers and the concepts that underpin them, a range of techniques including field-based studies, modelling analysis, and cloud computing techniques can be utilized. This thesis seeks to contribute to the knowledge on large braided river systems and provide insights into effective management of these rivers, which are of great ecological and economic importance.

Firstly, the present thesis reports thorough spatio-temporal variability of sand bar dynamics (2000-2019) and their influence on the braided belt disorderness in the large braided Brahmaputra River. The sand bar area is detected using the modified normalized difference water index (MNDWI), and an entropy-based intensity disorder index (IDI) is proposed to measure the spatio-temporal disorderness in the post-monsoon period. The IDI varies at a lowest value of less than 0.5 to a highest value of more than 0.9 for the selected study reach. Interestingly, IDI displays a declining trend for the first decade, followed by an increasing trend in the subsequent time slice, which signals the large-scale heterogeneity in process-form interactions for the Brahmaputra. An attempt was made to establish relationship between IDI, stream power derivatives (monsoon, peak flood, and post-monsoon), and bar classes in order to facilitate a process-based understanding of the geomorphic adjustments. In comparison with other stream power derivatives, the peak-flood stream power showed a better correlation with the disorderness measure of the reach. This study also highlighted that smaller (highly immobile) bars have significant control on the IDI variations and govern the temporal planform variability.

The interaction of the river corridor with the surrounding ecosystem is a complex hydro-geomorphological process that presents challenges for comprehension. Therefore, the second objective of this thesis was to shed light on the spatiotemporal heterogeneity in the vegetation-flow regime of the Brahmaputra river, providing valuable insights into this mighty river's behaviour. A detailed statistical analysis for the last three decades (1990 to 2019) was performed to demonstrate the in-stream vegetation characteristics for the selected braided reach (240 km) of the river. Google Earth Engine (GEE) platform and advanced geospatial techniques have been used in this study. The findings revealed a significant increase in moderate and dense vegetation cover over the last decade, triggering its role in the stability of the reach. Using this information, a process-based indicator referred to as Stability Trajectory Indicator (STI) was developed to identify the stability state of the braided reach utilizing vegetation as a filter.

Mid-channel bars play a crucial role in shaping the evolution of fluvial systems. Vegetation cover on these bars interacts with the flow, complicating the system and necessitating a fundamental interpretation of the flow-turbulence structure to understand braiding dynamics. Despite the importance of this topic, studies in this area are scarce. The final objective of the thesis work aims to bridge this gap by demonstrating the process-form-vegetation interaction through experimental investigation at a flume-scale mid-channel bar model with varying vegetation cover arrangements. Experiments were conducted using natural plant forms (paddy, leafy, and rigid stem) arranged in staggered manner over the bar in submerged condition. The flow-turbulence behaviour has been observed through the bifurcated channel using the three-dimensional Acoustic Doppler Velocimeter (ADV). Results showed that the longitudinal velocity component varied with the different vegetated cover arrangements and it was highest with leafy vegetation (about 32%) since it provided more resistance to the flow. Similarly, the Reynolds Stress and Turbulence Intensity were also observed to be more significant in case of flexible leafy vegetation. Moreover, it was found that vegetation structure influences both velocity reduction and momentum transfer at and top of the canopy, as well as the shear layer thickness. The insights provided in this thesis may facilitate a comprehensive understanding of braiding dynamics, and could be valuable to river engineers seeking to develop a management strategy for monitoring river health.

# CONTENTS

List of Figures	v
List of Tables	vii
List of Symbols	ix
List of Abbreviations	xi
<b>1 INTRODUCTION</b>	
1.1 OVERVIEW	3
1.2 BRAIDED RIVER AND ASSOCIATED MORPHOLOGICAL PROCESSES	3
1.3 THE LARGE BRAIDED BRAHMAPUTRA RIVER	4
1.4 AIM AND OBJECTIVE OF THE THESIS	7
1.5 STRUCTURE OF THE THESIS	7
<b>2 REVIEW OF LITERATURE AND CONCEPTUALIZATION</b>	
2.1 OVERVIEW	11
2.2 ENERGY DISSIPATION PROCESSES IN A HIGHLY BRAIDED RIVER SYSTEM	11
2.2.1 Braided belt width mobility and the implication of composite cohesive banks	11
2.2.2 Channel bar dynamics and formation of large-scale confluence-bifurcation	15
2.2.3 Process-morphodynamics-vegetation interactions at landform scale	21
2.3 CONCLUSIONS AND RESEARCH DIRECTION	27
<b>3 SYSTEM DISORDERNESS AND ENERGY EXPENDITURE MECHANISM IN A LARGE BRAIDED RIVER</b>	
3.1 OVERVIEW	33
3.2 INTRODUCTION	33
3.3 STUDY AREA AND DATA PREPARATION	36
3.3.1 Study area description	36
3.3.2 Data preparation	39

3.4	METHODOLOGY	39
3.4.1	Calculation of bar area using MNDWI	40
3.4.2	Intensity disorder index	41
3.4.3	Stream power	42
3.5	RESULTS	43
3.5.1	Frequency distribution analysis	43
3.5.2	Temporal variability of intensity disorder index	46
3.5.3	Relationship between stream power, IDI, and bar classes	48
3.6	DISCUSSION	50
3.6.1	Role of sand bar dynamics in the morphological uncertainty	50
3.6.2	IDI variation and its influence on the system's disorderness	51
3.6.3	Contribution of stream power to the IDI variation and morphological variability	52
3.6.4	Interpretation of process-based sand bar disorderness and energy expenditure mechanism	53
3.7	CONCLUSIONS	55
<b>4</b>	<b>REFLECTIVITY HYETOGRAPH PREDICTION</b>	
4.1	OVERVIEW	59
4.2	INTRODUCTION	59
4.3	DATA AND METHODS	62
4.3.1	Identification of zone-wise braided reach with reference to the local nodal point	62
4.3.2	Morphological assessment of the braided reach within the selected study area	63
4.3.3	Hydrological data preparation	65
4.3.4	Formulation of process-based indicator for identification of stability trajectory of the reach	66
4.4	RESULTS AND DISCUSSION	67
4.4.1	Bio-geomorphic characterization of Brahmaputra river	67
4.4.2	Spatio-temporal sandbar and in-stream vegetation dynamics within the river corridor in terms of erosional and depositional activity	69
4.4.3	Interpretation of vegetation dynamics through NDVI based classification of different type and its trend analysis	73
4.4.4	Interpretation of the vegetation type as a stabilizing agent for the sandbars of the braided reach	80
4.4.5	Conceptualization of braided reach behavior in accordance with in-stream vegetation cover dynamics	84
4.5	CONCLUSIONS	86

<b>5</b>	<b>MORPHODYNAMICS OF VEGETATED MID-CHANNEL BAR</b>	
5.1	OVERVIEW	91
5.2	INTRODUCTION	91
5.3	DESIGN OF EXPERIMENTAL PROGRAM	94
5.3.1	Experimental setup	94
5.3.2	Flow conditions and velocity measurement	95
5.3.3	In-stream vegetation arrangements	97
5.4	RESULTS	99
5.4.1	Streamwise velocity	99
5.4.2	Reynold's shear stress	101
5.4.3	Turbulent intensity	103
5.5	DISCUSSION	105
5.6	CONCLUSIONS	110
<b>6</b>	<b>CONCLUSIONS AND RECOMENDATIONS</b>	
6.1	CONCLUSIONS	115
6.1.1	System disorderness and energy expenditure mechanism in a large braided river	115
6.1.2	Vegetation and its impact on stability criteria of a braided reach	116
6.1.3	Morphodynamics of vegetated mid-channel bar	117
6.5	FUTURE RECOMMENDATIONS	117
	<b>REFERENCES</b>	119
	<b>PUBLICATIONS</b>	141



# LIST OF FIGURES

1.1	Spatial variability of at-a-station hydraulic geometries and vegetated landforms in the Brahmaputra.	5
2.1	(a) Braided belt width variability in the Brahmaputra River (b) Conceptualization of temporal variability of morphological activities and associated (de)stabilizing factors.	14
2.2	(a) Confluence-bifurcation, bar assemblages, and classification based on mobility and surface area (b) Variation of surface water occurrence (SWO) (in percentage) for a dynamic reach of the Brahmaputra (obtained from Google earth engine cloud computing of JRC surface water dataset, Pekel et al., 2016).	20
2.3	(a) Vegetated mid-channel bar, (b) vegetated floodplain, and (c) non-vegetated mid-channel bar in the Brahmaputra River.	23
2.4	(a) Classification of sand bars based on surface area (b) Classification of vegetated sand bars (islands) based on vegetation strength (NDVI) (c) Zone wise summary based on braided belt width and island to bar ratio (IBR) (classification suggested by Gurnell et al., 2000).	25
2.5	Conceptualizing hierarchies of hydro-morphological processes and spatio-temporal progression of the riparian vegetation corridor for highly braided rivers like the Brahmaputra.	26
2.6	Probable energy dissipation and associated dominant processes (braided belt width dynamics, spatial sand-bar distribution, and vegetation dynamics) for the highly braided Brahmaputra River (Conceptualize based on the synthesis of previous literatures).	28
3.1	a) Selected study reach for the Brahmaputra River and nodal points (Tezpur, Guwahati, and Jogighopa); b) Flow duration curve, and temporal variation of monthly average discharge at Guwahati nodal point.	37
3.2	Methodological framework utilized to understand the entropy-based bar disorderness and associated underlying processes.	40
3.3	Conceptual illustration of bar classes based on surface area along the braided belt.	41
3.4	Yearly variation of frequency of bar classes in the post-monsoon season along the study reach.	44
3.5	Yearly class wise bar frequency comparison for two sub-reaches.	44
3.6	Longitudinal variation of cumulative bar area for the different classes.	45
3.7	Yearly variation of Intensity Disorder Index (IDI) for the study reach and the sub-reaches along the post-monsoon season.	47
3.8	Yearly comparison plot of different bar classes with their relative frequency, monsoon stream power, post-monsoon stream power, peak flood stream power, and IDI; (a) for the decreasing IDI period; (b) for increasing IDI period.	49
3.9	Conceptualization of energy expenditure by the different sand-bar class with in the fluvial territory.	54
4.1	Zonal classification of the study reach using the Joint Research Centre (JRC) surface water dataset; a) monthly water occurrence in the channel with color coding from 0 to 12 (0 for no water, and 12 for water occurrence throughout the year i.e. 12 month); b) no of water pixels counted through the braided belt in the study reach (lowest count considered as the local nodal point).	63

4.2	Methodological framework used for calculation of Modified Normalized Differenced Water Index (MNDWI) and Normalized Differenced Vegetation Index (NDVI).	65
4.3	Variation of normalized peak discharge for last three decades (1990 – 2019).	66
4.4	Field photographs of instream-vegetation cover observed in the selected study reach of Brahmaputra river.	69
4.5	Variation in annual percentage change of a) sandbar area; b) vegetation cover area for the study period (1990-2019) in the selected reach of Brahmaputra river.	71
4.6	Annual vegetation cover area sharing for three different type (light, moderate and dense) of vegetation in the selected study reach (1990-2019).	71
4.7	Trend analysis of the different types of vegetation cover; a) light vegetation; b) moderate vegetation; c) dense vegetation, for the last three decades (1990-2019) using the improved, innovative trend analysis (ITA) adopted from Güçlü (2020).	79
4.8	Quadrant analysis showing the stability trajectory of different zones along the three decades (1990-2019).	83
4.9	Conceptual illustration of different degrees of vegetation in a large braided river system with the major interdependency characteristics - prevalence of moist environment, bio-geomorphological processes, and the stability criteria. The flow energy and sandbar density variation for a) low-vegetated reach, b) moderately-vegetated reach, and c) highly-vegetated reach are also demonstrated.	85
5.1	Experimental setup in Fluvial hydro-ecological laboratory, IIT Guwahati; a) plan view of the physical model setup; b) side view showing the details of experimental arrangements (vegetated bar, measuring platform etc.).	95
5.2	Experimental flume setup showing the symmetric mid-channel bar layout with details of test section with velocity measurement locations; a) in-channel bar arrangements with dimensions; b) detailed measuring locations.	96
5.3	Illustration of in-stream vegetation cover arrangements in real river scenarios and flume-scale lay outs used for the experimental study, a) scenario of different vegetation cover in the Brahmaputra river (photographs collected in field survey); b) leafy vegetation arrangement; c) rigid vegetation arrangements; d) paddy vegetation arrangements; e) without vegetation (bare mid-bar condition).	98
5.4	Vertical profile for normalized stream-wise velocity distribution for with and without vegetated mid channel bar with different vegetation arrangements; a) for cross-section 1; b) for cross-section 2; c) for cross-section 3.	100
5.5	Vertical distribution of normalized Reynolds shear stress; i) lateral RSS; ii) depth-wise RSS; iii) stream-wise RSS; a) variation at CS1; b) variation at CS2; c) variation at CS3.	102
5.6	Vertical distribution of normalized Turbulence Intensity; i) stream-wise TI; ii) lateral TI; iii) vertical TI; a) variation at CS1; b) variation at CS2; c) variation at CS3.	104
5.7	Normalized streamwise velocity contour for different mid-bar vegetation cover arrangements; a) no-vegetation b) rigid c) paddy d) leafy.	106
5.8	Conceptual illustration of vertical velocity profile at different zones due to the flow-vegetation interaction.	107
5.9	Conceptualization of the effects of different vegetation form on the turbulence parameter (momentum exchange, shear layer thickness, horizontal and vertical coherent vertex, secondary current etc.) of bifurcated channel of symmetric configuration. The vegetation configuration considered here is: a) No-vegetation; b) rigid vegetation; c) paddy/grass vegetation; d) leafy vegetation.	109

# LIST OF TABLES

2.1	The bar frequency statistics and confluence-bifurcation geometries in the last twenty years (2000-2019) for two large braided reaches of the Brahmaputra River.	19
3.1	Hydraulics and morphological characteristics of the study reach.	39
3.2	Details of bar classes and corresponding surface area	43
3.3	Details of Mann-Kendall and Sen's slope statistics for IDI variation trend analysis.	47
3.4	Details of regression statistics of IDI with different stream powers.	49
4.1	Detail statistic table of trend analysis for different zones for the case of light vegetation type.	76
4.2	Detail statistic table of trend analysis for different zones for the case of moderate vegetation type.	77
4.3	Detail statistic table of trend analysis for different zones for the case of dense vegetation type.	78
5.1	Property and characteristics of different plant type used in this experiment for the vegetation cover arrangements over the mid-channel bar.	97



# LIST OF SYMBOLS

<u>Symbol</u>	<u>Description</u>
$\Omega$	Stream power (W/m)
$f_i$	Frequency of sand-bar
$N$	Total frequency of sand-bar
$\gamma$	Specific unit weight (N/m <sup>3</sup> )
$Q$	Discharge (m <sup>3</sup> /s)
$S$	Bed slope
$\Omega_m$	Monsoon stream power (W/m)
$\Omega_{pm}$	Post-monsoon stream power (W/m)
$\Omega_{pf}$	Peak flood stream power (W/m)
$R$	Correlation coefficient
$R^2$	Coefficient of determination
$S$	Standard deviation
$d_{50}$	Bed particle size (mm)
$U_*$	Shear velocity (m/s)



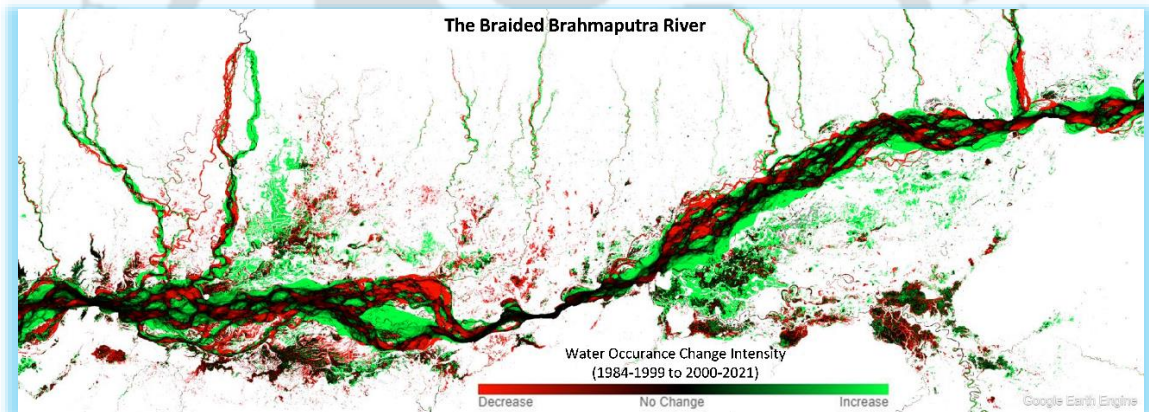
# LIST OF ABBREVIATIONS

<b><u>Terms</u></b>	<b><u>Abbreviations</u></b>
SWO	Surface Water Occurrence
JRC	Joint Research Center
IBR	Island to Bar Ratio
GEE	Google Earth Engine
NDVI	Normalized Differenced Vegetation Index
MNDWI	Modified Normalized Difference Water Index
UAV	Unmanned Aerial Vehicle
DEM	Digital Elevation Model
IDI	Intensity Disorder Index
IE	Intensity of Entropy
ETM	Enhanced Thematic Mapper
ETM+	Enhanced Thematic Mapper Plus
OLI	Operational Land Imager
TIRS	Thermal Infrared Sensor
NIR	Near Infrared
SWIR	Short Wave Infrared
DTM	Digital Terrain Model
SI	Stabilizing Indicator
CSI	Change in Stabilizing Indicators
CPD	Change in Peak Discharge
STI	Stability Trajectory Indicator
ITA	Innovative Trend Analysis
MI	Morphological Instability
ADV	Acoustic Doppler Velocimeter
RSS	Reynold's Shear Stress
TI	Turbulent Intensity



# 1

## INTRODUCTION





## 1.1 OVERVIEW

Braided rivers are unique and dynamic aquatic ecosystems characterized by a network of interconnected channels separated by bars and islands. High sediment loads, steep gradients, and unstable banks cause the river to bifurcate and shift its course frequently. Braided rivers occur in diverse landscapes, ranging from mountainous regions to lowlands and deltas, and they can support a rich array of flora and fauna. The ecological diversity and productivity of braided rivers are largely due to the heterogeneity of their habitat, including riffles, pools, islands, and wetlands, which create a variety of microhabitats that support different species. The complex interactions between the physical and biological components of braided rivers make them fascinating subjects for scientific study and management. Therefore, this thesis will investigate the eco-morphodynamics of the braided Brahmaputra river, as well as associated physical processes such as vegetation dynamics influence and management challenges.

## 1.2 BRAIDED RIVER AND ASSOCIATED MORPHOLOGICAL PROCESSES

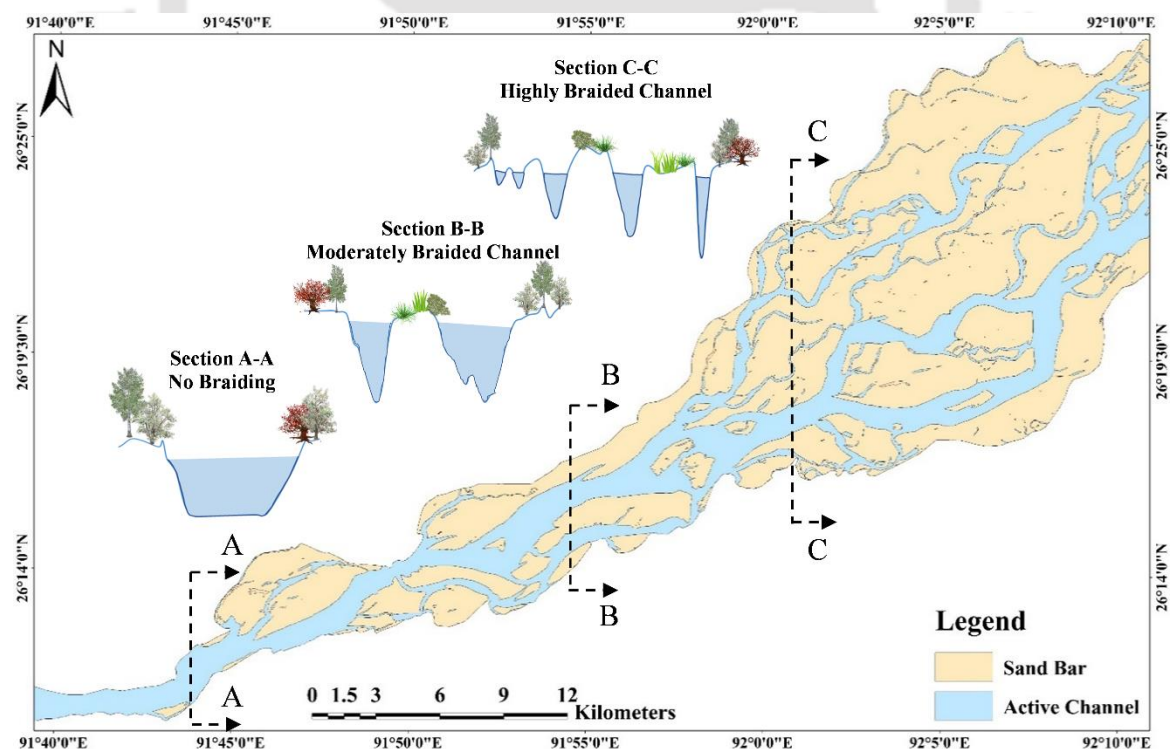
The braided rivers are equally beautiful and complex in nature. These systems comprise an unstable network of multiple channels, dynamic processes and are often observed in varied climatic regions and diverse physiographic settings (Surian, 2015). Furthermore, anthropogenic stresses develop transient morphological features and instream (or floodplain) geomorphic units in the braided rivers. In addition, braided streams are often synonymous with recurrent bar development, extreme bedload transport, and high rates of bank erosion. To understand the process-form relationships of braided channel pattern, many researches have been conducted in the last couple of decades, focused on laboratory-scale experiments (Ashmore, 1988, 1991; Hoey and Sutherland, 1991; Warburton, 1996) field-based studies (Davoren and Mosley, 1985; Ashworth et al., 1992; Goff and Ashmore, 1994; McLelland et al., 1996), numerical modelling (Paola, 2001; Brasington and Richards, 2007; Nicholas, 2013; Hardy, 2013; Wright and Hargreaves, 2013; Javernick et al., 2016), and integration of geo-spatial techniques (Surian, 1999; Piégay et al., 2009; Fotherby, 2009; Bertoldi et al., 2011; Wheaton et al., 2013; Belletti et al., 2014; Lallias-Tacon et al., 2014; Williams et al., 2014; Javernick et al., 2014; Pradhan et al., 2017, 2019).

Braided rivers show the interdependence of the associated processes and channel form evolution (Simon, 1992; Pradhan et al., 2021a). In general, channel segmentation, bar erosion, and migration are common morphological processes resulting in significant energy dissipation (Chembolu and Dutta, 2018; Dubey et al., 2020). It should also be noted that a considerable amount of energy in a braided river system is utilized through bedform changes and the braided belt width variability (Ashworth et al., 2000; Chembolu and Dutta, 2018). Simon (1992) investigated two different fluvial systems (coarse-grained and fine-grained sediment feedings) and observed that channel widening dominated the energy dissipation process in coarse-grained rivers. In contrast, fine-grained systems subjected to low energy are mostly dissipated through channel adjustment and deepening (Chorley, 1962). Few other studies have reported the bedform (ripples, mega-ripples, dunes, and sand waves) has a significant influence on the water surface turbulence pattern (boils, vortices, and macro-turbulent structures) and acts as a significant contributor to energy dissipation processes (Coleman, 1969). Furthermore, the flow resistance by vegetation colonization may dissipate a large portion of available fluvial energy in braided rivers (Wetzel, 2002; Gurnell and Petts, 2006; Bertoldi et al., 2009b, 2011; Pradhan et al., 2021b). In low-energy vegetated channels, retention and stabilization of organic and mineral deposits create a supportive environment for establishing “tree islands” (Wetzel, 2002). In addition, the vegetation may entrap, transport sediment, and interact with high fluvial energy, which progressively drives the island growth (Bertoldi et al., 2009b). A detailed discussion is given in the following sections in accordance with the energy dissipation processes in large braided river systems.

### 1.3 THE LARGE BRAIDED BRAHMAPUTRA RIVER

The Brahmaputra is a classic example of a large sand-bed braided river system (Coleman, 1969; Thorne et al., 1993; Mosselman et al., 1995), where the seasonal morphological changes are frequent due to large variability of the processes (flow and sediment transport) and geological factors (bed slope, nodal points, braided belt width and high erodible banks) (Goswami, 1985; Singh et al., 2004; Karmaker and Dutta, 2011, 2013, 2015; Chembolu and Dutta, 2018). Such extreme non-uniform nature of process-form interactions have enabled the river system to dissipate the fluvial energy at different scales. The previous studies on the Brahmaputra river have

focused on flow-sediment variability (Goswami, 1985; Karmaker and Dutta, 2015; Fischer et al., 2017), morphological dynamics, and ecological responses through numerical modelling (Surabuddin et al., 2013; Biswas et al., 2016; Karmaker and Dutta, 2016), field investigations (Karmaker and Dutta, 2013; Gul et al., 2018), laboratory experiments (Chembolu and Dutta, 2018; Khan et al., 2021) and geospatial techniques (Sarma, 2005; Akhtar et al., 2011; Dubey et al., 2014). In the Brahmaputra, instream, and floodplain geomorphic units such as sand-bars, low-flow channels, chutes, cut-offs, and vegetated landforms are dynamic in nature and display a hierarchy of energy dissipation potentials. The river is also prone to large-scale bank erosion along composite cohesive banks and supplies abundant sediment load to the morphologically active channels. The bed material composition is fine sand and silt ( $d_{50}$ : 0.16 to 0.21 mm), which makes it extremely sensitive to the changes in fluvial process variables (Sarma, 2005; Karmaker and Dutta, 2011). The shifting of river channels is also common throughout the braided belt resulting in flow separation, formation of mid-channel bars, and further development of different degrees of braiding (Richardson and Thorne, 2001).



**Figure 1.1** Spatial variability of at-a-station hydraulic geometries and vegetated landforms in the Brahmaputra.

## *INTRODUCTION*

A conceptual illustration of different stages of braiding and corresponding vegetated landforms is shown in Figure 1.1. The channel behaves as a single channel at section A-A (nodal points), a moderately braided channel at section B-B, and a highly braided channel at section C-C. The synthesis of these literatures has established the energy expenditure can be targeted towards a single (or multiple) fluvial processes. However, in order to understand such a complex river system, the attention must be concentrated on the dominant fluvial processes which acquire a large portion of available energy. For example, the inexorable bank erosion combined with non-uniform flow-sediment transport has resulted in a mobile braided belt for the Brahmaputra. The migration of braided belt and associated geomorphic units (bars, islands, chutes, low-flow channel, and flood channels) dissipate large chunk of fluvial energy. In addition, sand-bar disorderliness and eventual development confluence and bifurcation nodes signify the high energy expenditure potential of the Brahmaputra. The bio-geomorphic interactions, functionalities, and feedback between braided geomorphic units and vegetated landforms are also crucial to address this dynamic river system. The succession of large instream islands (surface area close to 100 km<sup>2</sup>) significantly governs the processes and dissipates the energy as a natural barrier. Therefore, the objective of the thesis is to understand the complex process associated with Brahmaputra river. Integration of high-resolution satellite imagery, field-scale in-situ studies, and laboratory scale experimental studies was designed and carried out in order to achieve the objectives. The research objectives are designed to address the critical knowledge gaps in this field, including identifying the dominant fluvial processes, investigating the feedbacks system, and examining the implications of morphological changes on the river's ecology. In this regard, some of the research questions have been addressed in this thesis. These are as follows:

- What are the dominant fluvial processes that acquire a large portion of available energy in the Brahmaputra river system?
- How do the succession of large instream islands govern the processes and dissipate energy as a natural barrier in the Brahmaputra river system?
- How the local scale morphodynamics behaves due to the in-stream flow-vegetation interaction.

#### 1.4 AIM AND OBJECTIVE OF THE THESIS

In this thesis, an attempt has been made to advance the understanding of the complex ecomorphodynamics of the Brahmaputra river, a large sand-bed braided system. To accomplish this goal, a comprehensive methodological framework has been developed that integrates the diverse factors influencing the river's morphological and ecological dynamics.

- Understanding the entropy-based morphological variability and energy expenditure mechanism of the large braided Brahmaputra river
- Establishment the role of in-stream vegetation on the morphological variability of the large braided Brahmaputra river.
- To investigate the impact of vegetated mid-channel bar on channel morphodynamics through laboratory scale experimental study.

#### 1.5 STRUCTURE OF THE THESIS

The content of this thesis is composed of six chapters. The organization of this thesis tracks three perspective: spatio-temporal variability of sand-bar disorderness using entropy theory; in-stream vegetation dynamics and its impact on the stability criteria; and finally, study of local scale hydrodynamics for a vegetated bar using laboratory experiments. The three perspectives of the thesis divided into chapters based on the aims of the present research work. The chapter-wise brief description of the thesis is given below:

**Chapter 1:** This chapter outlines the background of work, an overview of braided rivers and the Brahmaputra river system, and formation of research aims and scope.

**Chapter 2:** It presents state of the art relevant to the area of river morphology and conceptualize the research problems of this thesis.

**Chapter 3:** This chapter presents the understanding of entropy-based morphological variability and energy expenditure mechanism in the Brahmaputra river.

## INTRODUCTION

**Chapter 4:** This chapter deals with the development of process-based stability trajectory indicator using reach-scale approach for the middle reach of Brahmaputra river.

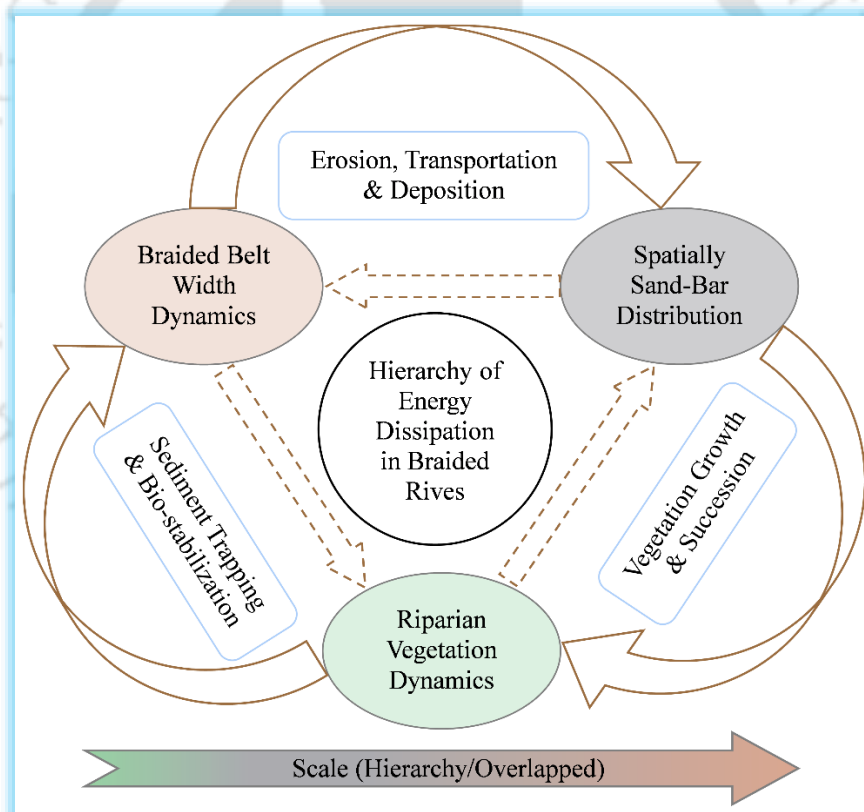
**Chapter 5:** This chapter provides the understanding of flow and turbulence along the bifurcated channel owing to vegetated mid-channel bar.

**Chapter 6:** This chapter contains a summary of the major findings of this study as well as suggestions for future research.



# REVIEW OF LITERATURE AND CONCEPTUALIZATION

(Synthesis of Literature and  
Conceptualization of Research Problem)



**Contribution from this chapter:** Nandi, K. K., Pradhan, C., Dutta, S., & Khatua, K. K. (2022). How dynamic is the Brahmaputra? Understanding the process-form-vegetation interactions for hierarchies of energy dissipation. *Ecohydrology*, 15(3), e2416. <https://doi.org/10.1002/eco.2416>



## **2.1 OVERVIEW**

This chapter will attempt to synthesize the previous understandings of the braided river mechanism and formulate a conceptual basis for probable hierarchical (or overlapped) energy dissipation processes. Such conceptual understanding of the dominant processes (braided belt mobility, bar disorderness and instream vegetated landforms dynamics) in the highly braided rivers like the Brahmaputra will develop a foundation for the research questions in this thesis. In addition, field investigated datasets along with geo-spatial imageries and Google earth engine computed fluvial information are integrated to conceptualize and understand the complex underlying processes in the river. Therefore, this chapter is sub-divided into the synthesis of previous literature concerning braided rivers like the Brahmaputra, research gaps, and conceptualize problem statement.

## **2.2 ENERGY DISSIPATION PROCESSES IN A HIGHLY BRAIDED RIVER SYSTEM**

### **2.2.1 Braided belt width mobility and the implication of composite cohesive banks**

In a highly braided river system, lateral migration and bank erosion are related to the complex flow-sediment dynamics and associated geo-morphological activities in terms of bar disorderness, thalweg migration, and intense water level variation. For rivers such as the Brahmaputra, these braided river dynamics are scaled up by many folds due to the aggravated sediment waves (Karmaker et al., 2010; Fischer et al., 2017), macroturbulence structures (Sharma et al., 2017), variability in the vegetated landforms (Chembolu et al., 2020), cohesive banks (Karmaker et al., 2015) and nodal points (Chembolu et al., 2018). Generally, in cohesive banks, erosion occurs after the breaking of electromechanical forces between the aggregates. Both shallow water and extreme flood events can be responsible for the shuddering of cohesive banks, leading to accelerated bank erosion. Interestingly, this cohesive bank erosion and timing of peak discharges are weakly related in the Brahmaputra (Sarker et al., 2014). This may establish that the bank erosion process in the Brahmaputra may not depend only upon the high energy expenditure potential of extreme events, rather gradual soil saturation by periodic low-moderate floods, deflection angle, longitudinal slope, and

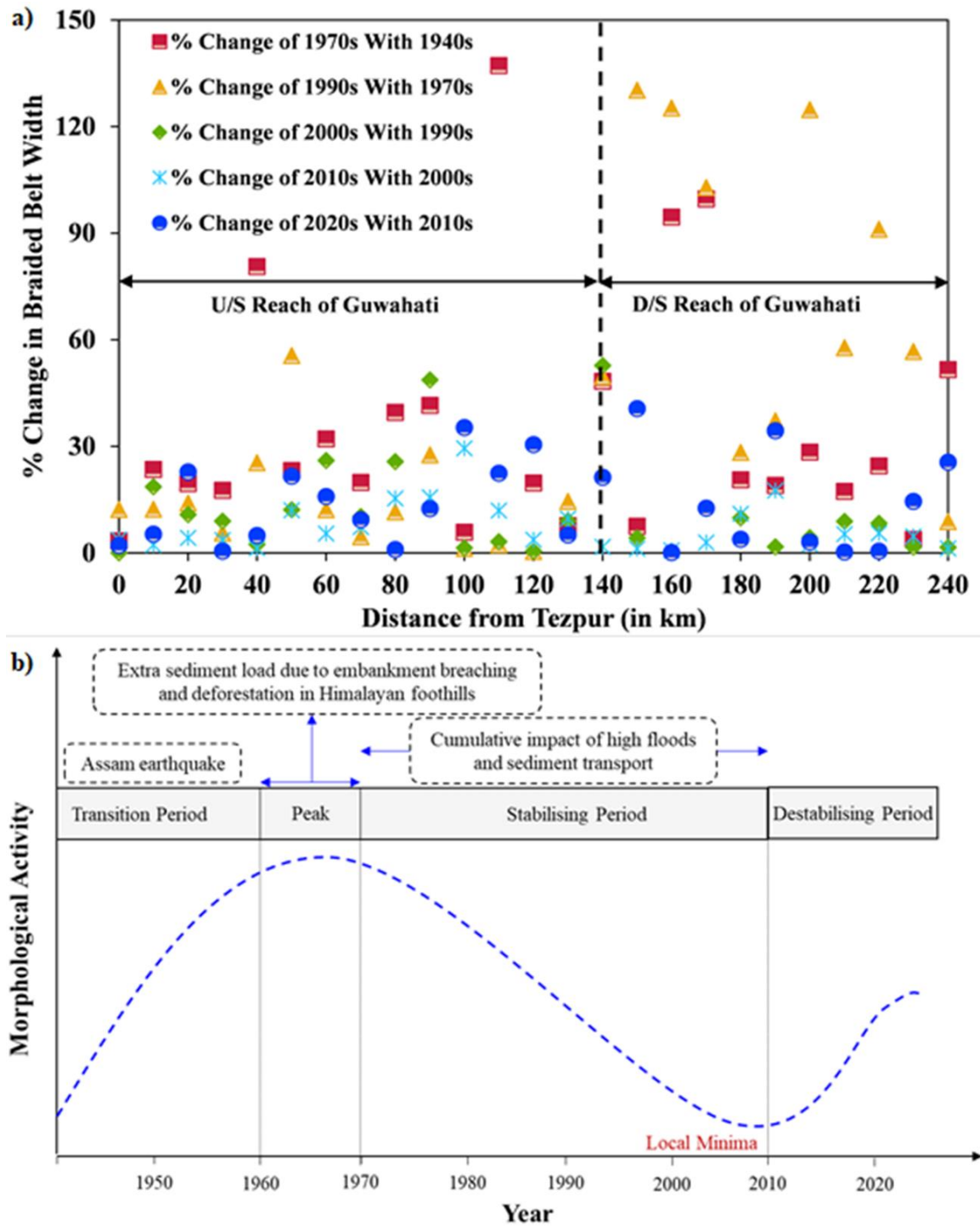
local bed material size can affect the extensive bank erosion (Mosselman, 2006; Surian et al., 2009; Karmaker et al., 2015).

The synthesis of literatures pertinent to fluvial bank erosion suggests a varying annual rate across the world's large rivers. For example, rivers like the Sacramento River (US), the Nile (Africa), the Tagliamento River (Italy), and the Yangtze (China) have an annual erosion rate up to 10-50 m/year (Larsen et al., 2006; Surian et al., 2009; Ayman and Ahmed, 2019; Deng et al., 2019). On the other hand, the annual bank erosion rate in the Brahmaputra is significantly higher in comparison to these notable dynamic river reaches. In fact, high bank erosion of 100 m/year (Mosselman, 2006; Mount et al., 2013) along with local scale erosion up to 1-2 km/year are even observed in these river reaches (Sarkar et al., 2014). The spatio-temporal variability in the bank erosion process has further developed a dynamic braided belt width in the Brahmaputra River. The old maps of the 1800s in the Bangladesh region suggest the Brahmaputra may have followed a meandering channel pattern (Thorne et al., 1993). In the later period, with the increase of both fluvial and anthropogenic disturbances, the river has significantly altered the process-form relationships. The meandering planform is eventually replaced by a considerably wider braided channel pattern accompanied by a significant rate of bank line retreat.

As suggested by Lawler (1995), one or combination of the processes such as sub-aerial erosion, fluvial entrainment, and mass failure caused by weakened bank materials are majorly responsible for river bank erosion. It has been observed that, in the Brahmaputra river, the water level falls rapidly during the recession limb and the pressure against the wall decreases, which resulted in the backwater movement from the bank and causes subaqueous failure by lateral flowage of sand and silt to the river (Karmaker and Dutta, 2011). Furthermore, the river experiences frequent channel migration, which enables the migrating channel intersects the bank-line at some locations. Eventually, that uplifts the water level in the bank, saturates the sand and silt, and in the subsequent falling limb, saturated sediments are liquified by forming well-defined shear planes. These processes contribute to the braided belt dynamics of the Brahmaputra River. The mean width of the Brahmaputra River in Assam valley is about 5949 m during the year 1912-1928 (Sarma and Acharjee, 2018). The mean width has increased up to 7455 m due to intense bed aggradation after the great

Assam earthquake of 1950 (Takagi et al., 2007; Goswami, 1985). The braided belt width has rapidly increased up to 1980-90s and gradually stabilized in the next two decades (Takagi et al., 2007) (reproduced from Karmaker et al., 2017 and integrating recent satellite imageries). In the 2000s, the mean braided belt width of Brahmaputra River is observed close to 9012 m, with distinct nodal locations and multi-channel segments. Figure 2.1a shows spatio-temporal variability of braided belt width for the middle stretch of the Brahmaputra (approximately 240 km). The percentage change in braided belt width variation is higher in the 1970s as compared to the 1990s, 2000s, and 2010s. This further indicates the reach is approaching a dynamic stable state after the 1970s. However, in recent years, the braided belt width variability is relatively higher, resulting in a dynamic, unstable (or transient) state. The downstream stretch from Guwahati is morphologically more dynamic in terms of braided belt width variability, which is more than 80 percentages (in the early 1990s) and 30 to 60 percentages (in the late 2010s), respectively.

The temporal dynamics in braided belt width (channel instability) can be attributed to numerous hydrological (floods and sediment wave), topographical (nodal points and local bed slope), and geological factors (bank erodibility, earthquakes, and landslides). The Brahmaputra river has experienced a sequence of geomorphological stages (1950 to 2020) with an interval of 5 to 10 years (Takagi et al., 2007). Furthermore, during the monsoon season, this river generates a considerable quantity of energy in the system due to a sequence of large flood waves. The morphological parameters mainly affected by this huge incoming energy are thalweg shifting (sinuosity), bank erosion, deposition, alteration in bed slope, channel wideing etc. According to previous studies, flood stream power arguably regulates the morphodynamics of the braided rivers (Akhtar et al., 2011; Bizzi and Lerner, 2012; Magilligan et al., 2015). However, in case of Brahmaputra river, the stream power has no direct influence on the braided belt variation (Karmaker et al., 2017). The fluvial energy is dissipated within the system by forming a series of braided loops, resulting in the generation of new secondary/tertiary channels as well as the blockage of the existing defined water ways (Chembolu and Dutta, 2016).



**Figure 2.1** (a) Braided belt width variability in the Brahmaputra River (b) Conceptualization of temporal variability of morphological activities and associated (de)stabilizing factors.

This process leads to the increase in planform disorderness of the system. Additionally, the energy associated with the rising peak flood has a significant erosion potential, which can be capable of reshaping the shallower channel to deeper,

washing out smaller unstable (mobile) bars, and triggering acute bank erosion. Part of the fluvial energy is also stored/absorbed within the system eventually before it initiates a new planform change (Charlton, 2007). A conceptualization of the channel instability in the Brahmaputra River basin integrating the studies of Goswami (1985), Takagi et al. (2007), Karmaker et al. (2017), and Chembolu et al. (2018) is shown in Figure 2.2b. After the 1950s, the extreme earthquake and series of landslides stimulated high sediment loads completely dominated the morphological processes. This resulted in an instability of the braided belt width and initiation of (de)stabilizing waves. The propagation of these waves was unclear in the succeeding decades, and the river was in a quasi-dynamic equilibrium state. But from the 1980s onward, the river was morphologically active and showed high fluctuations in the braided belt width with complex landform distributions. The sand bar disorderness study has established a stabilizing state in the first decade of the 2000s. However, after the 2010s, the river has again increased the channel instability in terms of bar disorderness as observed from the recent satellite imageries and field observations. This knowledge indicates a higher magnitude of energy is expended during the braided belt adjustments, which cannot be overlooked and needs to be addressed in process-based understanding.

### **2.2.2 Channel bar dynamics and formation of large-scale confluence-bifurcation**

Bars are the key geomorphic unit and the fundamental building block of a braided river system. Several braiding formation processes are formulated, entailing the bar development as a single unit or assemblages. In most cases, braiding is related to the conversion of the alternate bar to a multiple row bar or mid-channel bar via cut-offs formation. In sandy braided rivers, the lobate bars are known as “unit bars” (Smith, 1974; Ashmore, 1991a), which have individual downstream restrictions with avalanche faces (Bridge, 1993). However, with the progression of time, these unit bars are gradually deposited, sculpted, or dissected and developed into braid or compound bar in the braided rivers (Bridge, 2003; Bridge and Lunt, 2006). Depending upon the mobility of bars, forced bar (less migration rate) and free bar (high migration rate) are taxonomized for braided river systems (Bridge, 2003).

The growth and dynamics of confluence-bifurcation are also key features of braided channel networks (Leopold & Wolman, 1957; Tubino and Bertoldi, 2008; Ashmore, 2013). A number of studies have focused on understanding the formation and evolution of channel bifurcations through laboratory experiments (Ashmore, 1991b; Federici and Paola, 2003; Bertoldi and Tubino, 2007), field observations (Ferguson et al., 1992; Richardson and Thorne, 2001; Zolezzi et al., 2006) and numerical modelling (Bolla Pittaluga et al., 2003; Jagers, 2003). Ashmore (1991a) has reported four dominant mechanisms responsible for bifurcation commencement in braided rivers, such as (i) chute cut-off, (ii) initiation of the central bar, (iii) transverse bar alteration, and (iv) multiple bar braiding. Bifurcations may also be symmetric or asymmetric depending upon the division of flow-sediment an individual branch. In particular, the sand-bed rivers (relative to gravel-bed channels) are more prone to symmetrical bifurcations due to the increased Shield's stress (Best et al., 2007). It should also be noted that the flow-sediment partitioning of the active channel relies on the bifurcation dynamics (Bairstow & Best, 1993; Bolla Pittaluga et al., 2001), and this activity may switch between the individual branch depending upon the upstream bar migration rate.

The confluence node points serve as an interface zone for upstream lateral erosion and downstream deposition. Similar to the bifurcation nodes, confluences may also have symmetric and un-symmetric formations. To understand the dynamic confluence morphology, precise field observations of the flow structure near the zone, shear stress distribution, and sediment discharge pattern are necessary (Davoren & Mosley, 1986; Ashmore et al., 1992; Ferguson et al., 1992; Ashworth et al., 1992). Numerous factors also influence the morphology of confluences, including total and relative discharge at confluent anabranches, bedload yield to the confluence, boundary shear stress, particle size distribution, angle of confluence, and several anabranches (Mosley, 1976; Ashmore, 1993). In addition, the confluence angle and discharge of the anabranches control the size and depth of scouring (Ashmore, 1993, 2013). In the case of high angle confluences and equivalent anabranch discharge, scour depth is more expensive. This scour depth is marginally less for considerable variation in anabranch discharges, irrespective of confluence angle (Mosley, 1976; Ashmore and Parker, 1983; Best, 1986; Ashmore and Gardner, 2008).

In the Brahmaputra River, the formation of bars along with confluence-bifurcation nodes can be attributed to a number of dominant hydro-geomorphological factors. Due to its complicated flow-sediment discharge characteristics, the Brahmaputra is one of the few braided river systems in the world that exhibits dynamic morphological behavior (Goswami, 1958; Karmaker and Dutta, 2011, 2013; Dubey et al., 2021; Pradhan et al., 2021d). A very limited number of studies have been conducted to understand the sandbar dynamics (growth/adjustment/propagation) in this river system. The formation of braided patterns in the river is mainly determined by the formation/growth of sand bars. In addition, the sandbar dynamics are linked to the series of erosion-deposition processes in the river system. During high-flooding episodes, the incoming energy to the river system eventually regulates the underlying sandbar dynamics. During this period, morphological processes such as bar displacement and river channel fragmentation become prominent, which disperse a significant amount of energy. Furthermore, it governs the grain size distribution of the sediment material and its conveyance to a bar head, which influences the size and stability criteria of a bar.

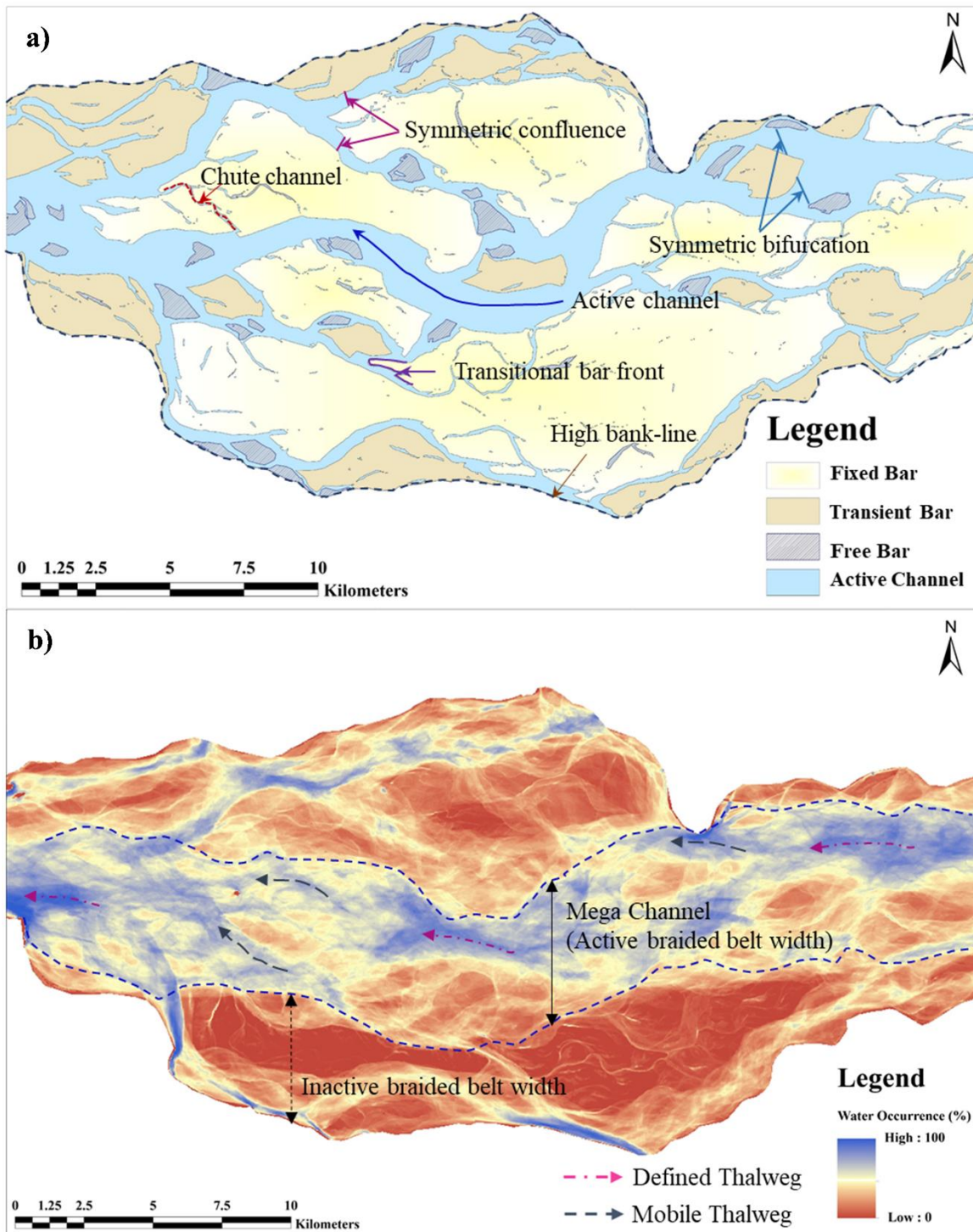
Depending upon the hydraulic regime and reach parameters, the river bed configuration (bed roughness) also provides varied resistance to the flow, which also dissipates a substantial amount of energy (Dubey et al., 2020; Pradhan et al., 2021c). According to Dubey et al., (2020), the channel has reduced roughness during the monsoon season compared to the non-monsoon season, which results in a steady river morphology in the course of monsoon period. During high floods, the flow energy increases and results in the erosion of mobile bars, which then gradually falls after the flood recedes, and irregular deposition of sediment material is observed (Chembolu and Dutta, 2018). At first, the river may encounter up to nine flood events of varying durations and sediment transport in a year (Karmaker and Dutta, 2010) and develop geomorphic units with multiple inundation surfaces. In addition, the substantial reduction of bed elevation at the India-China border (a drop of around 4800 m within a length of about 1700 km) and change in average bed slope from 2.8 m/km to 0.1 m/km in the Assam valley have produced a large braided channel of high energy dissipation potential. The nodal points also facilitate the channel to scour at the local scale and eventually deposit the excess sediment load across the widened braided belt sections. Table 2.1 shows the development of channel bars (based on

mobility) and probable bifurcation-confluence statistics along two braided reaches (Tezpur to Guwahati and Guwahati to Jogighopa) of the Brahmaputra. The morphometric analysis is performed focusing on the sand bar dynamics. The information in table 2.1 were obtained by analysing the twenty years (2000 to 2019) of satellite data using Google Earth Engine (GEE) platform. The data extracted from GEE was then processed in ArcGIS environment to determine statistics related to sand bar area and bifurcation/confluence configurations. The modified normalized difference water index (MNDWI) (Han-Qiu, 2005; Xu, 2006, 2007) was used with a threshold value ( $MNDWI < 0$ ) to identify the sand bars. Further, the sand bars were categorized into seven different classes based on their surface area to understand the influence of bar dynamics on the morphological behavior. Baki and Gan (2011) reported, the large bars are generally referred to as forced bars with low mobility (or immobile) rates in terms of shape, size, and location, whereas small bars are referred to as free bars with high mobility rates that further play a key role in morphological changes.

In the case of the Brahmaputra River, huge immobile bars form the large islands, whereas smaller mobile bars appear to have transient characteristics. It is interesting to note that bar surface area varies from 0.0006 to more than 100 km<sup>2</sup>, and clusters of mobile, moderate-low mobile, and immobile bars have formed as instream geomorphic units. Most of the bars can be classified as mid-channel longitudinal and diagonal bars, and occasionally side-channel and lateral bars are developed close to the cohesive high banks. Furthermore, more than eight hundred channel bars (temporal average of twenty years) have produced a complex braided planform of varying confluence-bifurcation geometries. The mobile bars have mostly asymmetric bifurcation (or confluence) configurations, whereas the large bars (surface area >1 km<sup>2</sup>) are symmetric in nature. Similarly, the configuration angle is less (close to 30-45°) for mobile bars, which gradually increases for static mid-channel islands.

**Table 2.1.** The bar frequency statistics and confluence-bifurcation geometries in the last twenty years (2000-2019) for two large braided reaches of the Brahmaputra River.

Bar Description (↓)/Braiding Process Description (→)			Bar Frequency Statistics						Bifurcation/Confluence Statistics		
Nature of Bar	Bar Class (Based on surface area)	Area (in km <sup>2</sup> )	Tezpur to Guwahati			Guwahati to Jogighopa			Average Angle Bifurcation (in degree)	Average Angle Confluence (in degree)	Configuration Details (Symmetry/Asymmetry)
			Max	Min	Avg.	Max	Min	Avg.			
Highly Mobile	Class 1	>0.0006 and ≤0.001	348	113	188	294	123	182	30	45	Mostly Asymmetry
	Class 2	>0.001 and ≤0.01	572	218	351	659	238	414	45	30	Mostly Asymmetry
Moderately Mobile	Class 3	>0.01 and ≤0.1	289	112	152	211	113	165	45	45	Mostly Asymmetry
	Class 4	>0.1 and ≤1	126	65	93	131	83	103	60	45	Mostly Asymmetry
Low Mobile	Class 5	>1 and ≤10	74	51	63	72	48	60	60	60	Mostly Symmetry
	Class 6	>10 and ≤100	23	14	19	31	9	16	90	60	Mostly Symmetry
Immobile	Class 7	>100	0	0	0	2	0	1	120	90	Mostly Symmetry



**Figure 2.2** (a) Confluence-bifurcation, bar assemblages, and classification based on mobility and surface area (b) Variation of surface water occurrence (SWO) (in percentage) for a dynamic reach of the Brahmaputra (obtained from Google earth engine cloud computing of JRC surface water dataset, Pekel et al., 2016).

Figure 2.2 illustrates in-channel geomorphic units of varying surface water occurrence (SWO) in the Brahmaputra. The active low-flow channel flows through

numerous confluences and bifurcations and develops transient morphological features across the variable braided belt (Figure 2.2a). The low-flow channels have SWO varying between 80-100%, signaling permanent water availability. However, the thalweg is not defined at few locations, which provides notable lateral freedom to the channel and attacks the fixed bars. The fixed bars are mostly emerged (SWO below 20%) and periodically subjected to sculpting during the high flows. The chutes are developed on the surface resulting in short-circuiting of flood channels. The bar assemblages are highly dynamic in nature resulting in a planform disorderness at spatio-temporal scales. For example, in the pre-monsoon season, the Brahmaputra is dominated by medium to large-sized sand bars. However, in the post-monsoon season, the same bars are dissected to smaller mobile and transient bars (SWO of 45 to 60%) and increases the entropy of the fluvial system. These smaller-sized bars are mostly submerged during floods and subjected to migration in the highly sediment-charged environment. Figure 2.2b signals the presence of probable channel-in-channel physiography of the Brahmaputra River. The low-flow channel (mega-channel) has maximum width up to 4-5 km and carries a significant portion of the flow-sediment discharge. In addition, these zones can be regarded as the active braided belt segment with a combination of dominant confluences and bifurcations. The fixed bars and floodplains can be considered as inactive braided belt zone, which are mostly active during high flows and extreme events. Therefore, a comprehensive evaluation of the bar dynamics along the active morphological reach is necessary and can aid in quantifying the energy utilization in braided physiographic settings.

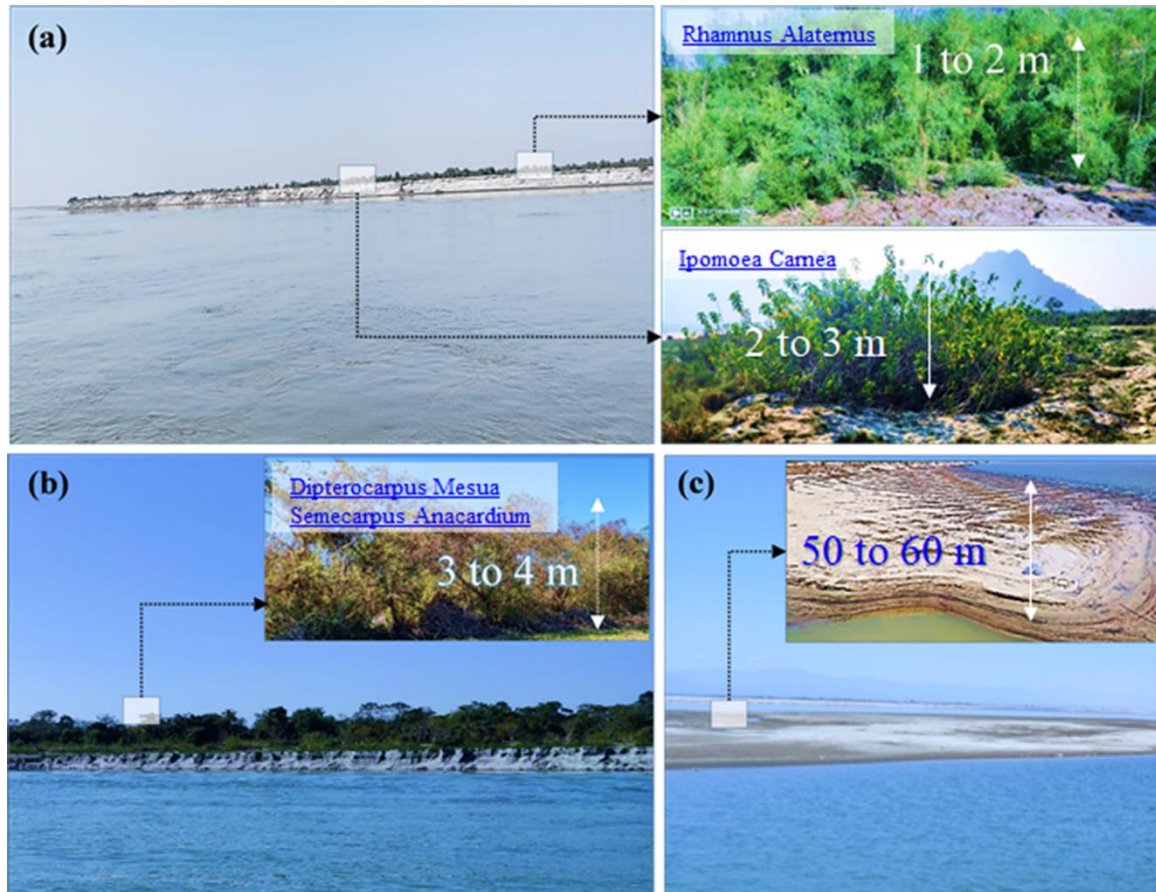
### **2.2.3 Process-morphodynamics-vegetation interactions at landform scale**

Instream vegetation is a vital component of fluvial systems and has a significant impact on river rejuvenation schemes by improving the physical features and ecological conditions (Wilson et al., 2003; Bennett and Simon, 2004; Nepf and Ghisalberti, 2008; Kondolf et al., 2013; Gurnell, 2014; Brachet et al., 2015; Gurbisz et al., 2016, 2017; Vargas-Luna et al., 2018; Lera et al., 2019; Nandi et al., 2021). Similarly, riparian vegetation has a significant impact on river morphodynamics since it interacts with the flow/sediment discharge at different spatiotemporal scales, triggering a series of intricate feedbacks and linkages (Gurnell & Petts, 2002; Camporeale et al., 2013; Gurnell, 2014; Camporeale et al., 2019; Henriques et al.,

2021). In addition, aquatic vegetation considerably adjusts the flow and turbulent structure and affect the riverine habitat (Boruah et al., 2008; Bornette and Puijalon, 2011), water quality (Dosskey et al., 2010), pollutant-nutrient distributions (Perucca et al., 2009; Shucksmith et al., 2010), and sediment transport process (Lopez and Gracia, 1998; Jordanova and Jame, 2003; Baptist, 2003; Kothyari et al., 2009; Bertoldi et al., 2009a; Gonzalez et al., 2019). Vegetation is also related to the morphodynamics by governing the braiding intensity (Gran and Paola, 2001; Tal and Paola, 2007; Belletti et al., 2015; Kui et al., 2017), promoting bar accretion and bank stabilization (Bertoldi et al., 2011; Gurnell, 2014). A number of laboratory-scale studies (Gran and Paola, 2001; Coulthard, 2005; Tal and Paola, 2010) have been performed to understand the vegetation interactions with braided river morphodynamics integrating non-natural rigid (Bennett et al., 2002; Liu et al., 2008; King et al., 2012) and flexible cylindrical stem (Velasco et al., 2008; Chen et al., 2011; Chembolu et al., 2019) submerged (or emergent) vegetation.

In the braided rivers, instream/riparian vegetations and aquatic plants represent the fluvial environment, climatic conditions, and local geological factors. The vegetation can either actively or passively contribute to the morphological activity of rivers (Camporeale et al., 2013; Camporeale et al., 2019). The passive role represents the impact of vegetation on roughness, hydraulic resistance and erosion/deposition characteristics which have alike morphological and mechanical properties. On the other hand, the active role refers to the biotic process linked with plant community colonization and life cycle, which regulates the morphodynamics of the river. Furthermore, certain species have the ability to colonize exposed or flooded alluvial sediments and create pioneer landforms (Bertoldi and Gurnell, 2020). Thus, individual species or patches in a braided fluvial system can operate as an ecosystem concocts in a variety of environmental conditions. Through a spatiotemporal series of interaction between the vegetation and geomorphic processes, the associated energy in the braided reach can be dissipated by various means. The growing vegetation root networks has been demonstrated to stabilize sediment deposits by diverting the flow and strengthen the soil (Polvi et al., 2014; Bywater-Reyes et al., 2018), which further reduce the flow velocity (Vargas-Luna et al., 2015) and increase the deposition of sediment minerals (Cotton et al., 2006; Nepf, 2012; Meier et al., 2013). This also leads to the formation of pioneer planforms (bars/islands) which affects the local physical

conditions and accelerate eventual colonization of different species (Gurnell, 2014). Additionally, the pioneer islands actively contribute to the hydro-geomorphological processes, giving rise to the establishment of a larger island with a broader space during the lean seasons and segregated during the extreme flood events.

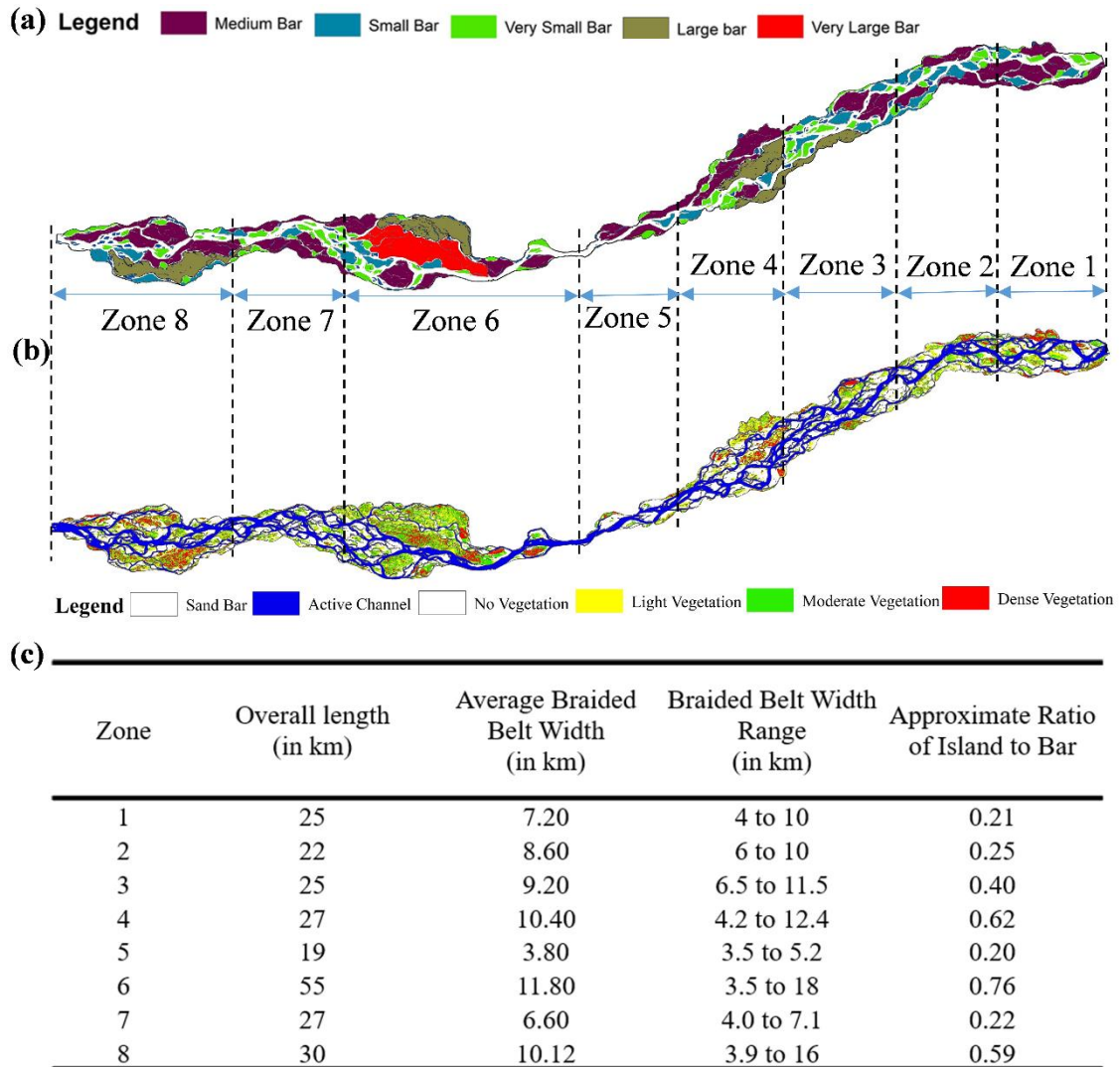


**Figure 2.3** (a) Vegetated mid-channel bar, (b) vegetated floodplain, and (c) non-vegetated mid-channel bar in the Brahmaputra River.

In this way, vegetation can operate as an "ecosystem engineer," aiding its development and establishment (Gurnell & Petts, 2006; Gurnell, 2014), which is the primary stairway toward the accretion of river banks, the formation of river islands, and, as a result, changes in river characteristics and planforms (Bertoldiet al., 2014; Wintenberger et al., 2015). There are limited studies available for understanding the interactions between active channels and instream/flood plain green corridors in the braided rivers. Further, for a highly braided river like the Brahmaputra, these bio-morphological processes become extremely complex and unpredictable due to the variable growth cycle of vegetation species and their controlling factors. The Brahmaputra has varied instream or floodplain vegetated landforms that affect the

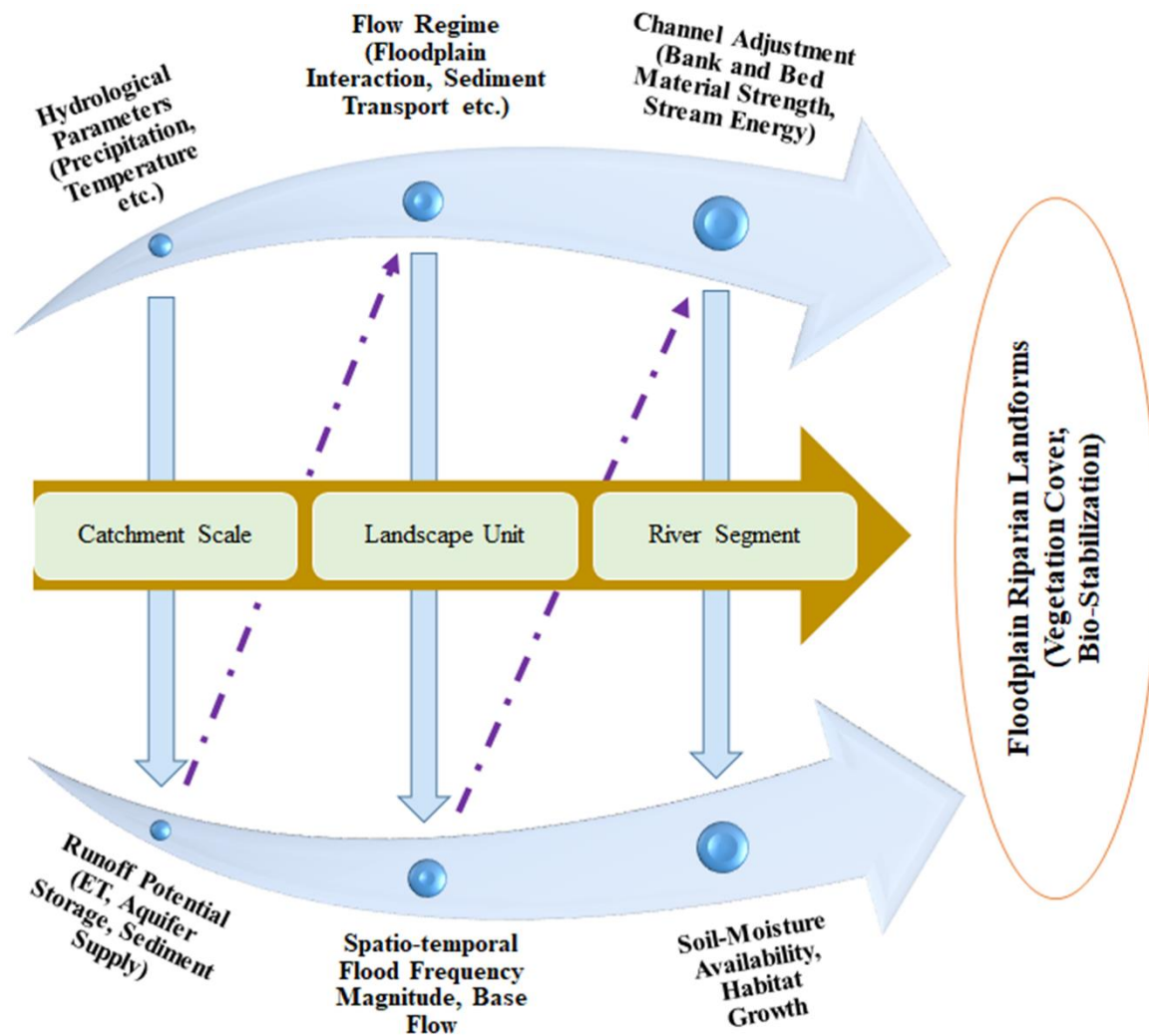
bio-morphological processes (Figure 2.3). During the high flows and extreme events, these vegetated structures offer resistance to the incoming flow and further helps in stabilizing the submerged landforms.

To establish a framework for a more comprehensive investigation of island distribution, its character, and dynamics, a precise understanding of an island in terms of size, form, and structure is required. It is important to carry out this objective as size of island provides significant information on its stability-structure and can be used as a parameter for identifying islands from maps and aerial imageries (Gurnell et al., 2000). The braided rivers can be classified based on the ratio of island area to gravel (sand) area (IBR) as bar-braided (no island present), bar-braided with occasional islands ( $<0.25$ ), island-braided (in between 0.25 to 0.5), and heavily island-braided ( $>0.5$ ) (Gurnell et al., 2000). This classification is applied to the Brahmaputra by dividing the entire study reach into eight zones with lengths varying between 19 and 55 km (Figure 2.4a). The zones are defined by local nodals identified using the high-resolution global surface water maps (Pekel et al., 2016). The vegetation cover information was also mapped for the whole stretch using the normalized differenced vegetation index (NDVI) (Figure 2.4b). The GEE platform was used to obtain NDVI images for the selected study reach, and the vegetated pixels were identified using a threshold value ( $NDVI > 0.2$ ) (Bertoldi et al., 2011). In addition, the vegetated area was calculated, and the previously determined sand bar area (section 3.2) is included in the IBR value computation. Zone 1, zone 5, and zone 7 confirm to occasional islands category, zone 2 and zone 3 fall under island-braided, and zone 4, zone 6, and zone 8 represent heavily island braided segments (Figure 2.4c). Interestingly, zone without vegetation cover on the bar surface is not present in the entire study area. The heavily island-braided zones (4, 6, and 8) (IBR of 0.62, 0.76, and 0.59, respectively) have higher braided belt variability (average of 10 to 11 km). These reaches accommodate larger bars that are stable in nature and provide a favorable condition for vegetation growth and succession. On the other hand, zone 2 and zone 3 (IBR of 0.25, 0.76, and 0.40) featuring medium and small-size bars have a low island-to-bar ratio due to less growth of vegetation. However, zone 1, zone 5, and zone 7 (IBR of 0.21, 0.20, and 0.22, respectively) have the lower island-to-bar ratio attributed to the presence of smaller size bars that are mobile in nature and possess the least vegetation cover.



**Figure 2.4** (a) Classification of sand bars based on surface area (b) Classification of vegetated sand bars (islands) based on vegetation strength (NDVI) (c) Zone wise summary based on braided belt width and island to bar ratio (IBR) (classification suggested by Gurnell et al., 2000).

In the Brahmaputra River, the island formation process begins with the deposition of fine sediments around vegetated landforms, and further trapping of sediments provides stability characteristics (Orton & Reading, 1993; Charlton et al., 2007; Rogers and Goodbred, 2014; Latrubesse, 2015; Pradhan et al., 2020). This concept encompasses varieties of interdependent processes occurring on instream and riparian vegetation, such as seed dispersal, recruitment, growth, and mortality. The spatial scale hydro-morphological cascade processes and the landforms appear according to vegetation growth-succession, which are further responsible for the bio-morphological stabilization, river rejuvenation, and restoration (Figure 2.5).



**Figure 2.5** Conceptualizing hierarchies of hydro-morphological processes and spatio-temporal progression of the riparian vegetation corridor for highly braided rivers like the Brahmaputra.

In the Brahmaputra, a multiscale approach can be considered (reach to catchment or catchment to reach scale) for instream or riparian vegetation characterization and succession. In the first approach, recruiting and establishing pioneer species on bare alluvial bars can be facilitated by water availability, flood disturbance, and geomorphic unit re-creation at the local scale (i.e., location-specific shear stress, time and frequency of flood) (Johnson, 2000; Karrenberg et al., 2002; Gonz'alez et al., 2018). In the second approach, scale-dependent dominance of climatic conditions, geographic formation and progressively flow regime, valley contexts, and local lateral flood plains control channel dynamics and geomorphic unit development and maintenance (Fryirs and Brierley, 2013). River corridor vegetation

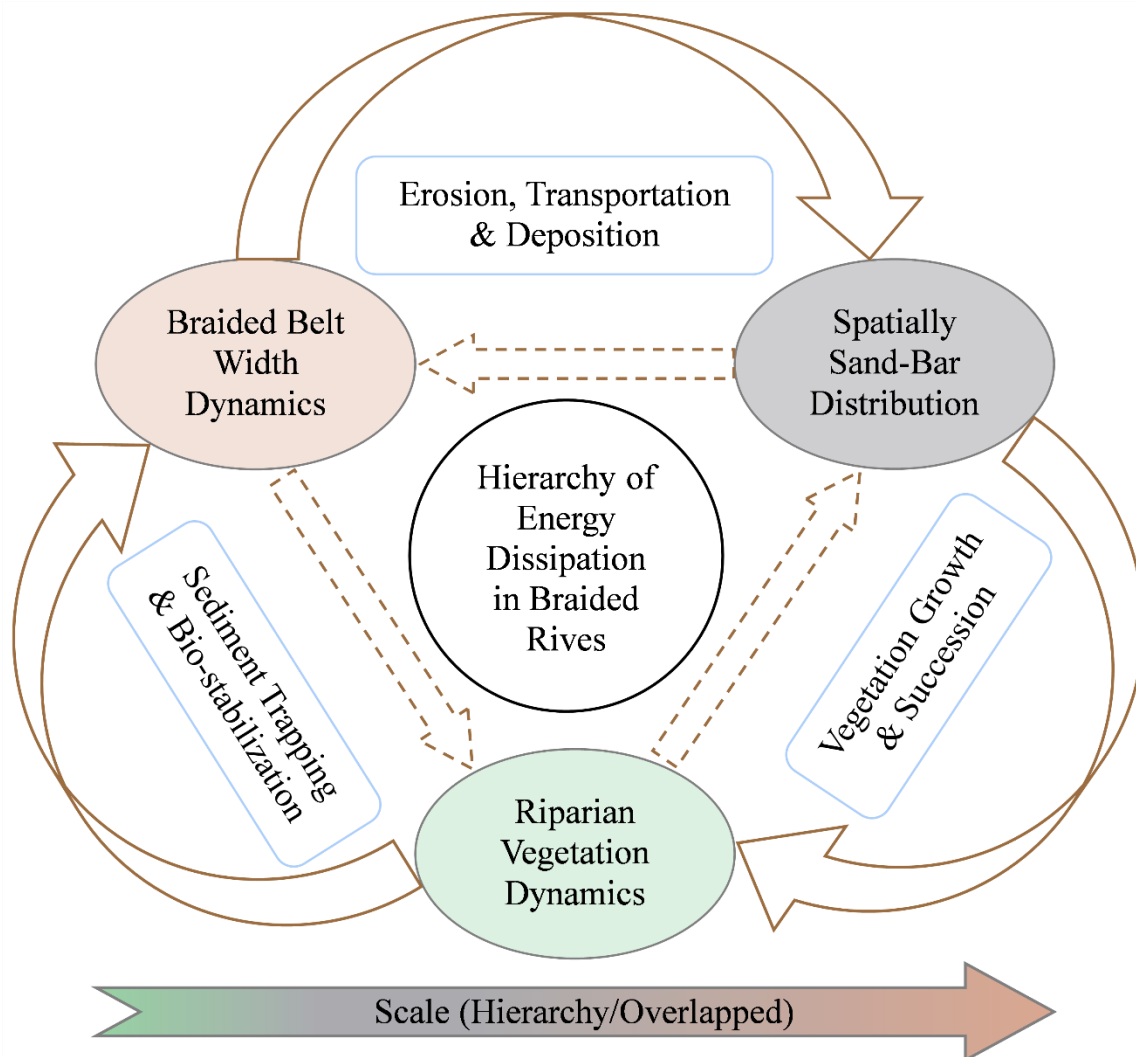
serves as a substantial energy dissipation component and has the ability to operate as a morphogenetic agent by exerting a large influence on the processes of erosion, transportation, and deposition of sediment. Thus, it is decisive to acknowledge the process-form-interaction of instream-floodplain vegetation, which contributes to the stabilization of fluvial landforms and control the braided morphology.

### **2.3 CONCLUSIONS AND RESEARCH DIRECTION**

The riverine problems of the Brahmaputra are significant concerns for river managers, hydrologists, and geomorphologists. For example, the bank erosion and braided belt width variability not only affect the morphological processes but also impact the individual, community, habitats, and economy (Mosselman, 2006; Sarker et al., 2014). According to Piegay et al. (2006), there is not such a unique solution for managing the braided rivers, and managers should take care of in-effect or apparent ecological values along with the evolutionary course of the river, besides human safety and protection of economic interests. Hence, estimating lateral mobility, bar disorderness, and vegetation-landform interactions are essential for a dynamic river like the Brahmaputra, and the undisturbed 'room for the river' concept should be promoted among the community and stakeholders level.

In this chapter, hierarchies of energy dissipation at three different scales (Figure 2.6) concerning the Brahmaputra River are discussed and further utilized to formulation of the research problem of the present thesis. Some of the points synthesized from this chapter are discussed here. A major portion of fluvial energy is getting dissipated by altering the braided belt width in the Brahmaputra River. The river passes through multiple geomorphic stages of 5 to 10-year duration, and (de)stabilizing agents like flow-sediment variability, geological factors (nodal, landslides, and earthquakes), and anthropogenic stresses (mining and deforestation) are among the contributing factors. The next energy expenditure potential can be referred to as formation of bar assemblage along with confluence-bifurcation nodes. The surface water dynamic analysis also signals the presence of a mega-channel and channel-in-channel physiography within the high cohesive banks. The Brahmaputra has varied instream or floodplain vegetated landforms that affect the bio-morphological processes. The flow resistance offered by vegetated landforms

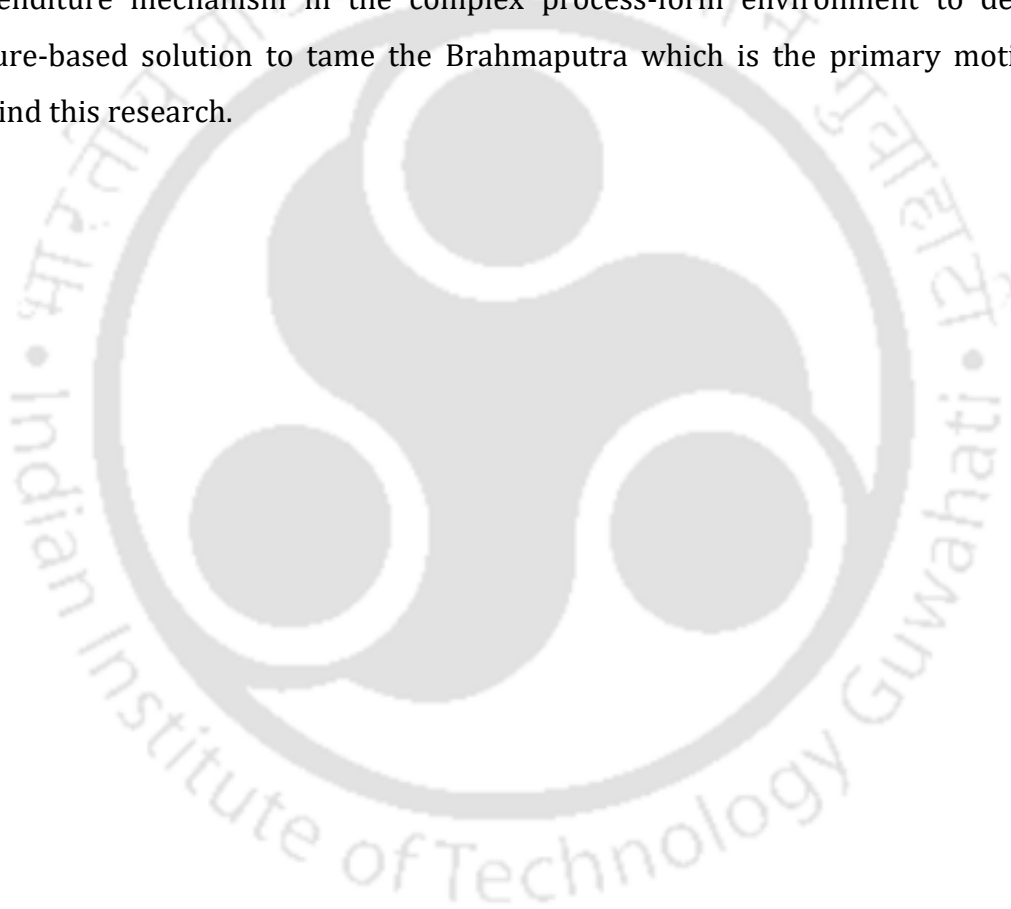
dissipates a share of fluvial energy and further helps to stabilize the dynamic geomorphic units at the landform scale.



**Figure 2.6** Probable energy dissipation and associated dominant processes (braided belt width dynamics, spatial sand-bar distribution, and vegetation dynamics) for the highly braided Brahmaputra River (Conceptualize based on the synthesis of previous literatures).

The morphological stability of the dynamic Brahmaputra river system can be improved through a better understanding of the complex interrelationships between cohesive and destructive forces that regulate succession and restoration dynamics within the fluvial corridor. However, the large-scale spatio-temporal heterogeneity in the governing processes creates several research issues that need to be addressed. Long-term goals should be prioritized over short-term objectives to unravel the

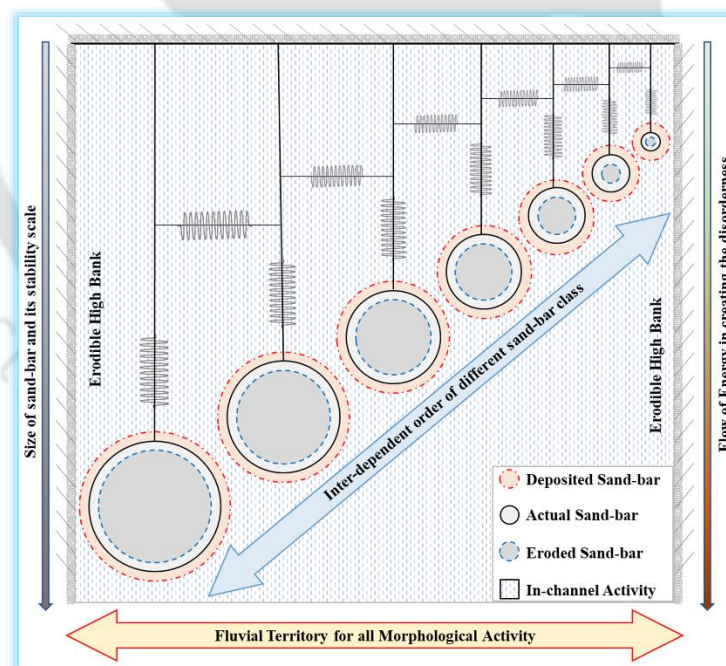
dynamics of this river system. To achieve this, eco-geomorphic river typology must be conceptualized, and dynamic prospective methods that incorporate the functional behavior of vegetation-landform corridors and associated fluvial processes must be developed. Additionally, for designing a proper methodology to characterize the extensive scale of the braided river system, several parameters such as sediment transport structure, erosion-deposition architecture, and planform changes should be considered. However, the unavailability of real-world river datasets and ungauged tributaries creates challenges during the formulation of numerical models and physical scale experiments. Hence, there is a need to comprehend the energy expenditure mechanism in the complex process-form environment to design a nature-based solution to tame the Brahmaputra which is the primary motivation behind this research.





# SYSTEM DISORDERNESS AND ENERGY EXPENDITURE MECHANISM IN A LARGE BRAIDED RIVER

(Understanding the entropy-based morphological variability and energy expenditure mechanism of a large braided river system)



**Contribution from this chapter:** Nandi, K. K., Pradhan, C., Padhee, S. K., Dutta, S., & Khatua, K. K. (2022). Understanding the entropy-based morphological variability and energy expenditure mechanism of a large braided river system. *Journal of Hydrology*, 615, 128662. <https://doi.org/10.1016/j.jhydrol.2022.128662>





### **3.1 OVERVIEW**

In the river like the Brahmaputra, large variability in discharge and sediment load results in extensive erosion-deposition process and instigate complex bar dynamics. This spatio-temporal variability in bar dynamics must be explored in order to comprehend the braided hydrodynamics. Further, it is also important to investigate the effect of bar dimension on the morphological changes of a braided reach. Consequently, the focus of this chapter is based on the interpretations indicated by change detection and variability of sand bar adjustment that addresses the following research questions:

- How can the spatiotemporal sand-bar dynamics of a large braided river be accessed using multiband water indices such as MNDWI?
- How can the concept of entropy be applied to study the disorderness of a braided river in reach scale?
- What is the mechanism by which the system uses the energy available within it to organize itself?

### **3.2 INTRODUCTION**

Braided rivers consist of complex network of channels or branches and bars (Leopold and Wolman, 1957), which are further characterized by large sediment loads, considerable discharge fluctuation, and steep topographic gradients (Charlton, 2007). Morphological processes like erosion, deposition, channel migration, and irregular planform formation pertaining to high stream power variability are crucial processes in understanding a braided river system (Bridge, 1993; Ferguson, 1993; Klaassen et al., 1993; Pradhan et al., 2021b). These processes in braided systems are recurrent and hasty enough to be measured over a short period. Majority of the studies are focused on integrating the flume-based experiments (Ashmore, 1982, 1991, 1993; Young & Davies, 1991), numerical modeling (Murray & Paola, 1994, 1997), satellite-based remote sensing products (Khan et al., 2014; Nykanen et al., 1998; Pradhan et al., 2017, 2019; Sapozhnikov and Foufoula-Georgiou, 1996, 1997; Walsh & Hicks, 2002), and advanced equipment like digital photogrammetry and laser altimetry (Lane et al., 2003; Westaway et al., 2000, 2001, 2003).

The Brahmaputra River is an ideal study region for assessment of morphological (sandbar) disorderness, as it is one of the largest sand-bed braided river systems in the world (Coleman, 1969; Mosselman et al., 1995; Thorne et al., 1993). The Brahmaputra ranks fourth in terms of the annual flow discharge (close to 20,000 cumecs - Goswami, 1985). In addition, the Brahmaputra is distinct from other large braided rivers owing to the extreme inter-seasonal variability of flow-sediment load and spatio-temporal variations in morphological activities (Chembolu and Dutta 2018; Dubey et al., 2020; Goswami, 1985; Karmaker et al., 2017). A series of large and long-duration flood events along with tectonic activities have generated a complex morphodynamics response in this river system (Goswami, 1985; Sarker et al., 2014; Valdiya, 1999). The morphodynamics of this extensive braided river system is accredited for high rates of bank erosion, unstable braided belt and fluctuating channel courses (Dutta et al., 2010). More than 30 million people relying on the Brahmaputra River are severely affected by these morphological changes almost every year (Nayak and Panda, 2016). Therefore, understanding the spatio-temporal variability of complex morphodynamics is necessary to differentiate the stable and unstable reaches and develop sustainable engineering (or nature-based) solutions.

Satellite remote sensing has proven its utility in many morphological studies, where in-situ survey is difficult or of costly affair (Bertoldi et al., 2011; Dubey et al., 2020; Fotherby, 2009; Piégay et al., 2009; Surian, 1999). Li et al., (2020) characterize the braided rivers in high-elevation environments by using long term satellite image analysis. Furthermore, the influence of comprehensive human activities such as construction of dam, farming practices, afforestation/deforestation, and mining etc. on river morphology has been investigated using high resolution satellite images (You et al., 2022). Gao et al. (2022) also utilized the Google Earth Engine resources for accessing specific set of Landsat images that helps them in their study to characterize the functional behaviour of Upper Lancang River located in the Qinghai-Tibet Plateau, China (>3400 m elevation). Similarly, Lu et al. (2022) examined the altered water and sediment flux due to the glacier melting in the Source Region of Yangtze River using Unmanned Aerial Vehicle (UAV) surveys and DEM data. Several researches on morphological changes utilizing the remote sensing techniques have been conducted for the Brahmaputra River, with an emphasis on bank migration and complex erosion-

deposition processes (Alam et al., 2007; Baki and Gan, 2012; Gilfellow et al., 2003; Khan and Islam, 2003; Klaassen et al., 1993; Sarker et al., 2014; Sarma, 2005; Sarma and Phukan, 2006; Thorne et al., 1993), estimation of braiding parameters and their relation with stream power (Akhtar et al., 2011; Gilfellow et al., 2003; Karmaker et al., 2017; Takagi et al., 2007). The synthesis of all these literatures provides an adequate understanding of the morphology of the Brahmaputra. However, there are still challenges persisting in the poorly-gauged Brahmaputra River owing to the high degree of morphological variability and associated processes. Chembolu and Dutta (2018) utilized selective satellite imagery and digitization approaches to study the sand bars (islands) disorderness. However, the authors believe, methods involving satellite-based multiband water index and semi-automatic surface water classifications are more capable due to their high detection accuracy, low implementation cost, and ease of use. The Normalized Difference Water Index (NDWI) is extensively used as an efficient land-water classification parameter (Ji et al., 2009; Lira, 2006; McFeeters, 1996; Ouma and Tateishi, 2006). However, in some instances, NDWI misclassifies the water surface, which led to the development of a further derivative called Modified Normalized Difference Water Index (MNDWI) (Han-Qiu, 2005; Xu, 2006, 2007). Therefore, in the present study, MNDWI is used to identify the spatio-temporal variability of the sand bar area and associated disorderness integrating the optical imagery.

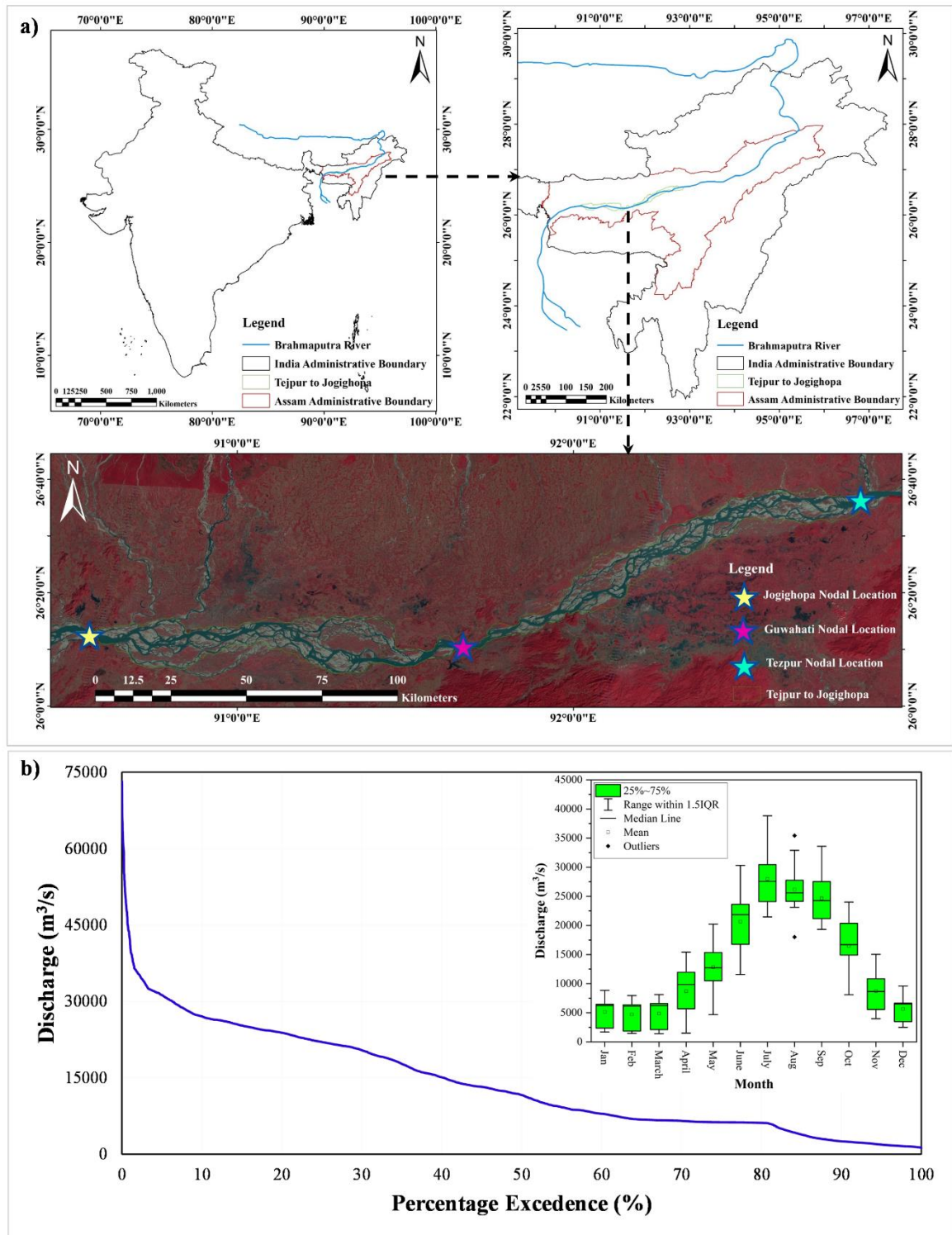
Entropy is defined as the measure of molecular disorder or randomness in the system. This concept is a thermodynamic-based principle, and it was first used in the field of fluvial-geomorphology by Leopold and Langbein (1962). Yang (1971c) demonstrated a relationship in a river system between potential energy and elevation that is analogous to the relationship between heat energy and temperature in a thermodynamic system as discussed by Leopold and Langbein (1962). Since then, the entropy concept has been used conveniently in several studies, primarily focused on the energy dissipation rate to explain the equilibrium in natural stream network (Brebner and Wilson, 1967; Leopold and Langbein, 1962; ra et al., 2019, 2021; Yang, 1971a, b, c). The entropy defined by Shannon (1948) and its different derivatives have been widely used in the morphological characterization. Few studies on fractal river networks use Shannon entropy-based derivation in developing the relationships between mean drainage elevation and river profiles (Claps et al., 1996; Fiorentino et

al., 1993). Tejedor et al. (2017) distributed optimal water-sediment in self-organized deltas by using the information entropy. Several studies have also focused on forecasting the equilibrium morphology, bed profile fluctuations, fluvial process-based evaluation, stream bank erosion modeling, bridge pier scouring, and river recovery potential using the entropy concept (Bandyopadhyay et al., 2014; Nield, 2006; Pitchford et al., 2015; Pizarro et al., 2017; Pradhan et al., 2021c, 2022; Sarker, 2021; Xu and Yang, 2012; Xu and Zhao, 2013). The application of entropy in large braided river morphodynamics is still an uncharted area, which is the motivation behind this study.

### **3.3 STUDY AREA AND DATA PREPARATION**

#### **3.3.1 Study area description**

The braided reach from Tezpur to Jogighopa of the Brahmaputra River is selected for this study (Figure 3.1). This stretch is approximately 240 km long and is made up of varied braided formations, with three nodal locations (Tezpur, Guwahati, and Jogighopa) having the narrowest channel width. The study reach is further divided into two different zones (upstream reach and downstream reach) based on the nodal point for analysis purposes. Nodal points are important physiographic location and have a greater impact on the morphology of the river. The nodal points govern the distribution of discharge and sediment flux as these locations are the converging points of upstream channels and subsequently diverges towards downstream. Furthermore, the riverbank is composed of highly erodible sand and silt composites that instigate additional dynamic characteristics to the braided Brahmaputra River (Karmaker and Dutta, 2011). The braided belt width variability of selected river reach is about 1.2 km to 18 km with an average bed-slope in order of 1/10,000. Daily discharge hydrograph is highly erratic in nature, and the mean daily discharge value varies from 4,420 cumecs in low flow to 51,156 cumecs in flooding conditions (Singh et al., 2004).



**Figure 3.1** a) Selected study reach for the Brahmaputra River and nodal points (Tezpur, Guwahati, and Jogighopa); b) Flow duration curve, and temporal variation of monthly average discharge at Guwahati nodal point.

The study area encompasses the middle reach of the mighty Brahmaputra river. This river originates from southern Tibet and is primarily a snow-fed trans Himalayan river. As far as its geological aspect is concerned, the Brahmaputra is considered the youngest of all major river systems (Sarma, 2004). The river has a total length of 2880 km and drainage basin area about 520,000 km<sup>2</sup>, which runs through China (1625 km; 293,000 km<sup>2</sup>), India (918 km; 195,000 km<sup>2</sup>) and Bangladesh (337 km; 47,000 km<sup>2</sup>). In Assam region of Indian part of Brahmaputra, the alluvium formation consists of clay, silt, sand and pebbles and is approximately 200-300 m thick (Geological Survey of India, 1974). The adjacent highlands to the Brahmaputra valley are extremely unstable seismically. The magnitudes of earthquake in 1897 and 1950 have been recorded as 8.7 in Richter scale. The severe earthquake caused massive land-failures and rockfalls on hill-slopes, as well as ground collapse and fractures. Furthermore, this leads to alteration in the course of many tributaries of Brahmaputra and ultimately affected the morphology of the river.

A wider braided belt width and flow-sediment variability create favourable circumstances for dynamic morphological activities in the river system. Wider braided belt width and flow-sediment variability together create favourable circumstances for morphological activities in the river system. The bed material composition is very fine, exposing the river to morphological activities in response to changes in fluvial parameters, such as channel shifting (Chembolu and Dutta, 2018; Karmaker and Dutta, 2011; Sarma, 2005). That eventually results in flow partition, and the formation of the mid-channel bar, and a further increase in the braiding of the reach (Richardson and Thorne, 2001). Inconsistent morphological activities like thalweg shifting, bank erosion, and bar migration are commonly seen in this river. Descriptive information about the study area is given in Table 3.1. There are three major tributaries in the north bank (Kameng, Dhansiri, and Manas) and one major tributary in the south bank (Kopili) that contribute flow and sediment to the study reach.

**Table 3.1** Hydraulics and morphological characteristics of the study reach.

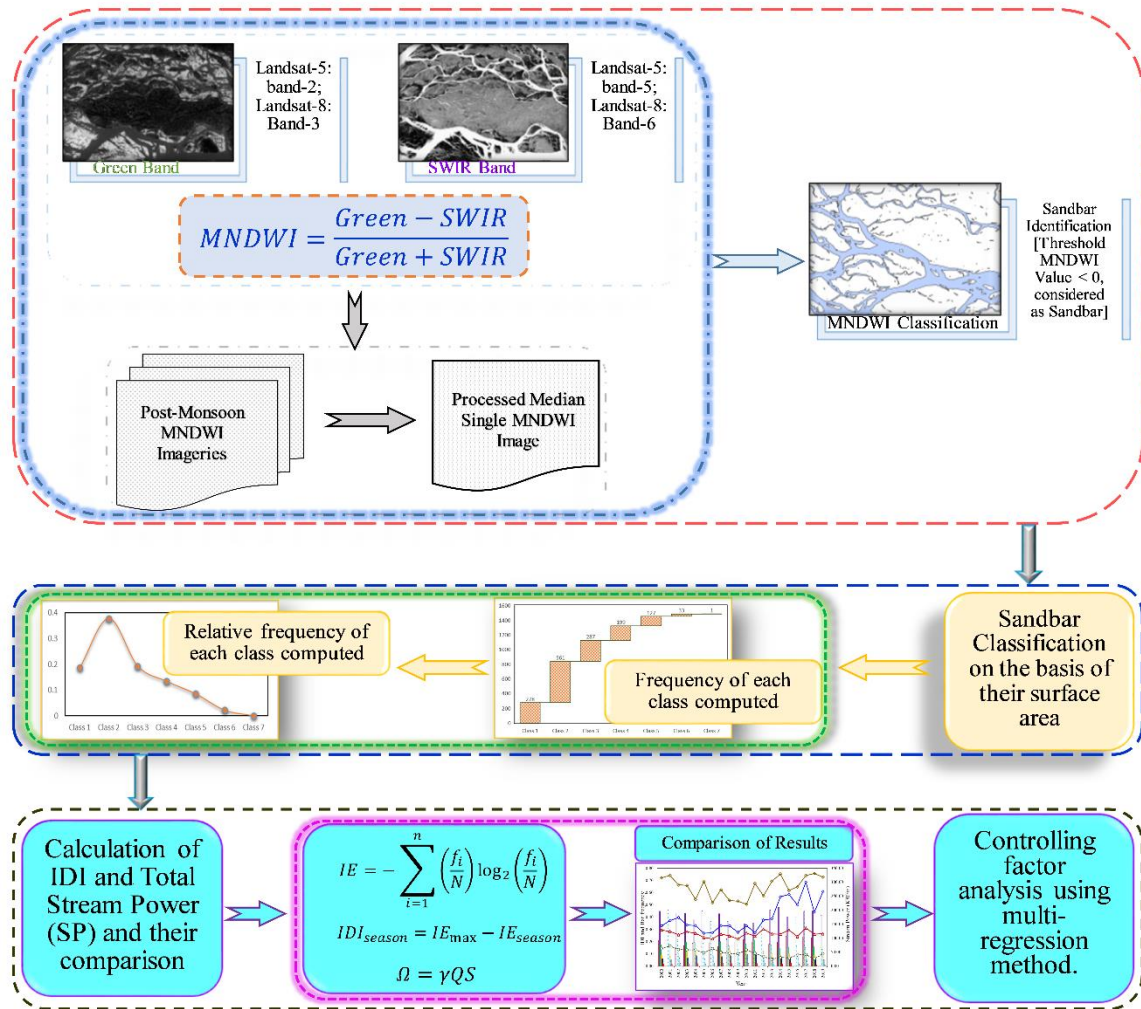
Study Reach Description	Average Length (in km)	Braided Width Details		Average Bed Slope	Major Tributaries	
		Width Range (in km)	Average Width (in km)		North Bank	South Bank
Tezpur to Jogighopa	240	12.6 - 0.59	4.5	0.00047	3	1
Tezpur to Guwahati	124.5	12.6 - 0.65	5.8	0.00038	2	1
Guwahati to Jogighopa	115.5	6.2 - 0.59	3.1	0.00032	1	0

### 3.3.2 Data preparation

The post-monsoon season (October to December) for the year from 2000 to 2019 is chosen for this study because major changes are anticipated to be captured after flooding events (Chembolu and Dutta, 2018). In Brahmaputra the % of annual discharge variation during the post monsoon season is highly fluctuates (about 10.3 % during October to about 2.6 % in December) (Vorosmarty et al., 1998). Data-set from both archive satellite imagery and in-situ observations are used in this study. The derivatives from optical images of Landsat TM/ETM+ at a high spatial resolution of 30m are obtained from Google Earth Engine. The in-situ data consists of hydrological observations (discharge and water level) acquired from the Central Water Commission (CWC) of India. Figure 3.1 (b) illustrates the flow duration curve and temporal variation of monthly average discharge prepared from the CWC data for the Pandu (Guwahati) gauging station.

### 3.4 METHODOLOGY

The morphometric analysis carried out in this study mainly focuses on the sand bar dynamics being a crucial feature in braiding (Ashworth and Lewin, 2012). The investigation is done for the post-monsoon period of 2000 to 2019 due to the active morphological changes of the river in this period. Figure 3.2 depicts the methodological flowchart, which includes procedures such as bar area detection (using MNDWI), bar frequency calculation, IDI computation, comparison of IDI with different stream powers, and lastly multi regression analysis for controlling factor assessment.



**Figure 3.2** Methodological framework utilized to understand the entropy-based bar disorderness and associated underlying processes.

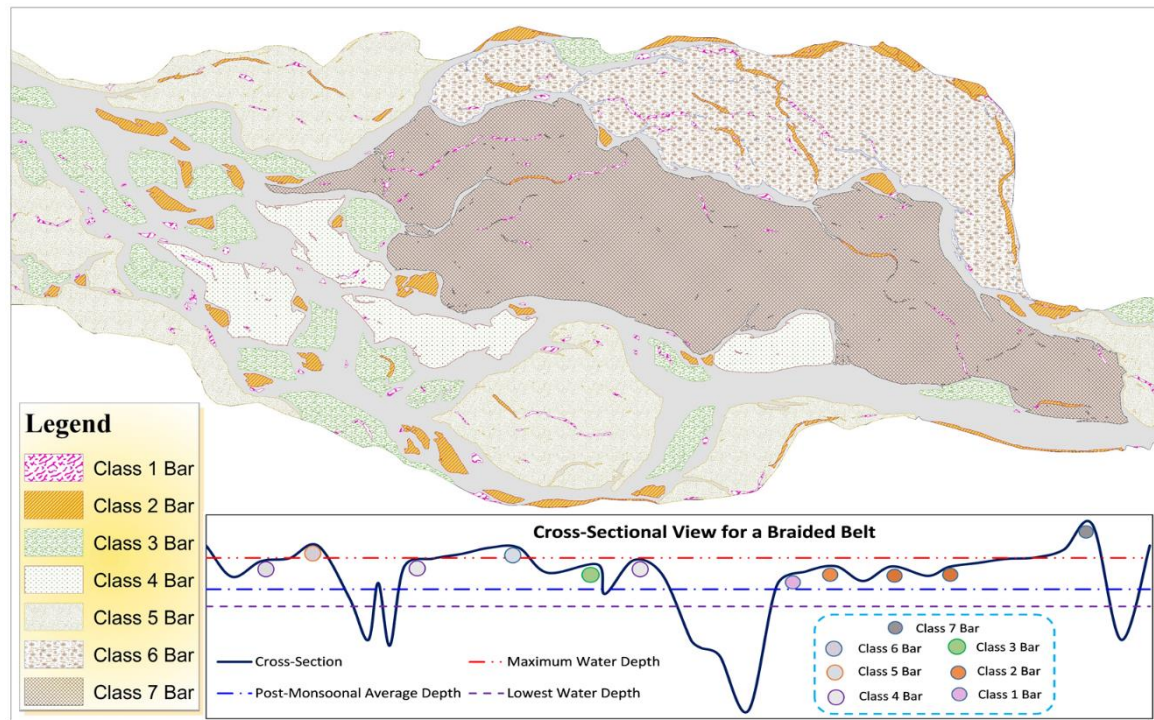
### 3.4.1 Calculation of bar area using MNDWI

The spectral index MNDWI was calculated by using reflectance from Landsat Archive in the google earth engine platform, and its corresponding images were downloaded. Xu (2006) proposed the MNDWI, which can be calculated using Eq. 3.1:

$$MNDWI = \frac{Green-SWIR}{Green+SWIR} \quad (3.1)$$

where, Green is the green band and SWIR is the short-wave infrared band in the electromagnetic spectrum. The ranges of MNDWI value ranges from (-1) to (+1). Negative values in MNDWI signify the absence of water, whereas the positive values signify the water features. A threshold value of 0 was used below which the sand bars

were identified, the rest of the features were identified as water. Furthermore, the detected sand bars were categorized depending on their surface area, and their approximate average elevations were observed through Google Earth Pro, which is conceptually illustrated in Figure 3.3 for a specific braided reach and cross-section.



**Figure 3.3** Conceptual illustration of bar classes based on surface area along the braided belt.

### 3.4.2 Intensity disorder index

In this study, the bars were classified into seven different classes as per their surface area, from the very small bar ( $<10^3 \text{ m}^2$ ) to the very large bar ( $>10^8 \text{ m}^2$ ) (Figure 3.3). Then the frequency of each class was calculated for obtaining the probability of its occurrence. This was further used to calculate entropy-based intensity disorder index (IDI) (Mishra et al., 2009). IDI explains the time-dependent alterations of the bars in a braided river system (Chembolu and Dutta, 2018). It is used to evaluate seasonal entropy-based heterogeneity. To estimate the IDI, the Intensity of Entropy (IE) for different bar classes is required. It is a metric for determining the disorder in the distribution of sandbar surface area in the study reach. This can be calculated using Eq. 3.2 in terms of relative frequency (Maruyama et al., 2005),

$$IE = -\sum_{i=1}^n \left(\frac{f_i}{N}\right) \log_2 \left(\frac{f_i}{N}\right) \quad (3.2)$$

where,  $f_i$  is the frequency of the sand bars for different classes,  $n$  is the number of classes,  $N$  is the total frequency of bars in a particular period. Here the unit used for IE is 'bit' having the logarithmic base 2 and defined over a range of IE is  $0 \leq IE < \infty$ . Smaller IE indicates less disordered intensity, implying a more skewed distribution of sandbar occurrence frequency, whereas higher IE indicates more highly disordered intensities spreading over a wider range. The IE provides an insight into ambiguity in the distribution of different sand bar areas. It varies from maximum value for equal distribution of different classes to 0 as the minimum value for most possible unequal distribution. Furthermore, IDI, mathematically defined as the difference between maximum probable entropy and the entropy of the individual distribution (Eq. 3.3).

$$IDI_{season} = IE_{max} - IE_{season} \quad (3.3)$$

Here,  $IDI_{season}$  is the intensity disorder index for a particular season,  $IE_{max}$  is the maximum possible entropy for uniform distribution, and IE is the individual intensity entropy for a particular season.

### 3.4.3 Stream power

The amount of available energy for river morphological processes is mostly determined by the stream power generated by the discharge flowing through the channel (Akhtar et al., 2011; Bawa et al., 2014; Karmakar et al., 2017). Stream power ( $\Omega$ ) is the rate of the deliverance of kinetic energy to potential energy during the flow (Bagnold, 1966) and mathematically defined by Eq. 3.4:

$$\Omega = \gamma QS \quad (3.4)$$

where,  $\gamma$  is the specific weight of water ( $\gamma = \rho g = 9810 \text{ N/m}^3$ ),  $\rho$  is the density of water ( $\text{kg/m}^3$ ),  $g$  is the acceleration due to gravity ( $\text{m/s}^2$ ),  $Q$  is the water discharge ( $\text{m}^3/\text{s}$ ), and  $S$  is the bed slope ( $\text{m/m}$ ).

### 3.5 RESULTS

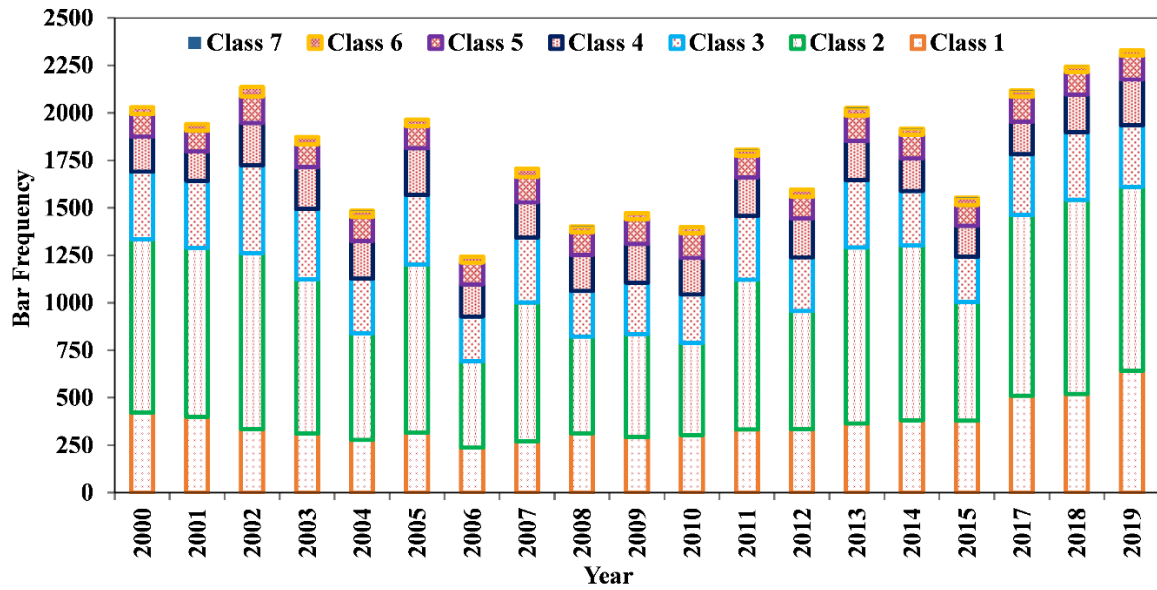
#### 3.5.1 Frequency distribution analysis

In this study, the frequency of the seven bar classes (Table 3.2) was calculated and shown in Figure 3.4. During the post-monsoon season, it is common for the large bars to get dissected and converted into small bars (Chembolu and Dutta, 2018). Similar to the previous findings, it was observed that the frequency of small bars was extremely high in comparison to the moderate, large class bars that are common during this season. As a result, the density of small bar classes increases, and it raises the disorderness. The large bars are generally referred to as forced bars with low mobility (or immobile) rates with respect to their shape, size, and location, while small bars are referred to as free bars with high mobility rates that play a key role in morphological changes (Baki and Gan, 2011). The detailed description of bar classes in the selected study reach is given in Table 3.2.

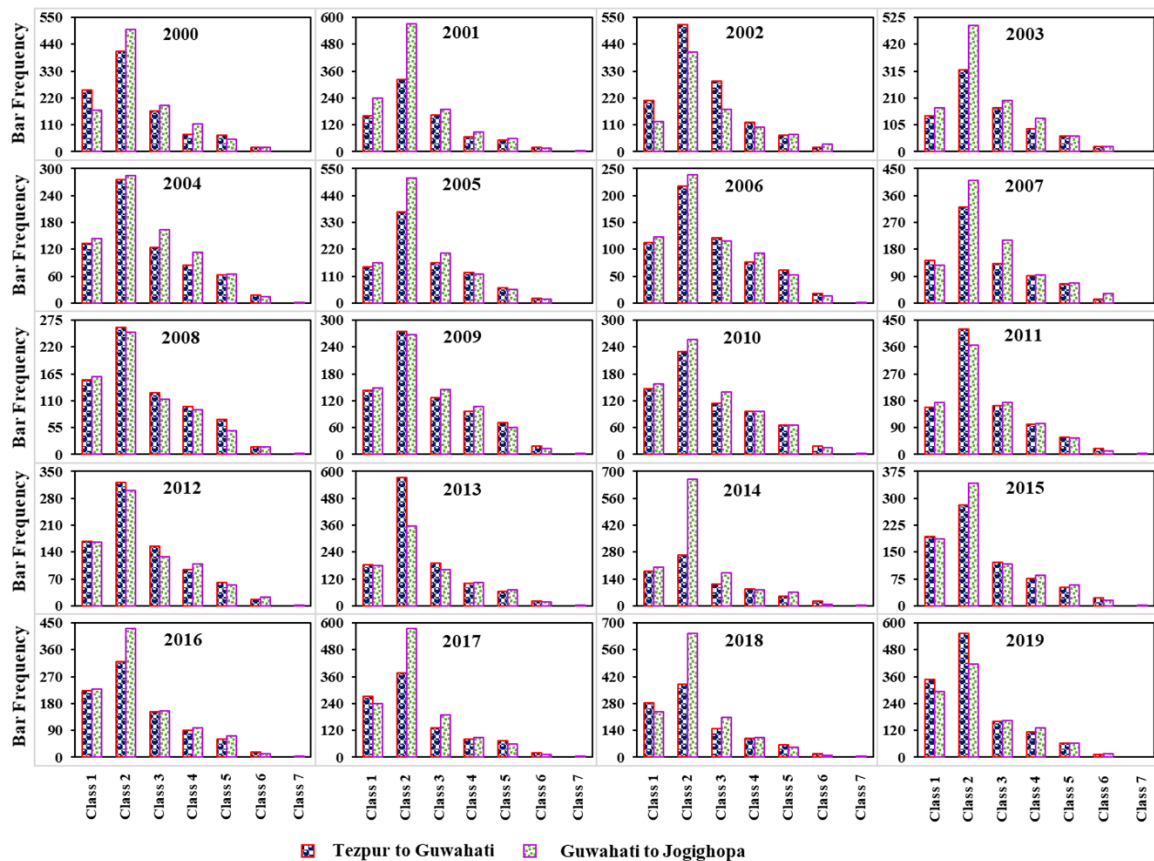
**Table 3.2** Details of bar classes and corresponding surface area

Bar Description	Bar Class	Area Range (in km <sup>2</sup> )	Average Area (in km <sup>2</sup> )	Average Area Fraction (in %)		
				Tezpur to Jogighopa	Tezpur to Guwahati	Guwahati to Jogighopa
Very Small	Class 1	< 0.001	0.0008	20.08	21.62	18.03
	Class 2	0.001 - 0.01	0.0031	40.16	40.00	41.04
Small	Class 3	0.01 - 0.1	0.0359	16.80	17.60	16.70
	Class 4	0.1 - 1	0.3688	11.09	11.01	10.09
Medium	Class 5	1 - 10	3.4548	6.13	7.54	5.63
	Class 6	10 - 100	24.4888	1.74	2.23	1.12
Very Large	Class 7	> 100	142.8372	4.00	0.00	7.39

The frequency of small bars (class 1, 2 and 3) was observed to be higher than that of medium and large-sized bars. The frequency of the class 2 bar was significantly higher than all other classes in each individual year. Except for 2005, the frequency of class 2 bar signaled a decreasing trend from 2000 to 2010. However, an increase in frequency was observed up to 2019 for class 2 and other lower bar classes (class 1 and 3).



**Figure 3.4** Yearly variation of frequency of bar classes in the post-monsoon season along the study reach.



**Figure 3.5** Yearly class wise bar frequency comparison for two sub-reaches.

Figure 3.5 depicts an annual class-wise bar frequency comparison for two different sub-reaches based on nodal point (upstream reach: Tezpur to Guwahati and

downstream reach: Guwahati to Jogighopa). Similar to the total reach, the frequency of class 2 bars was observed to be significantly higher than the frequency of other class bars along the sub-reaches. In most of the years, it was determined that the downstream reach has a higher number of class 2 bars than the upstream reach. This indicates that the downstream reach is morphologically more active than the upstream reach. The smaller class bar dominates along the sub-reaches and the higher-class bars (class 5, 6 and 7) did not undergo major changes, which further implies the formation of immobile bars (islands) over time.

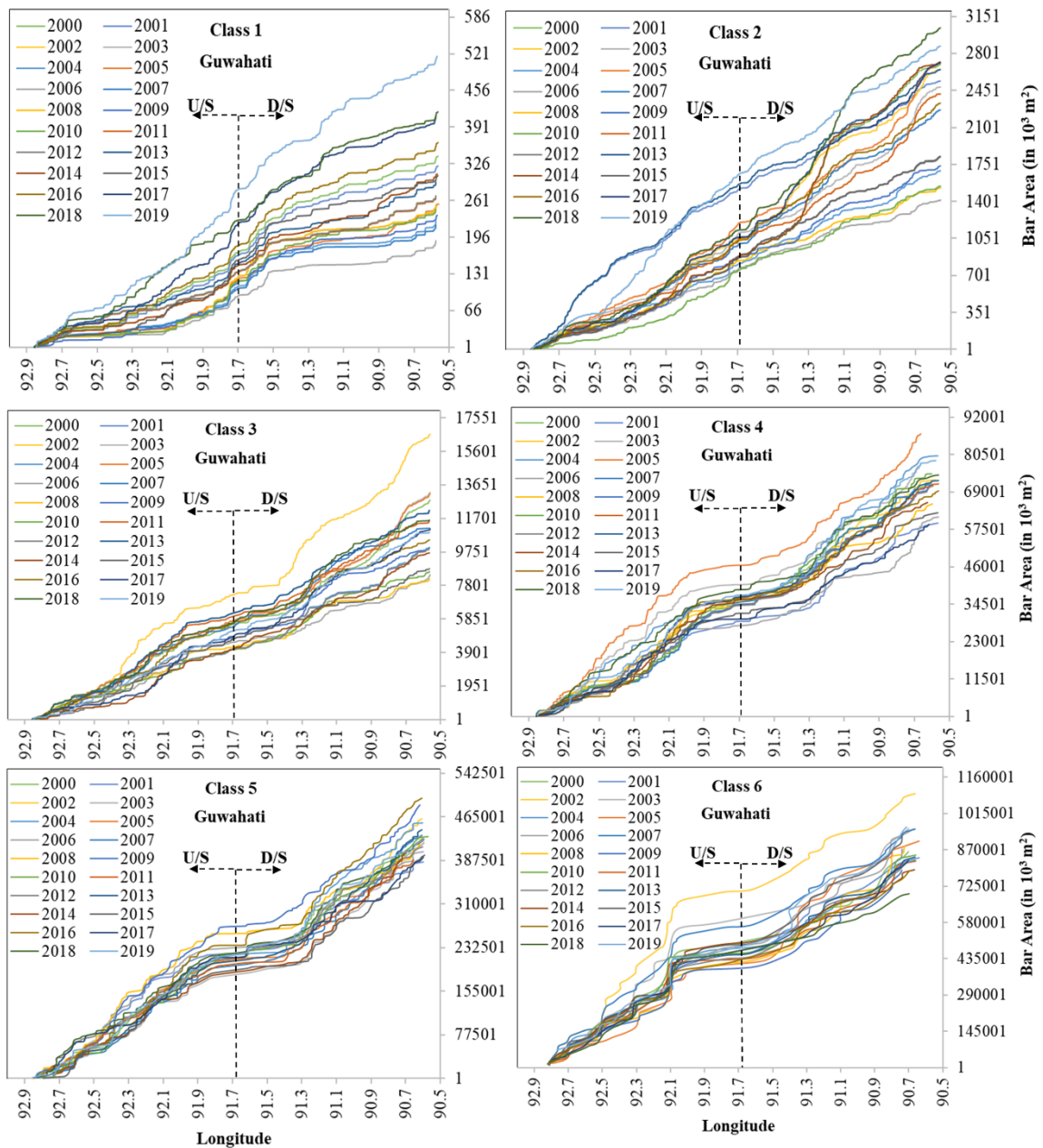


Figure 3.6 Longitudinal variation of cumulative bar area for the different classes.

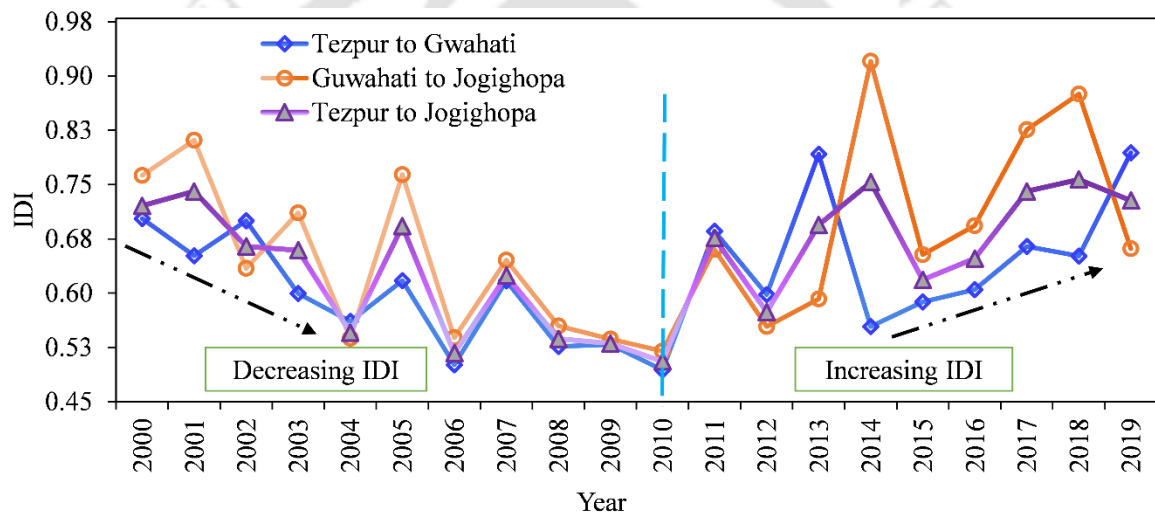
Figure 3.6 suggests that class 1 and 2 bars are more dynamic in comparison to the other classes and significantly contributing to the disorderness of the braided reach. In 2019, the class 1 bar had the highest cumulative area as compared to other years. In addition, class 2 bar showed higher fluctuations in 2001, 2013 and 2019, whereas in 2002, 2014, and 2018, the class 2 bar had a rise in the cumulative area (downstream of Guwahati). In 2002, the class 3 bar fluctuated higher in comparison to the other year. A constant variation was observed in classes 5 and 6 for almost all the years, indicating that these bars are stable and do not change notably with time and space. The class 6 bars in 2002, 2003, and 2007 and class 4 bars in 2011 had the greatest cumulative area in the downstream reach. Furthermore, the smaller bars were observed with less frequency (Figure 3.4) in these years, indicating that smaller bars may get eroded or combined (or deposited to adjacent bars) to form larger bars.

### **3.5.2 Temporal variability of intensity disorder index**

The bar classes variability in the study reach is a function of discharge, flow depth, erosion-deposition, and sediment transport. The Intensity Disorder Index (IDI) is used in the present study as a parameter for braided reach disorderness identification as proposed by Mishra et al. (2009). It is an indicator of uniformity of the bar distribution over the braided reach. Figure 3.7 depicts the variability of IDI for the whole study reach along with the two sub-reaches separated by the nodal points. The variability of IDI for the whole study reach as well as the two sub-reach were observed to be declining up to 2010, and then it showed more instability with an increasing trend up to 2019. A statistical analysis was performed to identify the trend of IDI variation using the Mann-Kendall test and Sen's slope ( $\alpha = 0.05$ ) analysis (Table 3.3). It was clear that from 2000 to 2010, the IDI showed significant changes for the entire reach and sub-reaches (p-values <  $\alpha$ -value). Negative Sen's slope and Kendall's tau value indicated declining trend of IDI for all the reaches in study period. However, from 2010 to 2019, the p-value is greater than the  $\alpha$  value, which implies no significant change. Still, there is an increasing trend for the IDI as the Sen's Slope and Kendall's tau have positive values.

**Table 3.3** Details of Mann-Kendall and Sen’s slope statistics for IDI variation trend analysis.

Statistical Parameter (Mann-Kendall and Sen's Slope analysis)	Tezpur to Jogighopa		Tezpur to Guwahati		Guwahati to Jogighopa	
	2000-2010	2010-2019	2000-2010	2010-2019	2000-2010	2010-2019
Kendall's tau	-0.689	0.389	-0.600	0.222	-0.556	0.389
Mann-Kendall Statistics(S)	-31.000	14.000	-27.000	8.000	-25.000	14.000
p-value (Two-tailed)	0.005	0.180	0.017	0.477	0.029	0.180
Alpha ( $\alpha$ )	0.05	0.05	0.05	0.05	0.05	0.05
Sen's slope	-0.022	0.012	-0.018	0.013	-0.024	0.031



**Figure 3.7** Yearly variation of Intensity Disorder Index (IDI) for the study reach and the sub-reaches along the post-monsoon season.

The dissection of larger bars into smaller bars and formation of chute channels on the diagonal bars increased the frequency of small bars. This process resulted higher IDI values in the second epoch (2010-2019). The IDI values were observed to be higher in the downstream reach (Guwahati to Jogighopa) than the upstream reach (Tezpur to Guwahati) except for few years (2012, 2013 and 2019). Furthermore, the downstream reach has a larger braided belt space than the upstream reach, which accommodates all the erosional and depositional processes and contributes to the higher disorderness of the reach. This is supported by the fact that in 2012, 2013 and 2019, the small bar classes (class 1, 2 and 3) frequencies were more prevalent in the downstream reach. The deviation of IDI was also higher in the downstream reach for

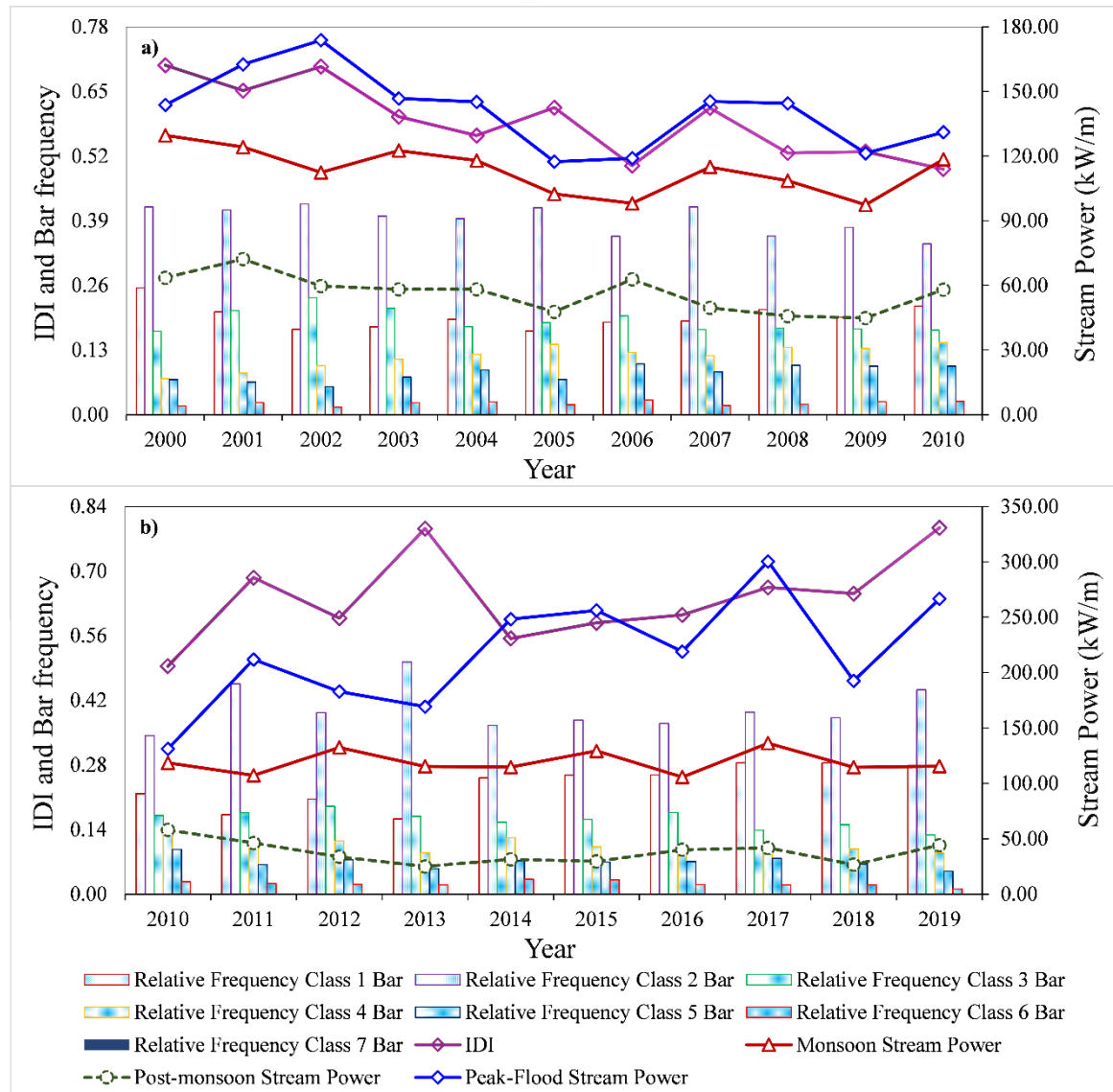
the second period (2010-2019). As noted in Figure 3.6, 2001, 2013, and 2019 have a higher class 2 bar fluctuation and therefore accounted for the higher IDI values. In 2002 and 2013, the IDI value was higher for the study reach in comparison with both the sub-reaches. Similarly, in 2002, 2014, and 2018, the class 2 bar has a higher frequency (Figure 3.4), that is reflected by the IDI variation. The cumulative area values of the class 6 bar are higher, indicating that growth in the larger bar class increases the stability of the reach and reduces the disorderness. Several studies reported about the shape similarity of different class of bar and its influence on the morphological behavior of the river (An et al., 2013; Sambrook Smith et al., 2005; Walsh and Hicks, 2002). However, this cannot be considered in a highly braided river such as the Brahmaputra, since the frequency of distinct classes of bar is significantly higher.

### **3.5.3 Relationship between stream power, IDI, and bar classes**

The morphological changes like thalweg shifting, channel alteration, the closing/opening of an existing/new channel, bank erosion are the effect of seasonal flood events. These processes in a braided reach may imitate the sand bar development and its variability. In the post-monsoon season, the braided planform disturbances increase due to the high flood discharge. Here total stream power for monsoon ( $\Omega_m$ ), post-monsoon ( $\Omega_{pm}$ ), and peak flood events ( $\Omega_{pf}$ ) was calculated and compared with yearly IDI variation and relative bar frequency of different classes (Figure 3.8). A regression analysis was performed to investigate how varying stream power correlated with the IDI fluctuation, considering IDI as the dependent variable (Table 3.4). According to Table 3.4, the R-statistics indicate that there is no stronger co-relation between the IDI and stream power derivatives, with values of 0.26, 0.18, and 0.39 for monsoon, post-monsoon, and peak-flood stream power, respectively. This demonstrates that the IDI variation was not significantly related to any stream powers, with the exception of a marginally better relationship with the peak-flood stream power. As the P-statistics suggested, the regression model does not demonstrate any significant relationship between the variables.

**Table 3.4** Details of regression statistics of IDI with different stream powers.

Statistical Parameter	Monsoon Stream Power ( $\Omega_m$ )	Post-Monsoon Stream Power ( $\Omega_{pm}$ )	Peak-Flood Stream Power ( $\Omega_{pf}$ )	Multiple Regression
R	0.26	0.18	0.39	0.41
R <sup>2</sup>	0.07	0.03	0.16	0.17
Adjusted R <sup>2</sup>	0.02	-0.02	0.11	0.01
Standard Error	0.08	0.09	0.08	0.09



**Figure 3.8** Yearly comparison plot of different bar classes with their relative frequency, monsoon stream power, post-monsoon stream power, peak flood stream power, and IDI; (a) for the decreasing IDI period; (b) for increasing IDI period.

Furthermore, the responses of the braided channels to flooding occurrences must not be overlooked since they may have an impact on the disorderness of the braided reach. This study showed that peak flood stream power is better related to IDI variation than monsoon and post-monsoon stream power. It is apparent that whenever the peak-flood stream power value increases, the smaller bar frequency decreases, as well as the larger bar frequency (or the surface area) increases for the succeeding year. For the second period (2010-2019), the peak flood stream power was increased, which may have contributed to the rising trend of IDI. There can be a significant effect of stream power on the different classes of bar variability in the braided reach. The class 2 bar, which is considered to be the most dominating bar class for IDI variation discussed earlier, showed an inverse relation to peak flood stream power. This is because extreme floods generate high velocity and erosive power, which can deepen the shallower channel, wash the smaller (mobile) bars, and cause substantial bank erosion. Further, the consequences of rising intensity floods require time to absorb within the system before it evolves towards a new planform, as evidenced by irregular patterns in sediment material depositions observed during flood receding (Charlton, 2007). Smaller bar growth established a direct relationship with the peak flood events for some of the year. The reason could be the peak flood episodes in those years sculpted sediment material from the bigger bars or banks and formed the smaller class bars through deposition (Moody, 2019; Wheaton et al., 2013; Williams et al., 2020). Furthermore, we may obtain a better process understanding by considering it as a whole system along with their geomorphic responses to the stream energy generated by fluctuating peak flooding events of varying durations.

### **3.6 DISCUSSION**

#### **3.6.1 Role of sand bar dynamics in the morphological uncertainty**

The fundamental morphological aspect of a braided river is bar creation, which is also associated with other morphological processes like bifurcation-confluence formations, alteration in channel sinuosity, thalweg shifting and lateral channel migration (Ashmore, 2013; Chembolu and Dutta, 2018; Nandi et al., 2022; Tubino and Bertoldi, 2007). The formation (or growth) of sandbars and their spatiotemporal evolution are strongly connected to a sequence of complex erosion-deposition processes, which must be understood to describe the morphodynamics of a highly

braided river system. Furthermore, the size of a sandbar is related to the stability and accompanying channel characteristics (Baki and Gan, 2012). This is supported in the present study where the frequency of small bars varies faster (highly unstable), and the frequency of large bars becomes relatively constant (stable) over the years (Figure 3.4 and 3.5). It should be noted that large sandbars with discrete areas are evidence of morphologic stress, in which wider or spreading portions capture the bed material exported from the contracting or constricted parts (Repetto et al., 2002; Ramirez and Allison, 2013; Szupiany et al., 2012; Wu & Yeh, 2005). The unit discharge and flow transport capacity decline substantially toward the bar head during the low- and medium-flow stages, facilitating suspended and bed sediment deposition. However, during floods (high flow), this process is opposite, resulting in erosions at the head and around the bar. Such processes are observed in the present study reaches, where the smaller bars are the prime target of the fluvial action. This further reduces the frequency at high flow and may deposit to the comparably larger bars. The antecedent state is reflected in the subsequent season by an increase in larger bar size (frequency) and a reduction in smaller bar frequency. The grain size distribution of the bed and suspended sediment material also governs the particles which are transported in suspension onto the bar head. The bed material is considerably coarser in the proposed study reaches of the Brahmaputra River, and these features may have an impact on the morphodynamic evolution of the bars. Furthermore, a process-based understanding of the sediment transport is required to evaluate the impact of flow conditions (secondary currents, turbulence structures, and boundary shear) on the sand bar dynamics resulting in extensive morphological changes along the Brahmaputra River.

### **3.6.2 IDI variation and its influence on the system's disorderness**

Chembolu and Dutta (2018) reported that the intensity of braiding depends on the braided belt width availability (due to multi-channel formation and sand bar disorderness). The available braided belt width ('room to move' or 'erodible corridor' or 'freedom space') helps the river to self-adjust or self-heal against the disturbances caused by floods and sediment load fluctuations (Biron et al., 2014; Piégay et al., 2005; Rapp and Abbs, 2003). The process-form-evolution comprises erosional (geomorphic unit removal, widening of active channels, river bank failure, scour, etc.) and

depositional processes (formation of new geomorphic units, sediment material accretion, etc.) (Fryirs et al., 2015). In the downstream reach of Guwahati, the braided belt space availability is larger as compared to the upstream reach and therefore, it facilitates the formation of major geomorphic units and an increased IDI (disorderness). Furthermore, the disorderness of a braided reach is an indicator of the morphological changes, and also depends on the hydrologic regime (Nicholas et al., 2013), anthropogenic stresses (Hicks et al., 2021) and periodic disturbances like earthquakes (Borgohain et al., 2017; Sarker and Thorne, 2006). According to Sarker and Thorne (2006), the impact of the great Assam earthquake (1950) on the morphological dynamics of the Brahmaputra River probably lasted for half a century due to substantial sediment wave generation. This may induce fluctuation in the sandbar evolution, which affects the IDI variation over the years. Therefore, any changes in the governing factors must be mapped as they induce a series of fluvial changes in the braided system at various spatio-temporal scales.

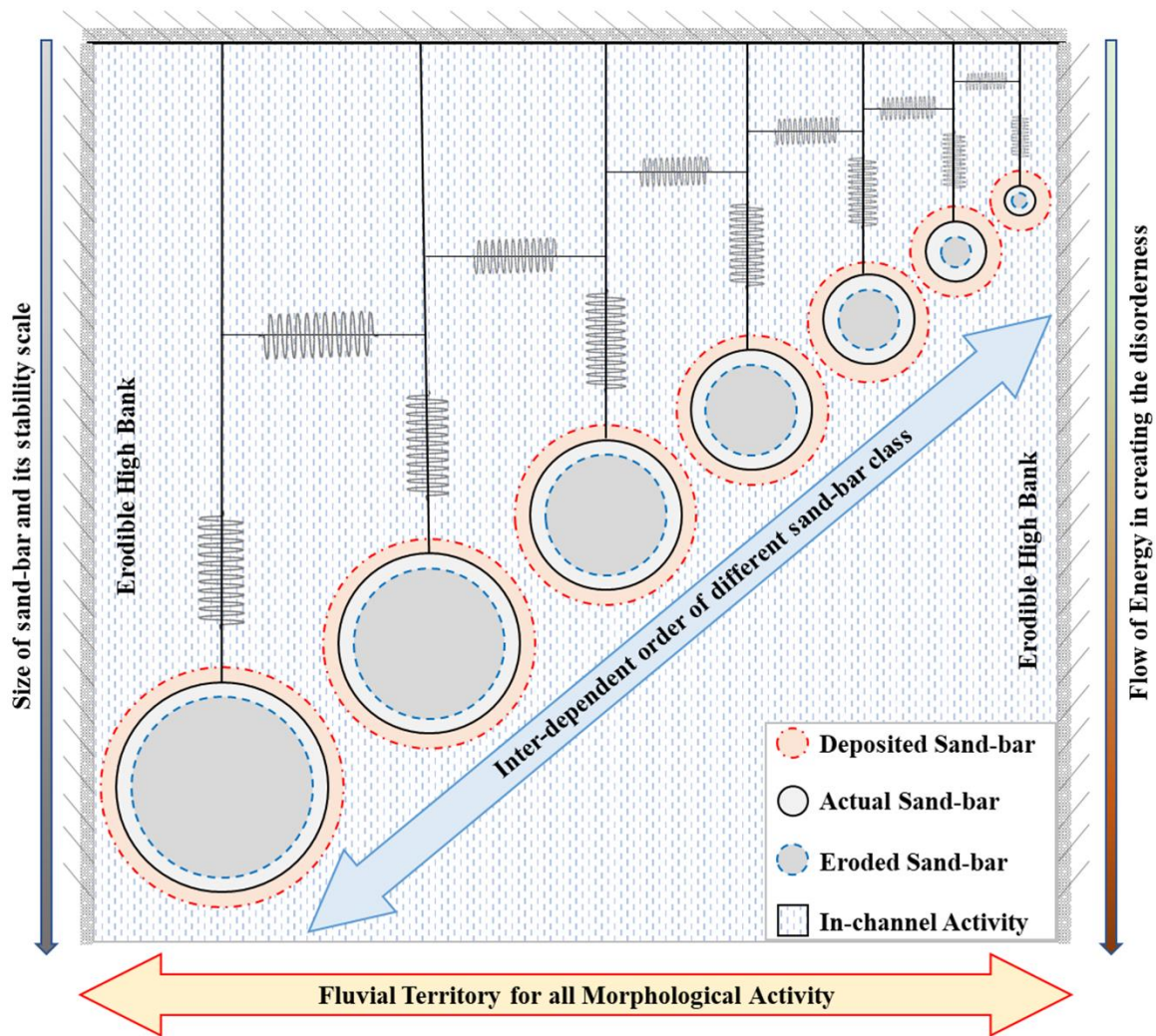
### **3.6.3 Contribution of stream power to the IDI variation and morphological variability**

Stream power is considered as the potential measure of geomorphic activities in braided river. The studies on sediment transport variability (Bagnold, 1966, 1977; Hassan et al., 1992; Reid and Frostick, 1986; Schneider et al., 2010; Yang, 1972), bank erosion processes (Lawler et al., 1999), braided belt disorderness (Chembolu and Dutta 2018), channel changes (Chang, 1979; Ferguson, 1987; Van den Berg, 1995), aggradation and degradation thresholds identification (Bull, 1979) have been carried out based on the stream-power variability. In this study, an attempt has been made to relate the stream power derivatives to the IDI variation of the reach. However, in the Brahmaputra River, lack of relationship signals the highly non-linear and complex processes, owing to the combined effects of anthropogenic activities, tectonic disturbances, and varied hydrologic regime. The previous literature synthesis indicated the dominant impact of flood stream power on the morphodynamics of alluvial rivers (Akhtar et al., 2011; Bawa et al., 2014; Kale, 2008; Magilligan et al., 2015; Pradhan et al., 2021b). In contrast, Karmaker et al. (2017) argued that braiding is not directly controlled by the stream power and geological characteristics control its spatial distribution, whereas the seasonal variability of

stream power is controlled by annual rainfall variability (Kaushal et al., 2020). Furthermore, the planform changes are not only the results of extreme events and smaller floods with regular intervals may have a higher cumulative impact on the changes (Charlton, 2007). It was reported that on average annually nine flood waves take place in the Brahmaputra River (Karmaker and Dutta, 2010). Figure 3.8 clearly demonstrates that when the disorderness of the reach increases, the corresponding stream power reduces, indicating a lower potential for energy expenditure. Majumdar and Mandal (2020) made a similar observation while attempting to correlate stream power with planform index and bank erosion for the Ganga River. Furthermore, high stream power can result in scour and formed chute bars, as well as a significant concentration of coarser material above the bar head and chute (Dietrich and Smith, 1984). In addition, if the stream power is reduced beyond a bar top due to an abrupt depth increment, it can result in a deposition at that bar tail due to the formation of a low-flow zone (Kasvi et al., 2013). This was also observed at few locations along the braided reach and the size of the larger bars has been augmented. In these conditions, the frequency of smaller bars was reduced due to erosion, resulting in the increment of larger bar area by deposition of the eroded material at the bar tail.

#### **3.6.4 Interpretation of process-based sand bar disorderness and energy expenditure mechanism**

The previous sections concluded the dynamics of the bar morphology may not be solely attributed to the stream power. The response of braided reach to the stream power is not only in the form of bar morphology, but also in the changes by other forms like thalweg shifting, sinuosity, erosion, and deposition (Chembolu and Dutta 2018). The excess energy available may be expended by the morphological activities at various hierarchical levels and overall self-adjustment of the braided system. A conceptual system representation based on the sand-bar dynamics of a large braided river has been illustrated in Figure 3.9.



**Figure 3.9** Conceptualization of energy expenditure by the different sand-bar class with in the fluvial territory.

A system scale has been employed to represent the bar classes and their interactions with flow energy within the fluvial territory. The sand bars are conceptualized based on the observed sand-bar classes in our study reach (Table 3.2). Further, the interdependent nature of sand-bars in terms of size, location, and erosion-deposition activity are hypothesized with respect to the incoming flow energy. The high magnitude floods produce huge amounts of energy and erosional power in the flow, which affects the sand bar depending upon the size and location (Baki and Gan, 2012; Goswami, 1985). The system can be suggested as a spring system; therefore, any disturbance caused by incoming flow energy to any of the attributes affects the entire system, and the disturbance propagates in both longitudinal and lateral directions. In accordance with the increasing flow energy magnitude, smaller (mobile) bars, or even

parts of larger bars (depending upon their stability criteria) get eroded and again deposited into the downstream bars (Chembolu and Dutta, 2018; Pradhan et al., 2021a; Nandi et al., 2022a). In similar fashion, part of the bank gets eroded and widens the channel, while part of the bank gets the deposited material and makes the channel narrower (Karmaker et al., 2017). As such, all of these processes control the channel-in-channel activity, such as forming new channels (secondary and tertiary), closing of the existing channels, modifying the thalweg sinuosity, and forming the chute channels (Bawa et al, 2014; Chembolu and Dutta, 2018). Therefore, such complex process-form interactions can (in)directly influence the braided belt variability, as well as all sorts of geomorphological activity of the large braided river system and dissipate a significant portion of the fluvial energy available to the system.

### **3.7 CONCLUSIONS**

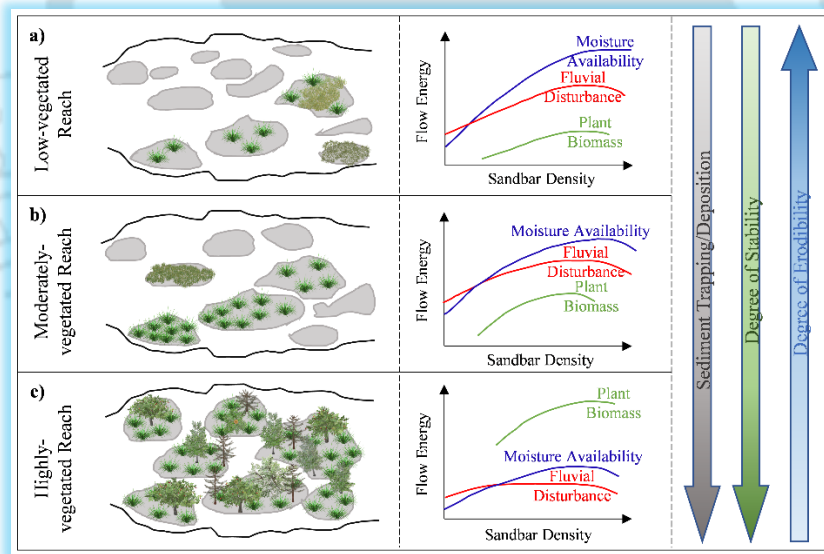
In this present chapter, the concept of entropy was utilized to assess the spatio-temporal variability of sand bar distribution over the selected braided planform of the Brahmaputra. Some of the major findings drawn from the analysis are listed in this section. First, the variations of IDI showed a decreasing trend in 2000-2010, followed by an increasing trend up to 2019, which further signals a decadal shift in morphological stability in the Brahmaputra. Second, the frequency of smaller (mobile) bars is high as compared to the medium and larger bars (immobile) in the second time period and controls the IDI variability. The inter-comparison of the two braided sub-reaches showed that the downstream reach had a higher IDI attributed to the prevalence of smaller-sized bars. Third, according to different stream power comparison, peak flood stream power was better correlated to IDI variation than monsoon and post-monsoon stream power. Finally, the disorderness of the braided reach does not fully expend the incoming stream power, but also the additional available fluvial energy may be dissipated by geomorphological activities such as sinuosity alteration, erosion-deposition mechanism, thalweg shifting etc. This study develops a new methodological approach to understand the system disorderness in a large braided river system. Further, the insights obtained from this research can be applied to develop a process-form-interaction approach, which can enhance our comprehension of intricate braiding patterns in large braided river systems.



# 4

## VEGETATION AND ITS IMPACT ON STABILITY CRITERIA OF A BRAIDED REACH

(Establishment of the role of in-stream vegetation on the morphological variability of the large braided Brahmaputra river)



**Contribution from this chapter:** Nandi, K. K., Pradhan, C., Dutta, S., & Khatua, K. K. (2023). Identifying the stability trajectory of a large braided Brahmaputra River using reach-scale process-based approach. *Journal of Hydrology*. (Under Review)





#### **4.1 OVERVIEW**

As discussed in the previous chapters a large braided river system operates sporadically, with its spatiotemporal evolution influenced by both natural and anthropogenic factors. The hydro-geomorphological interaction with the surrounding ecosystem within the river corridor is a complex process that makes understanding more difficult. It is necessary to comprehend the flow-vegetation interaction within the river corridor to appropriately design and manage the system. Additionally, understanding the river ecosystem's feedback mechanisms can help with flood mitigation measures and align the socioeconomic criteria. This chapter aimed to comprehend the spatiotemporal heterogeneity in the vegetation-flow regime of the mighty Brahmaputra river. This chapter addresses a few questions such as:

- How the in-stream vegetation dynamics can affect the river's morphodynamics?
- How river dynamics can influence the establishment/development of the vegetation cover?
- In what way the in-stream vegetation cover affects the stability criteria of the sandbars?

#### **4.2 INTRODUCTION**

The braided river systems are characterized by multi-channel flow-sediment networks and large alluvial formations that can last for decades to millennia (Schumm, 1985; Piégay et al., 2006; Tooth et al., 2008; Zolezzi et al., 2009). In recent years, process-form understandings of the braided river pertinent to the bio-geomorphic interactions have been developed as a new paradigm (Gurnell et al., 2001; Stallins, 2006, Bertoldi et al., 2011; Osterkamp et al., 2012; Camporeale et al., 2013; Gibling et al., 2014). In the braided rivers, the temporal evolution of bare alluvial deposits transforms them into islands with elevations close to the floodplains or high banks. The islands are non-erodible and significantly promote the succession of mature vegetation cover (Nanson and Kinghton, 1996). The plant communities are recognized as the physical ecosystem engineer and strongly influence the sediment transport, retain minerals, build the landforms and further promote rapid colonization (Gurnell et al., 2012). Therefore, understanding the flow-vegetation

interaction in different environmental settings on a spatiotemporal scale is required, and this study is still limited due to a lack of relevant information on vegetation dynamics.

The braided river corridor is subjected to continuous flood inundation with varying discharge, sediment transport, and associated bio-morphological changes (Bertoldi et al., 2011). The spatiotemporal erosion/succession of vegetation cover within the active territory of the river system is primarily regulated by floods (Lytle and Merritt, 2004; Camporeale and Ridolfi, 2006). The vegetation cover increases the flow resistance, which dissipates energy and deposits sediments, and further, the growing plant root system stabilizes alluvial deposits with time. There are increasing evidence that mutual interactions between vegetation and fluvial processes affect the system behavior and development over time (Gurnell et al., 2001, 2005; Corenblit al., 2007). The vegetation growth enables the system to control the morphology by increasing erosion resistance and stability to the sediment deposits (Pollen et al., 2004; Eaton, 2006). Furthermore, it can reduce near-surface flow velocity, and shear stress, allowing sediment, organic minerals, and plant propagules to be trapped (Gurnell et al., 2000) and eventually develop fluvial landforms (Gurnell et al., 2001; Abbe and Montgomery, 2003; Pettit and Naiman, 2006). Vegetation can also help reduce flood risk by extracting flow energy through process drag, adding adequate boundary flow resistance, and finally, lowering the channel conveyance (Nepf et al., 2007). In this way, the vegetation cover can control the flood risk, and sediment dynamics and guide the bio-geomorphic succession within the fluvial corridor (Corenblit al., 2009).

The study of the spatiotemporal evolution of fluvial deposits and vegetation cover dynamics within the river corridor primarily depends on field data collected from precisely defined spatial units such as quadrats across floodplains, islands, and bars (Gurnell et al., 2001; Corenblit et al., 2009). The availability of geospatial data sets such as high-resolution air photographs (Zanoni et al., 2008) and other airborne data sets (Bertoldi et al., 2011) can provide detailed information even for a large area, which is a significant advantage over ground observations. In addition, laboratory experiments (Coulthard, 2005; Tal and Paola, 2010) and developed numerical modelling (Millar, 2005; Camporeale and Ridolfi, 2006; Perona et al., 2009; Crosato

and Samir Saleh, 2011) are frequently used to assist researchers in understanding the importance of flow-vegetation interaction and its role in morphological evolution. The application of remote sensing in mapping and quantifying these vegetation dynamics in a larger riverscape at an unparalleled spatiotemporal scale can support the fluvial geomorphologist to properly plan and manage large river corridors (Boothroyd et al., 2021). The in-stream/riparian vegetation on the fluvial deposits and floodplain of a large braided river is regarded as an inseparable unit (Harvey and Gooseff, 2015). The fluvial dynamics and bio-geomorphological processes can be better explained with remote sensing data as they can provide better insight into these aspects (Henshaw et al., 2013).

To monitor the vegetation dynamics, the normalized difference vegetation index (NDVI) is the widely used spectral index in diverse ecosystem studies (Fu & Burgher, 2015; Kim et al., 2015). NDVI is an extensively used indicator for detecting the spatiotemporal trend of in-stream/riparian vegetation in large rivers (Bertoldi et al., 2011; Henshaw et al., 2013; Yi et al., 2019; Han et al., 2020; Boothroyd et al., 2021). Thus, in this study, the NDVI data was accessed via Google Earth Engine (GEE), which has access to petabytes of remotely sensed Earth observation data (Gorelick et al., 2017). GEE makes it possible for more purposeful geomorphological assessments at better spatial resolutions, over larger spatial extents, and at finer temporal resolutions (Boothroyd et al., 2021). GEE has previously been used on a large scale in studies such as river planform dynamics (Tobón-Marín and Caón Barriga, 2020), flood risk management by integrating Synthetic Aperture Radar (SAR) imagery for event scale flood detection (DeVries et al., 2020), flood risk index mapping (Phongsapan et al., 2019), etc. GEE has not yet been used much to examine the effectiveness of sediment and vegetation in channel conveyance.

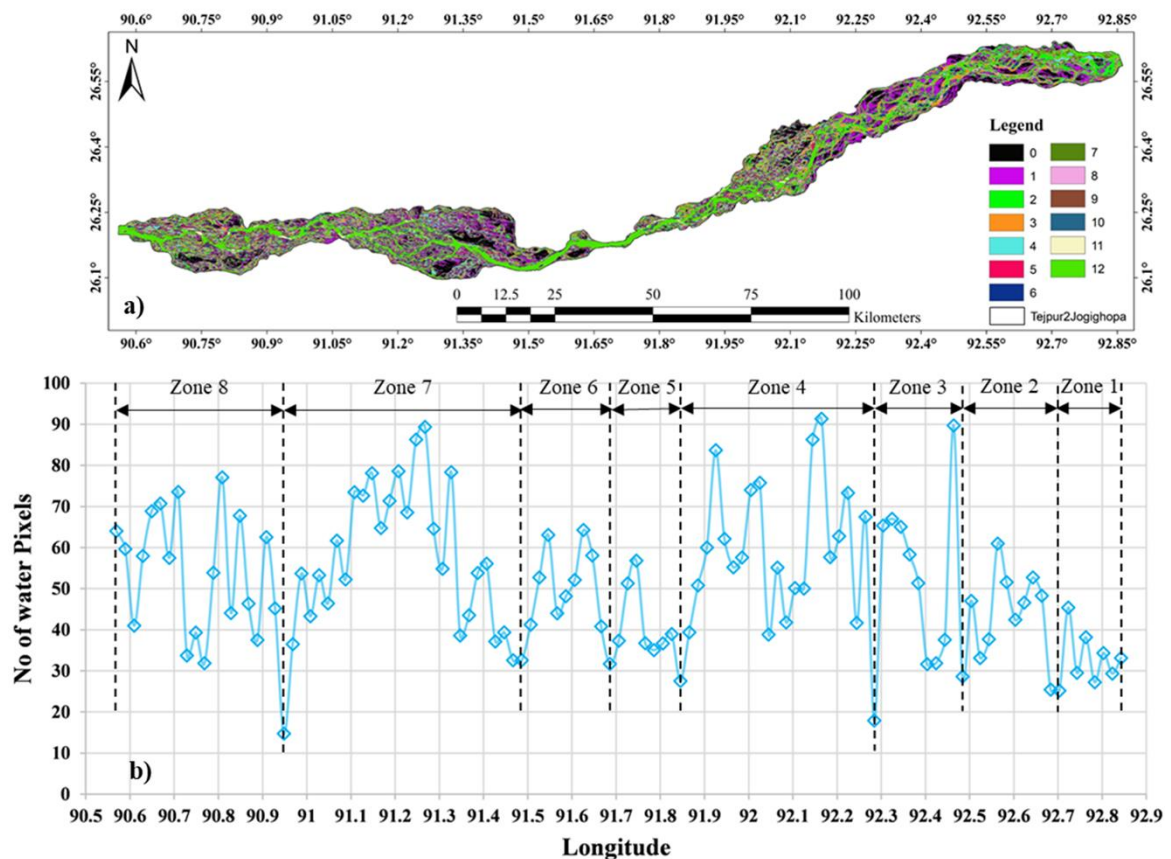
The Brahmaputra River is one of the world's most intricately braided river systems, with high morphological activity due to large flow-sediment variability (Goswami, 1985; Sarma, 2005; Nandi et al., 2021, 2022). Millions of people rely on the river for a living, such as agriculture, and their socioeconomic status has been significantly affected as a result of the river's morphological changes. Furthermore, people use not only the floodplain but also the fluvial deposits or sandbars for agricultural purposes (Talukdar et al., 2020) due to its fertile nature, causing these

bars to become stable over time (Best et al., 2007). Every year, a large part of the flood plain, as well as the sandbar deposit of the river, get eroded or disturbed by flood, leading to an alteration of the river's planform (Archana et al., 2012). There has been very limited research on the riverine ecosystem of the Brahmaputra, which is the motivation for this study.

### **4.3 DATA AND METHODS**

#### **4.3.1 Identification of zone-wise braided reach with reference to the local nodal point**

In this chapter, the same study area has been used as in chapter 3. Further, this study utilizes a variety of geo-informational data due to the nature of the work. The data set covers a range of spatiotemporal Landsat imageries that were downloaded and processed using the Google Earth Engine (GEE) platform and advanced geospatial techniques. To initiate, the high-resolution global surface water map (Pekel et al., 2016) was used to prepare the seasonal water availability in the selected braided reach. Pekel et al. (2016) developed high-resolution global surface water maps based on almost three million Landsat satellite images (over 32 years of data), considering historical changes in global water occurrences. Figure 4.1 (a) depicts seasonal water availability, where 0 indicates that there was no water in the channel even for a single month, and 12 indicates that there was water in the channel throughout all months. The spatial water pixels were calculated based on this information, and the locations with low values were identified as local nodes; thus, different zones within the study reach can be identified, as shown in Figure 4.1 (b). In the zones, lengths varied from 20 to 55 km, with complex braided planforms. Every zone has a distinct behaviour based on the braided activity that occurs within its available space (i.e "erodible corridor" (Piégay et al., 2006) or "fluvial territory" (Ollero, 2010)). Furthermore, zone-wise braided characteristics have been investigated through the identification of geomorphic units as well as process-based assessments.



**Figure 4.1** Zonal classification of the study reach using the Joint Research Centre (JRC) surface water dataset; a) monthly water occurrence in the channel with color coding from 0 to 12 (0 for no water, and 12 for water occurrence throughout the year i.e. 12 month); b) no of water pixels counted through the braided belt in the study reach (lowest count considered as the local nodal point)

#### 4.3.2 Morphological assessment of the braided reach within the selected study area

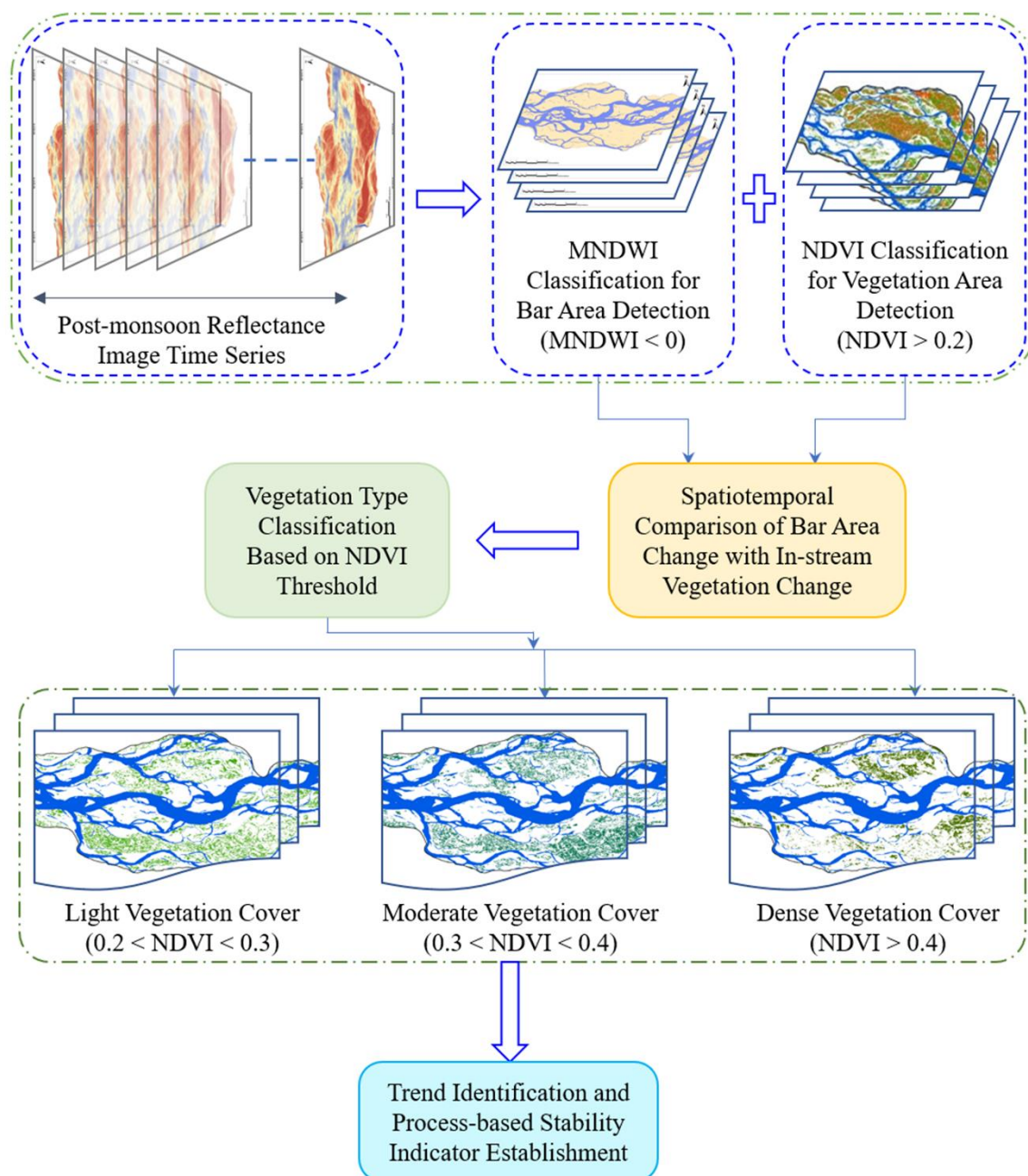
The atmospherically corrected and orthorectified surface reflectance from Landsat 5 ETM, 7 ETM+, and 8 OLI/TIRS sensors are accessible by using GEE (Boothroyd et al., 2021). For the given study period (1990 to 2019), these datasets were used to derive the seasonal Normalized Difference Vegetation Index (NDVI) and Modified Normalized Difference Water Index (MNDWI) time series. The methodological flowchart for the analysis used in this study is illustrated in Figure 4.2. Cloud-free satellite imagery was mostly accessible for the selected reach during lean periods. It has also been observed that the river is highly active in terms of morphological behavior during this period (Chemolu and Dutta, 2018). Therefore,

satellite images for the post-monsoon period were downloaded (October, November, and December) and processed. Each year, there were approximately 10 to 15 images available per season, and these images were statistically processed to create one median image. Reflectance images in green, red, and NIR bands of the electromagnetic spectrum from corresponding days of the acquisition were used to compute NDVI (eq. 4.1) (Rouse et al., 1973), and MNDWI (eq. 4.2) (Xu, 2006) derivative images by using the following equations:

$$NDVI = \frac{NIR-R}{NIR+R} \quad (4.1)$$

$$MNDWI = \frac{Green-SWIR}{Green+SWIR} \quad (4.2)$$

Where, NIR represents the near infrared, R represents the red, green represents the green band, and SWIR represents the short-wave infrared for respective Landsat imageries. MNDWI was utilized to identify the sandbar area. The threshold value of 0 has been used for MNDWI, below which the feature was identified as sandbar (Xu, 2006). NDVI was used to detect the vegetation cover as it has been shown to be responsive to the low-density vegetation type found in active braided river corridors (Bertoldi et al., 2011). A threshold of 0.2 has been used above which all the features were identified as active vegetation cover (Bertoldi et al., 2011).

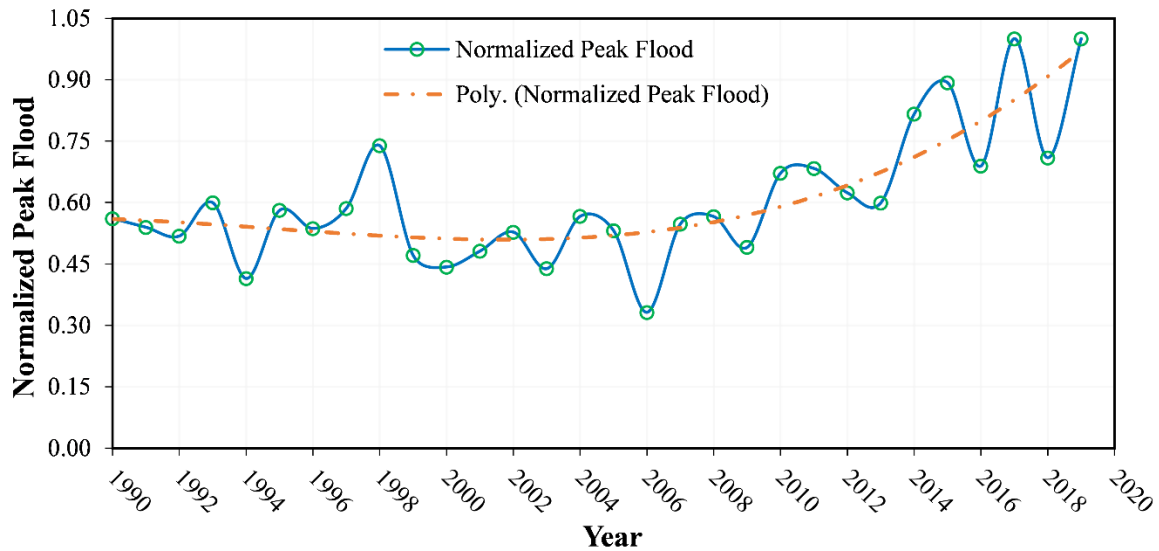


**Figure 4.2** Methodological framework used for calculation of Modified Normalized Differenced Water Index (MNDWI) and Normalized Differenced Vegetation Index (NDVI).

### 4.3.3 Hydrological data preparation

The hydrological data, such as daily discharge data, has been observed regularly by the Central Water Commission (CWC) of India. These data have been utilized in this study to understand the process behavior of braiding activities. The peak flood discharges, which are primarily responsible for various activities such as

erosion deposition, thalweg shifting, active channel alteration etc., have been analyzed. Figure 4.3 depicts the normalized peak flood for the Brahmaputra river during the study period. Peak flood discharges have shown an increasing trend in recent decades (2010-2019), as depicted in Figure 4.3. The effect of increased discharge on process-form alteration within the study reach is discussed later in this chapter.



**Figure 4.3** Variation of normalized peak discharge for last three decades (1990 – 2019).

#### 4.3.4 Formulation of process-based indicator for identification of stability trajectory of the reach

Large braided rivers like the Brahmaputra are characterized by mobile/immobile bars, large islands, and nodal points, which leads to complex planform configuration (Chembolu and Dutta, 2018). According to Roza et al. (2012), vegetation plays an essential part in stabilizing the reach because dense forests colonize different species and develop the island, which facilitates the consolidation of the soil. A factor called stabilizing indicator (SI) had been proposed, considering that the moderate and dense vegetation cover is accountable for stabilizing the bar. SI was proposed by calculating the percentage of cover encroached by moderate and dense vegetation in a given year. Furthermore, the yearly change in SI has been evaluated to define the change in stabilizing indicators (CSI). Additionally, the yearly change in peak discharge (CPD) has been evaluated as a disturbing factor for

vegetation growth. Finally, both CPD and CSI have been used to develop a new process-based indicator called stability trajectory indicator (STI), which is given in Eq. 4.3.

$$STI = \frac{CPD-CSI}{CPD+CSI} \quad (4.3)$$

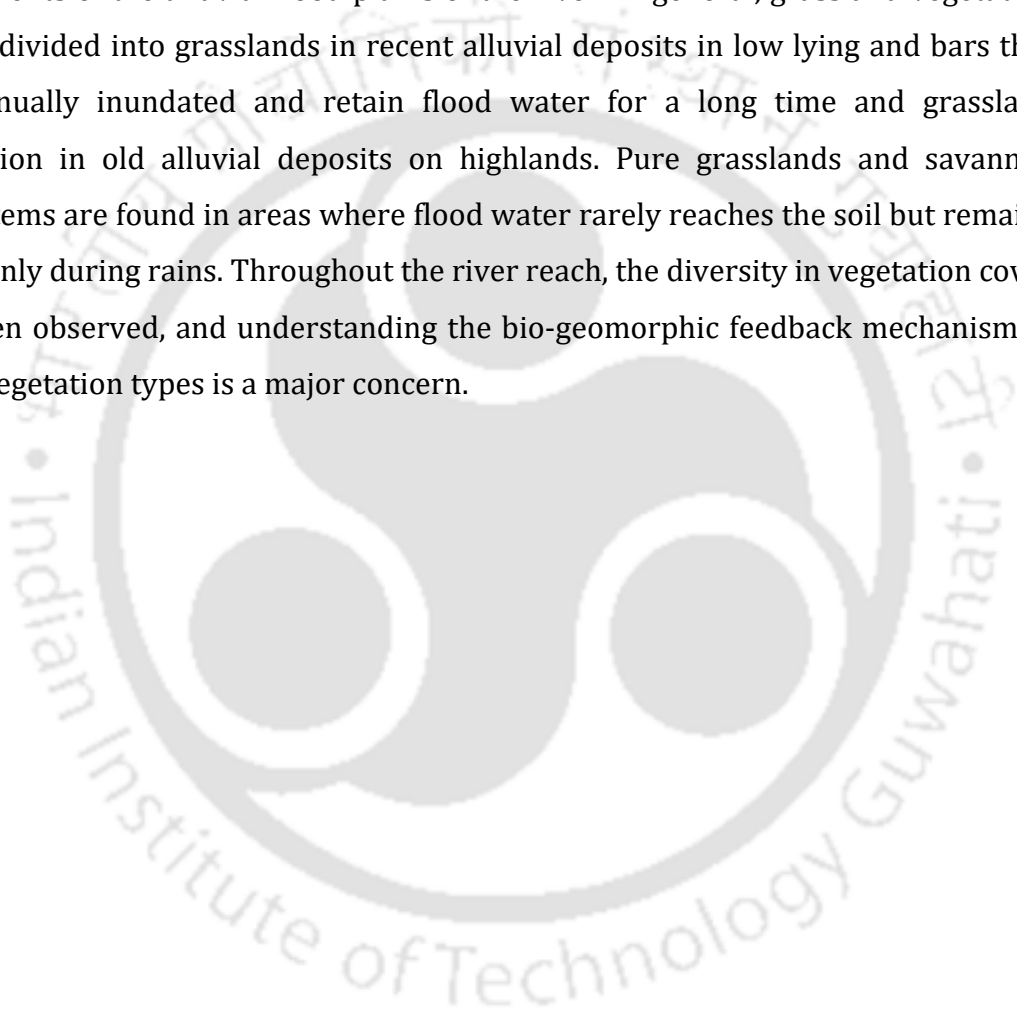
The novel index STI is compared to another parameter called morphological instability (MI). MI reflects the proportional change in sandbar area with respect to the maximum occupancy of the yearly percentage change. The analysis was carried out to determine the stability trajectory of the reach.

### 4.4 RESULTS AND DISCUSSION

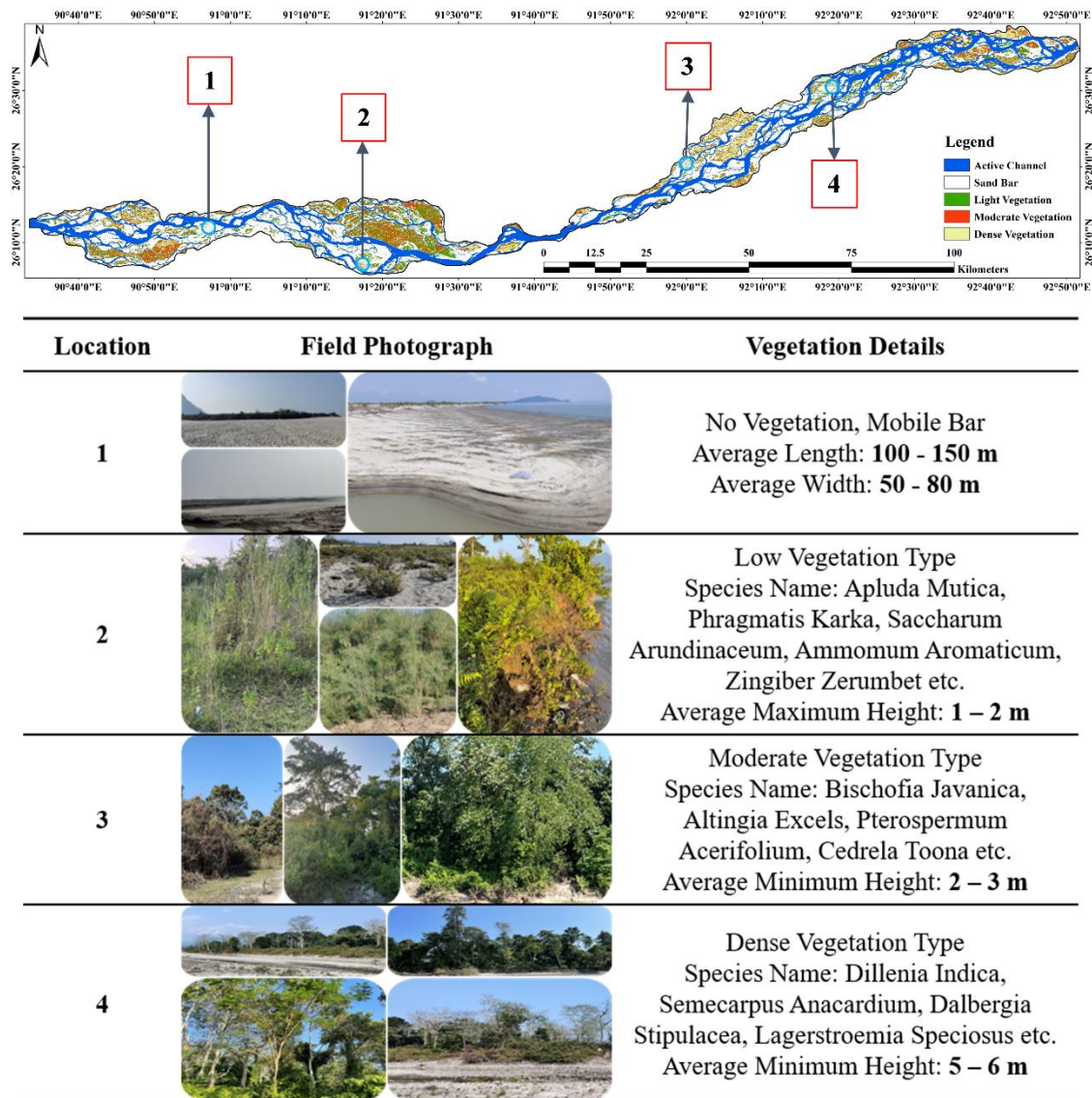
#### 4.4.1 Bio-geomorphic characterization of Brahmaputra river

The principal plant communities found in the Brahmaputra basin are classified as Moist Evergreen and Semi-Evergreen Forest, Moist and Dry Deciduous Forest, Hydrophytes in wide lengths of wetlands (riparian belts, swamps, and marshes), Bamboo brakes, Scrubland, and Grass Land (both wet and dry) (Srivastava et al., 2002). There is a huge concentration of tropical vegetation and extensive riparian forest along the river banks and braid bars. The diversity in plant communities and forest variety is driven mostly by varying physiographic, edaphic, and climate circumstances. Riverine vegetation is extremely dynamic, serving as an interface between terrestrial and aquatic habitats. These vegetations are mostly of a type that develops in the evergreen and semi-evergreen zones along river banks as well as over the sandbars under the influence of a waterway (Basumatary et al., 2021). A series of field surveys were conducted to collect vegetation information along the middle reach of the Brahmaputra River. Figure 4.4 was prepared on the information collected from the survey and highlighted the plant types along the River corridor. Commonly found species in these areas are *Dillenia indica*, *Anthocephalus indicus*, *Albizia lebbek*, *Bischofia javanica*, *Duabanga grandiflora*, *Bombax ceiba* etc. and these are of dense type forest. The middle storey of these forests is occupied by the species like *Albizia lucida*, *Alstonia scholaris*, *Dalbergia assamica*, *Pterospermum acerifolium* etc. Furthermore, it has been observed that the ground vegetation types are covered by the species like *Alpinia nigra*, *Lasia spinosa*, *Ammomum aromaticum*, *Carex breviculmis*, *Typha elephantina*, *Zingiber zerumbet*, etc. Every year, the seasonal flood

submerges these forests through some inches, resulting in new alluvium and consecutive silt deposits (Borah et al., 2015). These are first colonized by Tamarix and Salicornia seedlings, which expect to make themselves in a dense form, either in pure form or combined with other grassy species (Borogayary et al., 2018). It has been reported that the bare land, in terms of natural vegetation, is colonized by three categories: scrubland, grassland (savanna, grasslands, and steppes), and forests (Dikshit and Dikshit, 2014). Grassland and Savannahs are one of the dominant components of the alluvial flood plains of the river. In general, grassland vegetation can be divided into grasslands in recent alluvial deposits in low lying and bars that are annually inundated and retain flood water for a long time and grassland vegetation in old alluvial deposits on highlands. Pure grasslands and savannah ecosystems are found in areas where flood water rarely reaches the soil but remains moist only during rains. Throughout the river reach, the diversity in vegetation cover has been observed, and understanding the bio-geomorphic feedback mechanism of these vegetation types is a major concern.



## VEGETATION AND ITS IMPACT ON STABILITY CRITERIA



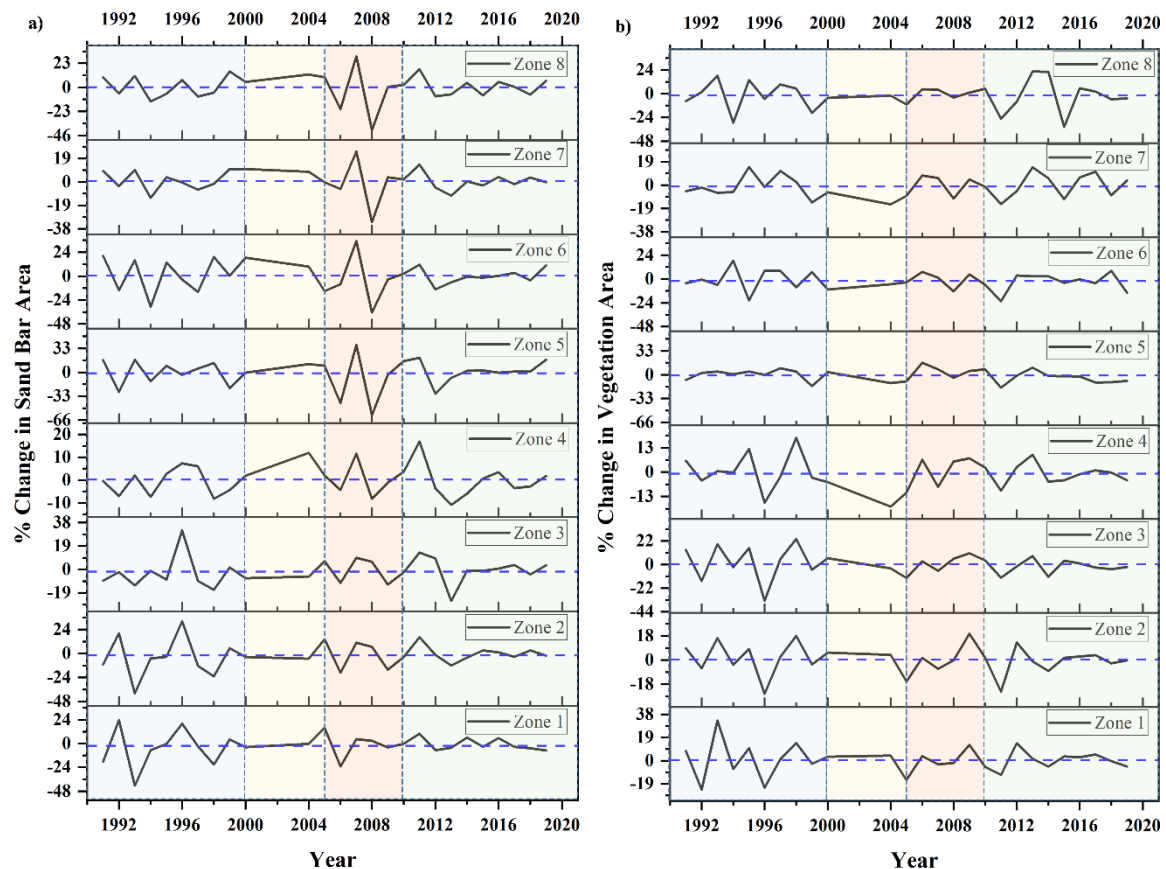
**Figure 4.4** Field photographs of instream-vegetation cover observed in the selected study reach of Brahmaputra river.

### 4.4.2 Spatio-temporal sandbar and in-stream vegetation dynamics within the river corridor in terms of erosional and depositional activity

The vegetation within the river corridor actively participates in the hydro-geomorphic process, acting as semipermeable membranes regulating energy and matter flow (Naiman and Decamps, 1997). In-stream vegetation during the spring and summer months is prevalent in nutritionally chalk streams and influences the in-stream ecosystem by interacting with river flows and trapping sediments (Cotton et al., 2006). Consequently, the changed sedimentation processes in the river and its

floodplains were affecting flood mitigation measures at the local level. The vegetation scenario of the river system is therefore influencing the erosion and deposition processes in the river corridor. We tried to comprehend the spatiotemporal erosion/deposition activity prior to actually linking the vegetation dynamics to the morphological response of the river. The percentage change in sandbar area for the last 30 years (1990-2019) has been analyzed for each zone of the study reach and demonstrated in Figure 4.5a. The positive scale represents the net erosion in that zone for a particular year, while the negative scale represents the net depositional activity. After a comprehensive assessment, four distinct time periods have been identified, notably 1990-2000, 2000-2005, 2005-2010, and 2010-2019, each with a distinct process characteristic. During the first phase (1990-2000), the cyclic erosion-deposition process could be seen with a larger magnitude, especially in the zones upstream of Guwahati (Tezpur to Guwahati). For the second time slice (2000-2005), a specific process behavior with a lower magnitude was observed. Most of the zones showed erosional behavior, except for zone 2 and 3, which displayed minimal depositional behavior. However, in the third time slice (2005-2010), a sudden increase in magnitude was seen, particularly in the zones downstream of the Guwahati (Guwahati to Jogighopa), whereas the other zones exhibited essentially identical behavior as in the first time slice. This could be due to the extreme flood event observed in 2004-05, which generated a huge sediment wave and triggered erosion/deposition activity as the wave dissipated within the system over time (Dubey et al., 2021). Finally, for all zones except zone 4, a gradual weakening of the erosion/deposition process was observed in the fourth time slice (2010-2019). In spite of the increase in discharge, a significant reduction in erosion/deposition occurred during this period which is unusual. This implies that the vegetation cover over the sandbars plays an important role in regulating the erosion/deposition process (Henriques et al., 2021). The net erosional/depositional behavior for the individual zones was in the sequence of Zone 7 > Zone 6 > Zone 8 > Zone 4 > Zone 5 > Zone 3 > Zone 2 > Zone 1. Among all the zones observed in the last three decades, Zone 7 showed the most active reach for morphological behaviors. Furthermore, zone 5 had no significant erosion or deposition because it is mainly constrained by a non-erodible stable bank configuration. The braided belt width variation at this zone is observed to be 1 to 2 km due to its proximity to the physiographic nodal point

(Chembolu and Dutta, 2018). While zone 7 has a higher mobility space for braiding activity with a braided belt variability of 4 to 16 km (Chembolu and Dutta, 2018; Nandi et al., 2022), this could be one of the reasons for the zone having the highest morphological activity. Furthermore, vegetation growth over the sandbars implies that the bars may have stabilized and regulated the erosion/deposition process.



**Figure 4.5** Variation in annual percentage change of a) sandbar area; b) vegetation cover area for the study period (1990-2019) in the selected reach of Brahmaputra river.

The in-stream vegetation cover over the sandbar area has been detected through NDVI classification ( $NDVI > 0.2$ ) using GEE platform. Further, the NDVI detected vegetation pixel area has been calculated for the entire reach as well as for different zones. The percentage change in vegetation area for the study period (1990 to 2019) was examined to better understand the process dynamics of the study reach owing to vegetation cover and illustrated in Figure 4.5b. The percentage change in the vegetation area exhibited nearly identical behaviour as of the percentage change in the sandbar area. In the case of vegetation cover change analysis, the same four

distinct time periods were observed, such as 1990-2000, 2000-2005, 2005-2010, and 2010-2019. During 1990-2000, there was a significant erosion and growth/succession of vegetation area for all the zones except zone 5. As discussed, zone 5 is located at the nodal point and has no significant size bar formations; as a result, there were no substantial vegetation covers present. A considerable size bar is essential to creating a pioneer plant community that further colonizes the sediment deposits. Subsequently, this leads to the accretion of the river bank and further conversion of these deposits to new islands (Asahi et al., 2013; Bertoldi et al., 2014; Wintenberger et al., 2015). For example, Gurnell et al., 2001 discussed that the bare sandbar is first inhabited by different plant species and may evolve into a bigger vegetated patch.

Furthermore, sediment entrapment and plant root reinforcement elevate the sandbar, resulting in pioneer landforms that eventually consolidate into larger islands. For all zones, the second time period (2000-2005) showed a consistent characteristic of either reduction or growth in vegetation area. It is an intriguing observation, and it might be due to the absence of major flooding during those years. From 2005 to 2010, some cyclical behavior in erosion and growth of vegetation was observed, the magnitude being greater in the upstream reach (Tezpur to Guwahati) than in the downstream of Guwahati. There was no such significant change in the vegetation area in the zones downstream of Guwahati. It was observed that the major flooding occurred in 2004-05, which may have caused changes in the upstream region and dissipated flow energy but had no significant impact in the downstream region. Further, due to the planform dynamics and vegetation arrangements, the flow with the high energy propagates as well as stored within the system (Gurnell, 2014; Karmaker et al., 2017). This stored energy is then utilized within the system to alter the planform, and in-stream vegetation configurations serve a crucial role in this process (Corenblit et al., 2007).

Finally, for the most recent period (2010-2019), the change in vegetation area was minimal for all zones except zones 7 and 8. The larger bars were located in zones 7 and 8, which facilitate the vegetation colonization, which was reflected in Figure 4.5b. These zones experienced a net vegetation succession in the recent decade, which may be the cause of bar elongation in those zones. Vargas-Luna et al. (2019) described

a similar mechanism of bar elongation caused by the accumulation of entrapped sediments as a result of vegetation colonization on the bar surface. During the floods, sandbars of varying sizes in the study area are subject to erosion/deposition, and vegetation cover scenario over these bars actively regulates this process (Tabacchi et al., 2005). Sporadic flow permits vegetation succession between the floods; further, the flow-vegetation interaction could regulate the morphodynamics of the river. However, because the timescale of plant growth is slower than that of flood recurrence, vegetation establishment is governed by the intensity of flow and the energy associated with it (Crouzy et al., 2014). Fielding et al., (1997) reported that the in-channel growth of different plant species altered the system environment, ensuring their survival by deviating from the flow. This promotes sediment deposition, which establishes favourable circumstances for seedling germination and growth (Tooth and Nanson, 2000).

### **4.4.3 Interpretation of vegetation dynamics through NDVI based classification of different type and its trend analysis**

It has been noted that the presence of various types of instream/riparian vegetation can provide bank stabilization, improve stream bank cohesiveness, and enable the formation of various planforms (Polvi et al., 2014; Gibling et al., 2014). Therefore, the erosion and growth/succession of the plants is one of the major concerns in understanding the planform evolution in the braided systems. The vegetation cover area has been determined by using NDVI thresholds (Bertoldi et al., 2011; Henshaw et al., 2013) and further classified into three different types light vegetation cover ( $0.2 > \text{NDVI} < 0.3$ ), moderate vegetation ( $0.3 > \text{NDVI} < 0.4$ ) and dense vegetation cover ( $\text{NDVI} > 0.4$ ) as per the ergodic reasoning. This investigation was carried out to better understand the variety of plant cover that exists within reach and its relevance in the river's morphodynamics. While light vegetation covers were destroyed during higher magnitude floods, mature vegetation offers resistance to the flow, interacts with it, and establishes sandbar stability. Figure 4.6 depicts the annual vegetation cover for the three major vegetation types in terms of the percentage share of total vegetation area for different zones.

VEGETATION AND ITS IMPACT ON STABILITY CRITERIA

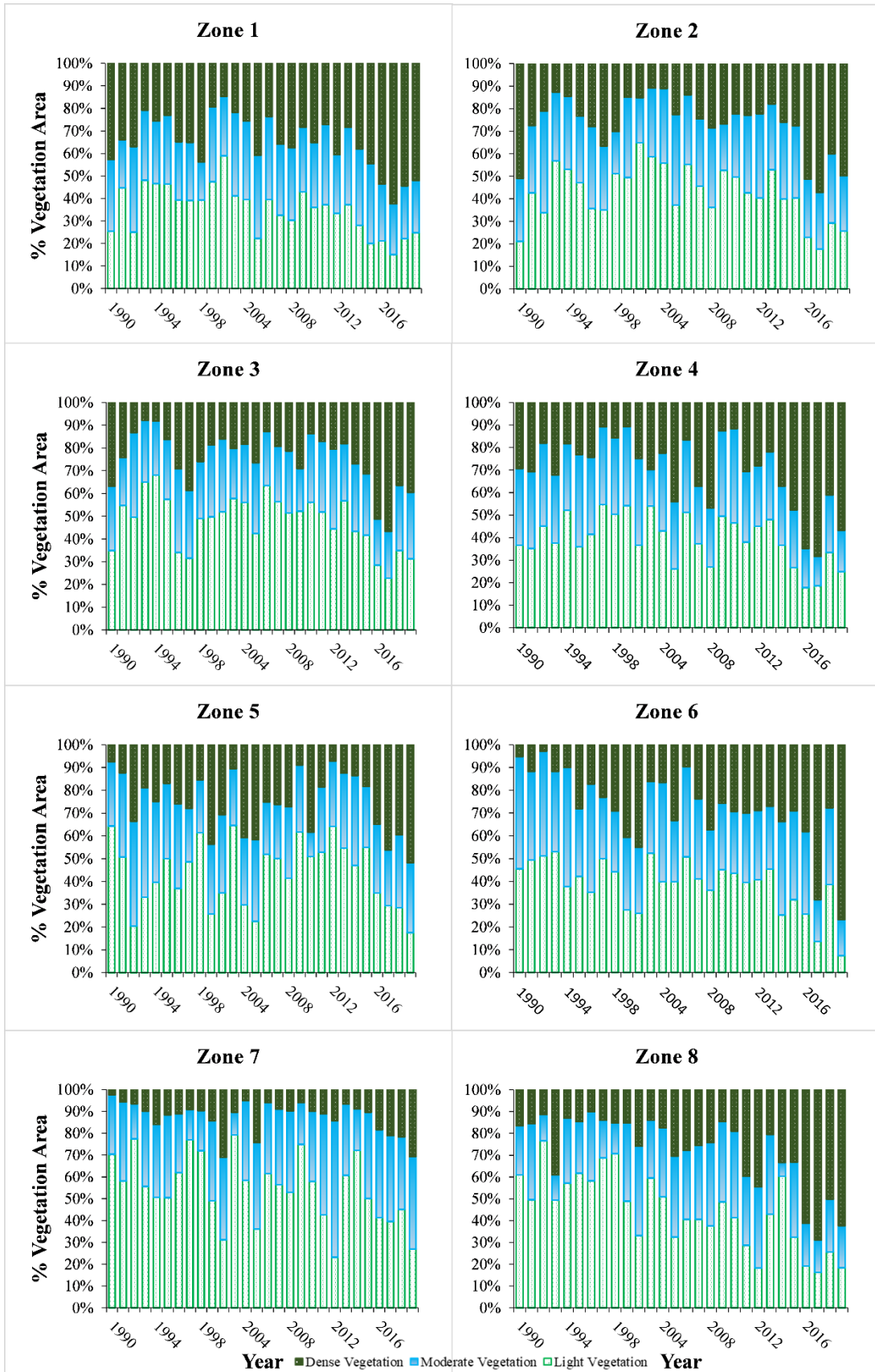


Figure 4.6 Annual vegetation cover area sharing for three different type (light, moderate and dense) of vegetation in the selected study reach (1990-2019).

It is obvious that the light vegetation area was decreasing with time since it is eroded during floods in almost all zones. The moderate vegetation cover was more or less the same during the study period. The percentage sharing of moderate vegetation cover was seen to be lower in some years, while the percentage sharing of dense vegetation cover was higher in those years. The most likely explanation is that some plant species (moderate type) grew and progressively transformed into dense vegetation with time. Furthermore, as illustrated in Figure 4.6, dense vegetation cover increased with time and seemed to be significant in nearly all zones. The vegetation that developed over the sandbars and matured over time contributed to the bar's stability (immobility) and the morphodynamic process of the river (Rozo et al., 2012; Asahi et al., 2013; Wintenberger et al., 2015).

A statistical trend analysis was performed to have a stronger insight into these vegetation reduction/growth patterns (Figure 4.7). Güçlü (2020) created an improved method for Sen-innovative trend analysis (ITA) that was employed in this investigation. The detailed procedure to perform this modified ITA has been discussed in the article published by Güçlü (2020). The analysis revealed that the light vegetation cover is declining with a negative 2.81 percent trend across the whole study reach. At the same time, the moderate and dense vegetation types showed a positive monotonic trend of 21.13 percent and 89.44 percent, respectively. Furthermore, the Pettit change point test was applied to the data series, and change points for light, moderate, and dense vegetation cover were observed in 2015, 2004, and 2010, respectively. The detailed comparison of trend analysis for the full reach as well as for different zones has been given in the following tables (Table 1, 2 and 3).

**Table 4.1** Detail statistic table of trend analysis for different zones for the case of light vegetation type.

		Light Vegetation								
Zone		Zone 1	Zone 2	Zone 3	Zone 4	Zone 5	Zone 6	Zone 7	Zone 8	Full Reach
<b>Mann Kendall Test</b>	<b>Kendall's tau</b>	-0.35	-0.06	-0.35	-0.37	-0.04	0.03	-0.05	-0.29	-0.21
	<b>S</b>	-153.00	-25.00	-153.00	-161.00	-19.00	13.00	-22.00	-127.00	-93.00
	<b>Var(S)</b>	3139.67	3139.67	3139.67	3139.67	3139.67	3139.67	3140.67	3139.67	0.00
	<b>p-value (Two-tailed)</b>	0.01	0.67	0.01	0.00	0.75	0.83	0.71	0.02	0.10
	<b>alpha</b>	0.05	0.05	0.05	0.05	0.05	0.05	0.05	0.05	0.05
	<b>Sen's Slope</b>	-0.25	-0.05	-0.35	-0.80	-0.01	0.01	-0.23	-0.68	-0.30
	<b>Remark</b>	Significant trend	No significant trend	Significant trend	Significant trend	No significant trend	No significant trend	No significant trend	Significant trend	No significant trend
	<b>Pettitt Change Point Test</b>	2011	2015	1997	2001	1995	2008	2015	2009	2015
<b>Improved ITA (Güçlü, 2020)</b>	<b>High Value Trend (%)</b>	-28.96	-13.84	-11.28	-15.79	5.78	-18.16	3.47		-10.16
	<b>Low Value Trend (%)</b>	-11.45	12.25	-20.75	-28.92	-24.13	16.73	14.10	-20.34	-2.82

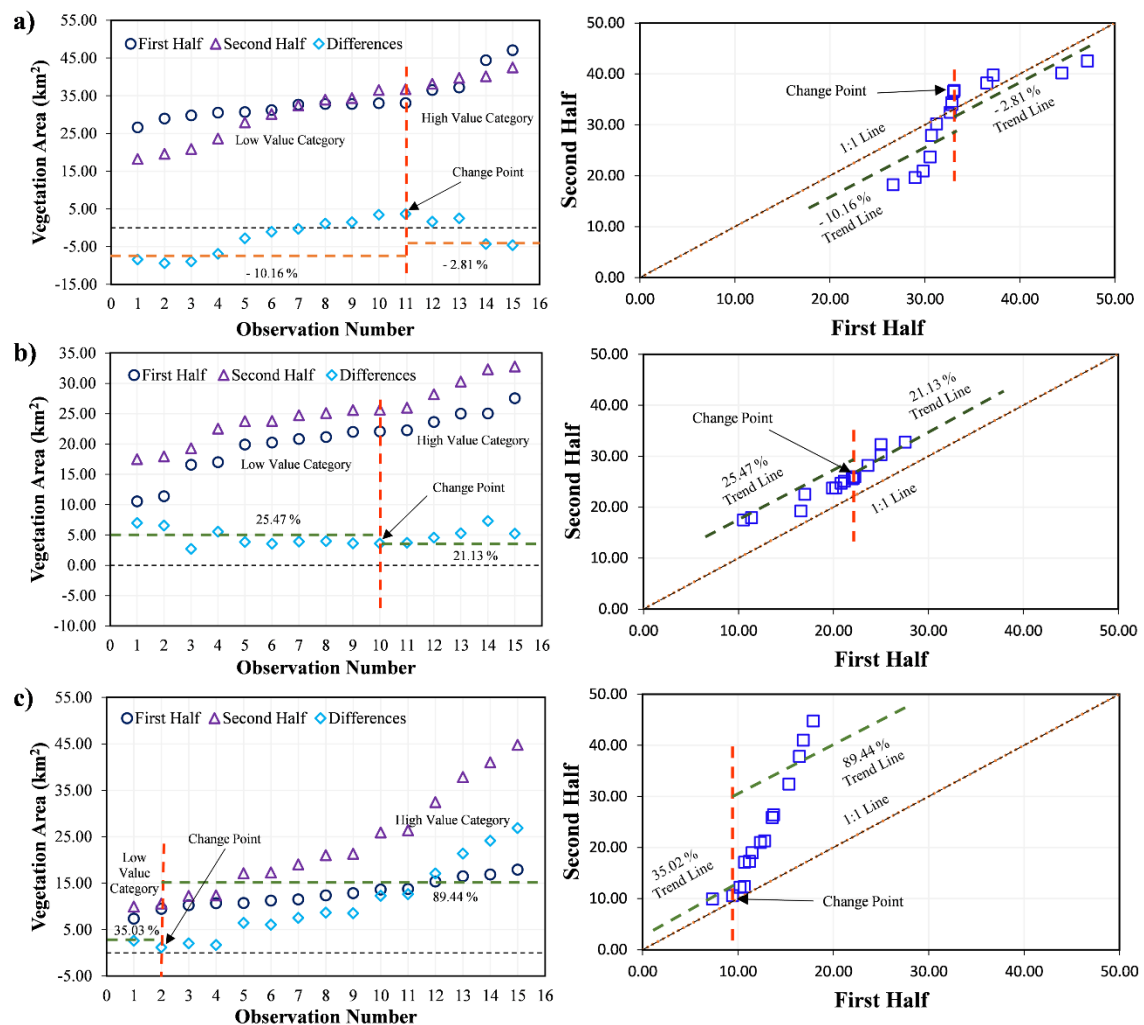
**Table 4.2** Detail statistic table of trend analysis for different zones for the case of moderate vegetation type.

		<b>Moderate Vegetation</b>								
<b>Zone</b>		<b>Zone 1</b>	<b>Zone 2</b>	<b>Zone 3</b>	<b>Zone 4</b>	<b>Zone 5</b>	<b>Zone 6</b>	<b>Zone 7</b>	<b>Zone 8</b>	<b>Full Reach</b>
<b>Mann Kendall Test</b>	<b>Kendall's tau</b>	-0.01	0.05	-0.08	-0.50	-0.16	0.12	0.31	0.32	0.19
	<b>S</b>	-5.00	21.00	-35.00	-215.00	-71.00	54.00	135.00	137.00	81.00
	<b>Var(S)</b>	3139.67	3139.67	3139.67	3139.67	3139.67	3140.67	0.00	3139.67	0.00
	<b>p-value</b>	0.94	0.72	0.54	0.00	0.21	0.34	0.02	0.02	0.16
	<b>(Two-tailed)</b>									
	<b>alpha</b>	0.05	0.05	0.05	0.05	0.05	0.05	0.05	0.05	0.05
	<b>Sen's Slope</b>	-0.01	0.03	-0.11	-0.74	-0.03	0.04	1.25	0.82	0.11
	<b>Remark</b>	No significant trend	No significant trend	No significant trend	Significant trend	No significant trend	No significant trend	Significant trend	Significant trend	No significant trend
	<b>Pettitt Change Point Test</b>	2015	2004	1997	2010	1996	2010	2004	2004	2004
<b>Improved ITA (Güçlü, 2020)</b>	<b>High Value Trend (%)</b>	1.75	17.88	-1.50	-21.32	-21.46	10.22	70.08	119.67	25.47
	<b>Low Value Trend (%)</b>	16.45	15.83	-36.32	-15.89	-10.11	20.79	38.68	29.86	21.13

**Table 4.3** Detail statistic table of trend analysis for different zones for the case of dense vegetation type.

		<b>Dense Vegetation</b>								
<b>Zone</b>		<b>Zone 1</b>	<b>Zone 2</b>	<b>Zone 3</b>	<b>Zone 4</b>	<b>Zone 5</b>	<b>Zone 6</b>	<b>Zone 7</b>	<b>Zone 8</b>	<b>Full Reach</b>
<b>Mann Kendall Test</b>	<b>Kendall's tau</b>	0.32	0.26	0.22	0.22	0.09	0.64	0.34	0.65	0.37
	<b>S</b>	141.00	112.00	95.00	95.00	39.00	280.00	148.00	281.00	159.00
	<b>Var(S)</b>	3139.67	3140.67	3139.67	3139.67	3139.67	3140.67	3140.67	3139.67	0.00
	<b>p-value (Two-tailed)</b>	0.01	0.05	0.09	0.09	0.50	< 0.0001	0.01	< 0.0001	0.00
	<b>alpha</b>	0.05	0.05	0.05	0.05	0.05	0.05	0.05	0.05	0.05
	<b>Sen's Slope</b>	0.23	0.34	0.21	0.98	0.02	0.42	0.67	1.97	0.53
	<b>Remark</b>	Significant trend	Significant trend	No significant trend	No significant trend	No significant trend	Significant trend	Significant trend	Significant trend	Significant trend
<b>Pettitt Change Point Test</b>		2015	2013	2013	2013	2015	2007	2014	2004	2010
<b>Improved ITA (Güçlü, 2020)</b>	<b>High Value Trend (%)</b>	70.11	93.85	28.18	3.92	-9.80	72.78	73.81	201.15	35.03
	<b>Low Value Trend (%)</b>	12.09	53.34	30.40	83.30	45.82	172.23	35.87	356.25	89.44

## VEGETATION AND ITS IMPACT ON STABILITY CRITERIA



**Figure 4.7** Trend analysis of the different types of vegetation cover; a) light vegetation; b) moderate vegetation; c) dense vegetation, for the last three decades (1990-2019) using the improved, innovative trend analysis (ITA) adopted from Güçlü (2020).

The stabilizing features of vegetation indicate an increase in sediment cohesiveness and a decrease in flow erosivity, thereby addressing the erosive influence of vegetation colonization (Tooth et al., 2008). Nandi et al., (2022) supported the fact that some of the zones (downstream of Guwahati) exhibit a constant frequency of a particular class of immobile bar with respect to size and location across all the years, with the only change being its surface area. Any modifications to the smaller (mobile) bars can influence the reach's disorder, while adjustments to the larger (immobile) bars actually affect the reach's stability criterion. Fast-growing plant species prefer depositional locations with wide surface

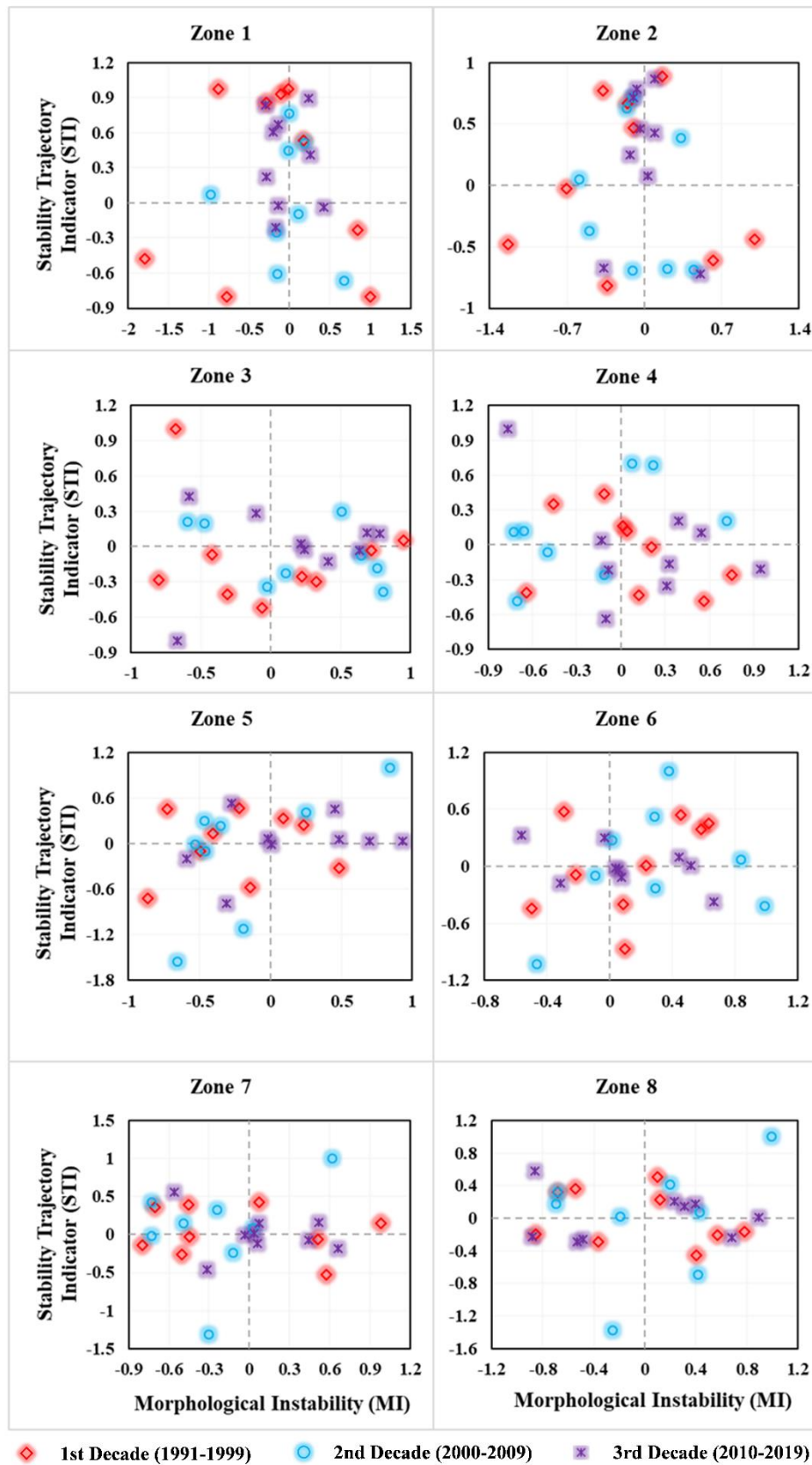
areas exposed to vegetation colonization, such as large immobile bars. Likewise, after the scroll bar is formed, vegetation grows and offers support for soil accumulation and island development. The processes associated with these activities take a long time based on the environmental and climatic conditions for large braided rivers like the Brahmaputra. Combining all, it is possible to state that "the instream morphology in alluvial rivers is a product of flow regime, sediment properties, and vegetation arrangements."

#### **4.4.4 Interpretation of the vegetation type as a stabilizing agent for the sandbars of the braided reach**

For a process-based understanding, the quadrant analysis has been carried out between the STI and MI for all the zones and is illustrated in Figure 4.8. The analysis was carried out with peak flood discharge as the driving/disturbing factor for destabilizing the reach and a combination of moderate and dense vegetation acting as a filter (stabilizing agent). The four quadrants demonstrated different states of the braided reach, such as the 1st quadrant showing amplifier dominance, the 3rd quadrant demonstrating filter dominance, and the remaining two (2nd and 4th quadrants) demonstrating transitional behavior. The total study period was divided into three decades to determine the reach-scale behavior and stability trajectories. For the first decade (1991 to 1999), there was no such particular observation in the data cluster, and it was showing random behavior except Zone 7. Zone 7 was observed to be the most stable zone among all the zones for all three decades. The frequency of larger bars was also seen to be higher in this zone (Nandi et al., 2022) and, therefore, exposed to higher vegetation growth. Zone 8 exhibited similar behavior to Zone 7 but with a little more scatter in the distribution. The second decade (2000 to 2009) was observed to be more scattered as compared to the other two decades for most of the zones. During those years, a series of regular flood waves with longer duration and a lack of significant vegetation growth has been observed. However, in the last decade (2010 to 2019), the cluster was observed to be around either of the axes, indicating comparable stability in the reach instead of a significant increase in flood peaks during this period. The vegetation changes were also observed to be almost constant during this period, suggesting that there is a substantial mature vegetation patch in most of the reach, which aids in the stability of the reach. Furthermore, it should be noted that

the formation of stable island bars is a time-consuming process that begins with bare substrate and progresses to pioneer shrublands, then to pioneer forest land, and finally to mature forests (Van Andel et al., 1993). Hence, the peak discharge may not show a sudden impact because the age of the vegetation also plays a part in the process. During the three decades, none of the zones displayed highly unstable behavior, and the majority of them displayed transitional behavior.

It has been evident that the type of vegetation may have a profound impact on the morphodynamics of the reach. According to Corenblit et al. (2007), the stages of vegetation inheritance in a river corridor are first vegetation recruitment, then vegetation establishment, and finally, vegetation succession. It becomes more intricate as the natural river system exhibits disturbance patch dynamics, suggesting that vegetation succession is a function of spatiotemporal variation in hydrogeomorphic mechanisms and fluvial formations (White, 1985). The trend analysis revealed, in particular, that during the study period, the moderate and dense vegetation type was most efficient and may actively participate in the river's morphological activity. One possibility proposed here is that the moderate and dense vegetation cover has a combined impact on stabilizing the sandbar over which it grows. Therefore, in this study, the combination of moderate and dense vegetation cover is considered a stability indicator of the reach. Furthermore, during flood occurrences, the arriving discharge has higher flow energy, which might destroy the vegetative cover and expose the bars to erosion (Chembolu and Dutta, 2018). As a result, during floods, the light vegetation cover possibly gets eroded, whereas moderate and dense vegetation cover obstructs and interacts with the flow, dissipating a significant amount of energy.



**Figure 4.8** Quadrant analysis showing the stability trajectory of different zones along the three decades (1990-2019).

The bars having large vegetation cover of moderate and dense type have higher dissipation capacity and are less prone to erosion during floods. Consequently, these bars became more stable over time as the vegetation grew, and it is evident that the vegetation cover and its type played a crucial role in this process (Rozo et al., 2012; Gautier et al., 2021). Yu et al., (2014) stated that the interaction between the hydrologic process and vegetation growth is one of the significant factors influencing channel planform change. There was no such definite temporal trajectory for any of the braided reach. The reason for this could be that a large river like the Brahmaputra responds to a set of hydrogeomorphic constraints such as climatic conditions, moisture availability, degree of fluvial disturbance, anthropogenic stresses, and so on. Previous studies have demonstrated that small (mobile) bars affected the braided reach's disorderness (Chembolu and Dutta, 2018; Nandi et al., 2021), whereas large (immobile) bars affect the reach's stability criteria by allowing vegetation to grow and survive erosion during high floods (Gautier et al., 2021).

Geomorphic systems respond to flooding with qualitative changes, in which minor events produce no significant change, while extreme events may obliterate the system. In general, the geomorphic disturbances are relatively discrete events (temporal scale dependence). The geomorphic disturbances cannot be assessed and understood properly without neglecting the ecological functions and feedback (Rice et al., 2012). Therefore, several studies have explored the ecological relationship in the context of geomorphic landscape sensitivity (Phillips, 1995; Brunsden, 2001; Thomas, 2001; Stallins and Corenblit, 2018) and postulated terminologies like bio-geomorphology and eco-geomorphology (Phillips, 1995; Thoms et al., 2018; Rice et al., 2011; Malavasi et al., 2021; Kirillova et al., 2022). Phillips (2009) introduced the "Four R" framework (response, resistance, resilience, and recursion) related to geomorphic disturbances. The response represents the system's reaction time, resistance is the capacity to absorb change, resilience is the ability to recover from a disturbance, and finally, recursion is the system's internal feedback. The four R concepts can be further utilized to identify the state of the system after the disturbances. A geomorphic system state can be characterized by its planform composition, structural relations, and prevalent flux and interaction networks.

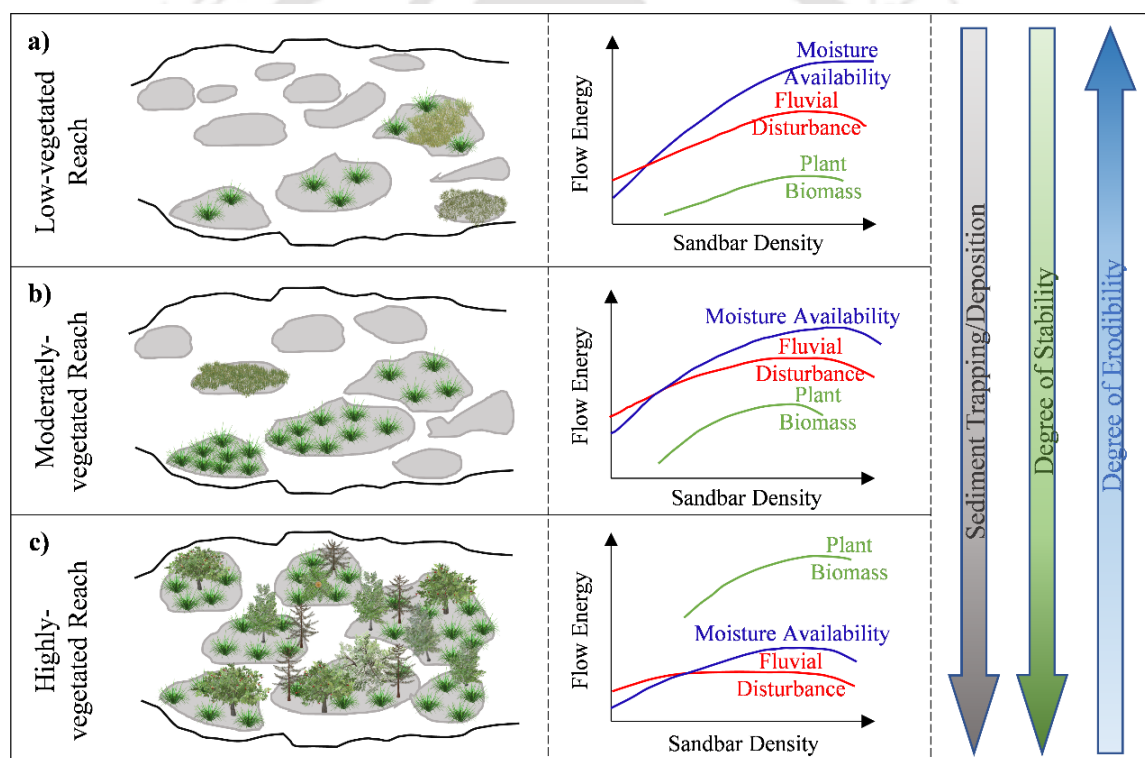
It was also reported that the disturbances in the geomorphic system might be characterized by amplifiers and filters (Phillips and Dyke, 2016). Amplifiers are systems with low resistance, long relaxation times, and dynamically unstable feedback. On the other hand, systems with high resilience, faster relaxation time, and stable recursive feedback can filter the impact of disturbances. Post-flooding, the system state can be modelled on the basis of conceptual patterns such as linear sequential, binary, convergent, divergent, random, or fully connected models (Phillips and Dyke, 2016). When the recovery of the system follows a fixed sequential developmental stage, it is referred to as a linear model. The systems having progression between two potentially stable states are binary models. The convergent model indicates that restoration from a number of states will be toward a single end-state after a disturbance. Random or fully connected models are not realistic representations of existing geomorphic systems, instead used as the reference condition. Again, the response of the system to extreme floods may vary as a function of the vegetation dynamics. The reach having denser vegetation cover are less vulnerable towards the fluvial landscape modification during higher floods indicating the stability of the reach. But in the case of a large braided river, it may follow a linear function as the reach induced a transient behavior in the intermediate states having variable recovery styles and non-recovery conditions. The immediate and after effect of an extreme event strongly depends on the filter dominance of the vegetated system that controls the bio-geomorphic process. The resilience of a vegetation-covered system to geomorphic modification can induce an enhanced recovery mechanism, whereas an un-vegetated fluvial system experiences an irreversible geomorphic effect.

#### **4.4.5 Conceptualization of braided reach behavior in accordance with in-stream vegetation cover dynamics**

Nandi et al., (2022) investigated the island information over the sandbar for the middle reach of the Brahmaputra River using the island-to-bar ratio (IBR) parameter developed by Gurnell et al., (2000). As per IBR, the braided rivers are classified as bar-braided (without vegetated land), bar-braided with occasional vegetated land (0.25 to 0.5), and severely island-braided (> 0.5). In the Brahmaputra river, the vegetation cover depends on the type and size of the sandbar distribution.

## VEGETATION AND ITS IMPACT ON STABILITY CRITERIA

The larger bar provides a more suited environment for vegetation growth than the smaller bar, which has less surface area, elevation, and erodible characteristics (Chembolu and Dutta, 2018; Gautier et al., 2021; Nandi et al., 2022). In general, the reach with larger bars has been observed to be highly vegetated, and naturally, it comprises a high degree of plant biomass (Figure 4.9c). Gurnell et al. (2016) investigated the hydro-geomorphological processes of the Tagliamento River (Italy) and noticed that during high flood events, the vegetated islands shrink and split due to erosion. The density of vegetation on these islands increased during low flow, resulting in area expansion and becoming more stable. Figures 4.9b and 4.9c depict a conceptualized process for the Brahmaputra river, showing a gradual transition of the braided reach from moderate to high vegetation cover.



**Figure 4.9** Conceptual illustration of different degrees of vegetation in a large braided river system with the major interdependency characteristics - prevalence of moist environment, bio-geomorphological processes, and the stability criteria. The flow energy and sandbar density variation for a) low-vegetated reach, b) moderately-vegetated reach, and c) highly-vegetated reach are also demonstrated.

The growth and succession of plant species and communities depend on three broad sets of constraints such as macroclimate (precipitation and temperature), moisture

availability and fluvial disturbance (Steiger et al., 2005; Evette et al., 2012; McShane et al., 2015). Figure 4.9 depicts a conceptual illustration for the braided reaches while considering variables like moisture availability, fluvial disturbance, and plant biomass density. In the reach scale, moisture availability is significantly governed by localized factors such as drainage area, the contribution from hillslopes, and the permeability of alluvial soils and sediments (Booth and Loheide, 2012; Kath et al., 2014). Furthermore, moisture availability is controlled by adjacent channel conveyance during low flow periods and gradually increases during high flood pulses. Anabranching of channels may occur as the frequency of smaller/moderate bars increases due to flood erosion. Larger size bars, on the other hand, may decrease the probability of channel branching. As a result, channel conveyance may be lower in highly vegetated reaches than in lightly vegetated reaches. Additionally, floods inundate vegetation communities, increasing shear stress and drag, potentially causing uprooting through erosion and finally depositing the eroded materials. During an extreme flood, densely vegetated bars can withstand erosion more effectively than less vegetated bars. Thus, sediments accumulate more over (at) the bars with a higher degree of vegetation, finally leading to their stability. In contrast, bars with light vegetation cover are more vulnerable to erosion by the flood.

#### **4.5 CONCLUSIONS**

Large rivers and associated ecosystem services provide an environment for sustaining biodiversity, with vegetation playing a significant role in controlling the hydro-geomorphological processes. It is essential to investigate the establishment and development of vegetation cover over the geological formation, as this will aid in river health management. In this study, we have attempted to demonstrate the relationship between morphodynamic patterns and in-stream vegetation dynamics, as well as their impact on the braided reach stabilization processes. According to the analysis, four distinct time periods have been identified in the vegetation cover assessment over the past 30 years (1990-2019), in which the previous decade (2000-2019) showing no significant changes in vegetation cover and erosion or deposition activities. Again, considering different vegetation types, it was noticed that the combination of moderate and dense vegetation has a higher rate of succession than the light vegetation cover. This owes to the fact that light vegetation is less resilient

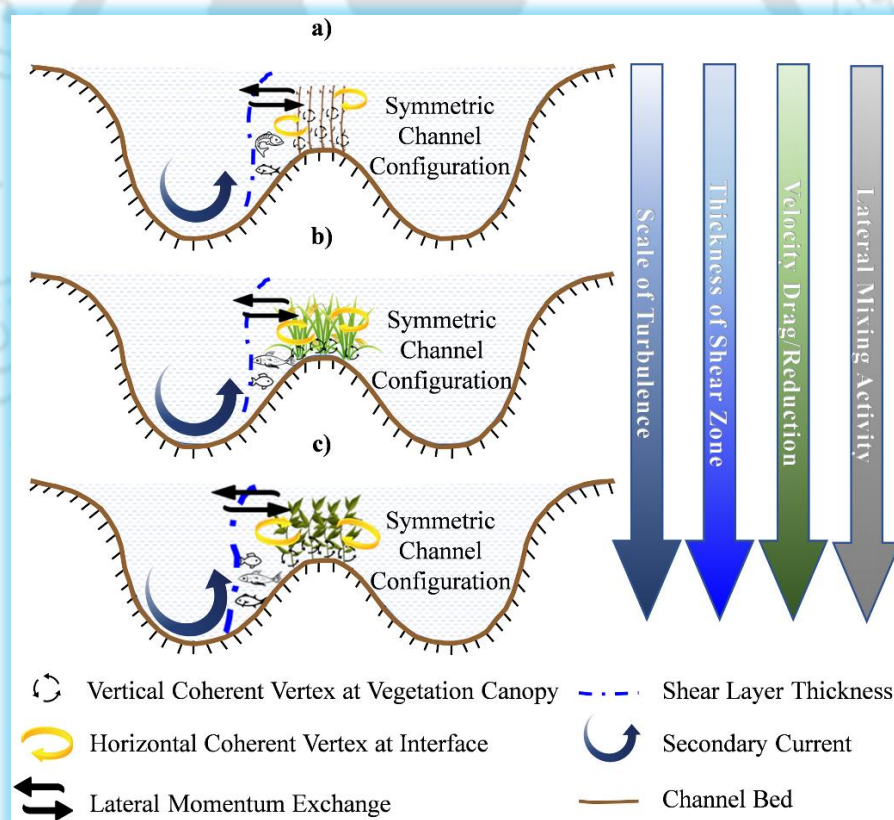
than moderate and dense vegetation types and gets eroded during higher floods. The detailed statistical trend analysis (improved ITA) revealed that the light vegetation cover showed a significant decreasing trend, whereas the moderate and dense vegetation cover had a positive increasing trend. An interesting transitional behavior of the stability trajectory has been observed in the large braided Brahmaputra River. This is due to the combined effect of non-linear hydro-geomorphic constraints like variable climatic conditions, moisture availability, degree of fluvial disturbances, and anthropogenic stresses. Further, the finding of this study can be utilized to determine the state of the river's health and to establish effective management strategies for sustaining the river's ecosystem. Finally, bio-geomorphological information can be incorporated to develop a nature-based management approach to continuously monitor the condition of different river types.





# MORPHODYNAMICS OF VEGETATED MID-CHANNEL BAR

(Understanding the Impact of different type of natural vegetation on the morphodynamics of mid-channel bar through laboratory scale experiments)



**Contribution from this chapter:** Nandi, K. K., Kakati, R., Dutta, S., & Khatua, K. K. (2022). Exploring the Influence of Vegetated Mid-Channel Bars on Flow and Turbulence in Bifurcated Channels: An Experimental Approach. *Advances in Water Resources* (Under Review)





## **5.1 OVERVIEW**

The present chapter demonstrates the process-form-vegetation-interaction through experimental investigation at a flume scale mid-channel bar model with different vegetation cover arrangements. Experiments were conducted using natural plant forms (paddy, leafy, and rigid stem) arranged in staggered manner over the bar in submerged condition. This chapter addresses the following questions:

- How does the natural vegetation cover on the mid-channel bar affects the flow dynamics?
- How does the interaction between the flow and the vegetation lead to the formation of a flow-turbulence structure in the bifurcated channel?
- What are the effects of different types of canopy structure on flow-turbulence due to flow-vegetation interaction?

## **5.2 INTRODUCTION**

In any fluvial system, bar formation is the fundamental building block that initiates the braiding (Ashmore, 1982; Ferguson, 1993; Sharma, 2004; Bridge & Lunt, 2006; Ashmore, 2013; Chembolu and Dutta 2018; Nandi et al., 2022a). Braiding process typically involves converting the alternate bar into a multiple row bar or a mid-channel bar through the use of cut-offs (Nandi et al., 2022a). Mid-channel bars divert the flow through the branch channel towards outer banks, causing erosion, as well as obstructing flow-sediment conveyance that resulted in a series of downstream deposits (Ashmore and Parker, 1983; Pradhan et al., 2021). Furthermore, the formation of the mid-bar also complicates the flow structure and the interaction between flow and sediment triggers the morphological dynamism. The bar formation resulted in a number of subsequent confluence-bifurcation nodes affecting the hydrogeomorphology of the river system.

Some of the studies related to braiding issue such as energy expenditure mechanism in large braided river system (Pradhan et al., 2021; Nandi et al., 2022b), bar erosion and migration process (Chembolu & Dutta, 2018; Dubey et al., 2021), application of geo-spatial techniques (Piegay et al., 2009; Wheaton et al., 2013; Belletti et al., 2014; Lallias-Tacon et al., 2014; Pradhan et al., 2022), numerical modelling approach (Paola, 2001; Hardy, 2013; Javernick et al., 2016), and flume scale

experimental studies (Hoey & Sutherland, 1991; Warburton, 1996; Khan et al., 2017, 2021, 2022) have been carried out in past few decades. Furthermore, presence of vegetation over the bar structures makes it more difficult to understand the system's behaviour. As vegetation grows over the bar with time, it transforms into an island. The riparian zone and the instream units of a natural river system are generally covered with woody deciduous shrubs whose branches and leaves are strewn over the height (Schnitzler et al., 2007). Furthermore, the hydrodynamic behaviour of these plants exhibits different bending and streamlining responses to flow depending upon their rigidity and flexibility (Gibson, 2012). As a consequence, the adjustment in the flow field caused by the presence of vegetation cover exemplifies the system's dynamic response. A very few studies have been conducted to understand micro-level flow behaviour due to the presence of vegetated mid-channel bar. This chapter attempts to understand the flow turbulence structure in the bifurcated channel due to presence of vegetated mid-channel bar.

Vegetation has a profound interference with the flow and enable the river to self-organise and resilient during the extreme events. Therefore, in many types of river restoration initiatives, vegetation is regarded as the prime nature-inspired solution for enhancing the fluvial system's bio-physical signatures (Nepf and Ghisalberti, 2008; Brachet, 2015; Vargas-Luna et al., 2018; Chembolu et al., 2019; Lera et al., 2019; Pradhan et al., 2022). Vegetation interacts actively with the flow and sediment, influencing the morphology of the fluvial system by generating additional resistance to the flow (Paola, 2011; Corenblit et al., 2009; Gurnell et al., 2012; Bertagni et al., 2018). Furthermore, vegetation has a significant impact on erosion-deposition rates, bank stability, water quality, and riverine habitat (Baptist, 2003; Perucca et al., 2009; Dosskey et al., 2010; Bornette and Puilalon, 2011). In large braided systems, vegetation becomes a controlling agent and shown a positive feedback by promoting the stabilization of geomorphic units (Allmendinger et al., 2005; Asahi et al., 2013; Bertoldi et al., 2014; Gurnell, 2014). The ability of vegetation in improving river health encourage the research community to understand the process underneath (Nepf, 2012; Curran and Hession, 2013). Therefore, the process understanding of flow-vegetation interaction creates an interesting research opportunity for the scientific community.

It should be noted that the vegetation cover can act as a filter by resisting flow depending on its type, rigidity and flexibility, submergence and emergence, vegetation cover density, and other biomechanical and morphological factors (Chen et al., 2013; Green, 2005). Previous studies have investigated the influence of different types of vegetation on flow dynamics, including artificial rigid, flexible, and cylindrical forms (Nepf, 1999; Bennett et al., 2002; Velasco et al., 2008; King et al., 2012; Chen et al., 2011; Tanino and Nepf, 2008; Siniscalchi et al., 2012). However, these studies have largely overlooked the role of plant morphology. In an effort to address this gap in the literature, Wilson et al. (2003) conducted an experimental investigation using flexible vegetation with and without fronds to explore their impact on flow characteristics. Further some studied tried different vegetation arrangement/pattern (Chen et al., 2011; Chembolu et al., 2019), varying vegetation density (Li et al., 2014; Devi et al., 2016; Zhang et al., 2018; Zhao et al., 2019) to understand the effect on turbulence behavior. Still, there are very few evidences on impact of natural vegetation on flow-turbulence structure. The majority of research studies have used straight, compound, and meandering channel setups. In this chapter, an attempt has been made to study the vegetation impact using a braided loop setup.

This chapter aimed to investigate the turbulence behavior of bifurcated channel due to the presence of mid-channel bar with and without vegetation arrangements through flume experiments. The flow condition maintained in the experiment was unidirectional and steady-uniform flow. In this research, we attempted to gain a better understanding of flow-vegetation interaction by considering the braided mechanism. This chapter attempted to relate the study to the natural river environment through the use of natural vegetation types, primarily in terms of planform stability and ecological implications. In order to achieve the objectives, a detailed three-dimensional flow measurement was conducted with the help of Acoustic Doppler Velocimeter (ADV) in the bifurcated channel with different types of natural vegetation arrangements (such as rigid stems, paddy and leafy types) on the mid bar. The time-averaged velocity along with the turbulence characteristics associated with the canopy and Reynolds stress distribution have also been analyzed and discussed in detail. During the experiments, submerged vegetation conditions were used to simulate a high-flow (flood) situation. This is one of the pioneering

experimental studies based on braided loop models using natural vegetation cover arrangements.

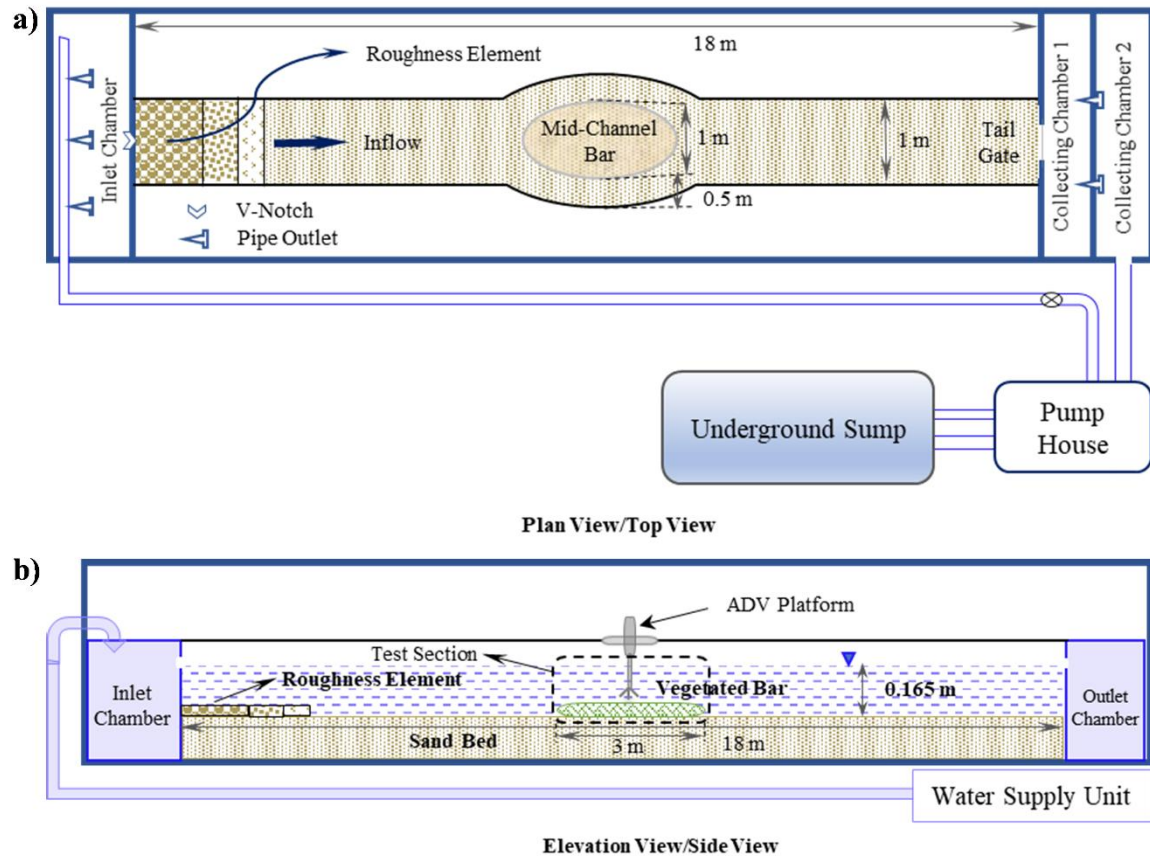
### **5.3 DESIGN OF EXPERIMENTAL PROGRAM**

#### **5.3.1 Experimental setup**

The Fluvial hydro-ecological laboratory constructed at the Indian Institute of Technology (IIT) Guwahati was being used for the experiments. The experiments were carried out in a flume with dimensions of 18 m in length and 4 m in width, of which 18 m X 2 m was used for the physical braided model installation (Figure 5.1a). The flume is built in such a way that the water flow maintains a recirculating system that comprises an inlet chamber (at upstream), an outlet chamber (at downstream), and an underground sump (storage and supply unit). Roughness elements such as stones, pebbles were placed at the upstream channel-bed to weaken the inflow turbulence and to straighten the flow. Figure 5.1a and b illustrates the experimental layout (plan view and side view) of the experimental setup. To achieve the desired discharge (about 37 l/s), two 15 HP and one 10 HP pump has been utilized. The flow depth has been maintained at 16.5 cm throughout all the experiments using the tail gate arrangements. In order to prepare the channel bed, river sand with a  $d_{50}$  value of 0.55 mm was used, and the bed slope of 0.001 was maintained in the channel. A V-notch was installed at the inlet of the channel to measure the flow discharge.

Nandi et al., (2022) found that different types of sand bars of various sizes with different morphological nature are present in the large braided river Brahmaputra, and categorized into 7 different classes. The class 6 bar (low mobile bar) has been selected and an idealized version has been modelled in the flume to simulate a braided loop flow characteristic. An elliptic shape of the bar was used and placed in the channel which replicate the river mid-channel bar deposition (Figure 5.1). It should be noted that, the size and shape of the bar constructed in the flume was not a direct scale down model of any actual scenario from the river. This is because, a flume scale representation of the prototype fluvial condition of a large braided river is not feasible without encountering from inherent scale effects (Khan et al., 2021). Therefore, a simplified version of mid-channel bar was designed in the flume to study the flow hydrodynamics and associated morphological activity. The bar was constructed at

distance from the inlet where the flow was in fully developed condition (Sharma and Kumar, 2017). Furthermore, the symmetric loop was maintained in the channel so as to achieve the discharge condition of symmetry. Symmetric loop offers the advantage that the main channel flow divides into two channel courses with equal discharge.

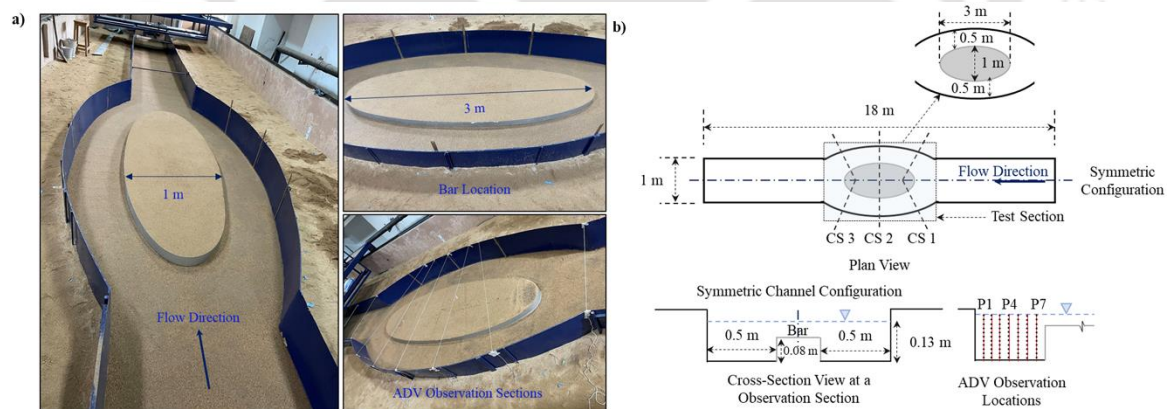


**Figure 5.1** Experimental setup in Fluvial hydro-ecological laboratory, IIT Guwahati; a) plan view of the physical model setup; b) side view showing the details of experimental arrangements (vegetated bar, measuring platform etc.)

### 5.3.2 Flow conditions and velocity measurement

The experiments were performed in four different conditions, with and without mid-bar vegetation, while maintaining a constant flow depth. There was no transport state maintained for the bed in all of the experiments by generating incipient motion condition. The flow depth was kept just below the incipient motion depth to achieve no transport condition (Devi and Kumar, 2016). As discussed earlier, the flow depth has been maintained at 16.5 cm throughout all the experiments using the tail gate arrangements. The test section was selected at the bar location for the

measurement of instantaneous velocity. Figure 5.2a and b shows the measurement location details in the physical setup used for the experiment. The velocity measurements were done using a three-dimensional Acoustic Doppler Velocimeter (ADV) at a sampling frequency of 200 Hz (Yagci et al., 2010; Devi, 2016; Chembolu et al., 2019). The ADV used in the experiment was manufactured by Nortek® and has four probes with a capacity of 10 MHz. Further the accelerating threshold method (Goring and Nikora, 2002; Dey et al., 2012; Devi, 2016; Pu et al., 2018; Chembolu et al., 2019; Modalavalasa et al., 2022) has been used to filter out the spikes from the velocity time series obtained from ADV. A threshold acceleration value of 1 - 1.5 was determined based on the careful trial and error method, so that velocity power spectra follow Kolmogorov's hypothesis (Pu et al., 2018). Three cross sections have been carefully selected in the text section for the measurement segments, each with seven points and about twenty depth locations (Figure 5.2b). The ADV measurements were taken at each point for about 20 depths with a 3 to 5 mm intervals from the surface to the bed. To analyze the vertical distribution of different kinds of flow parameters, three major points were used: near the left bank (P1), middle of the section/channel (P4), and near the mid-bar (P7).






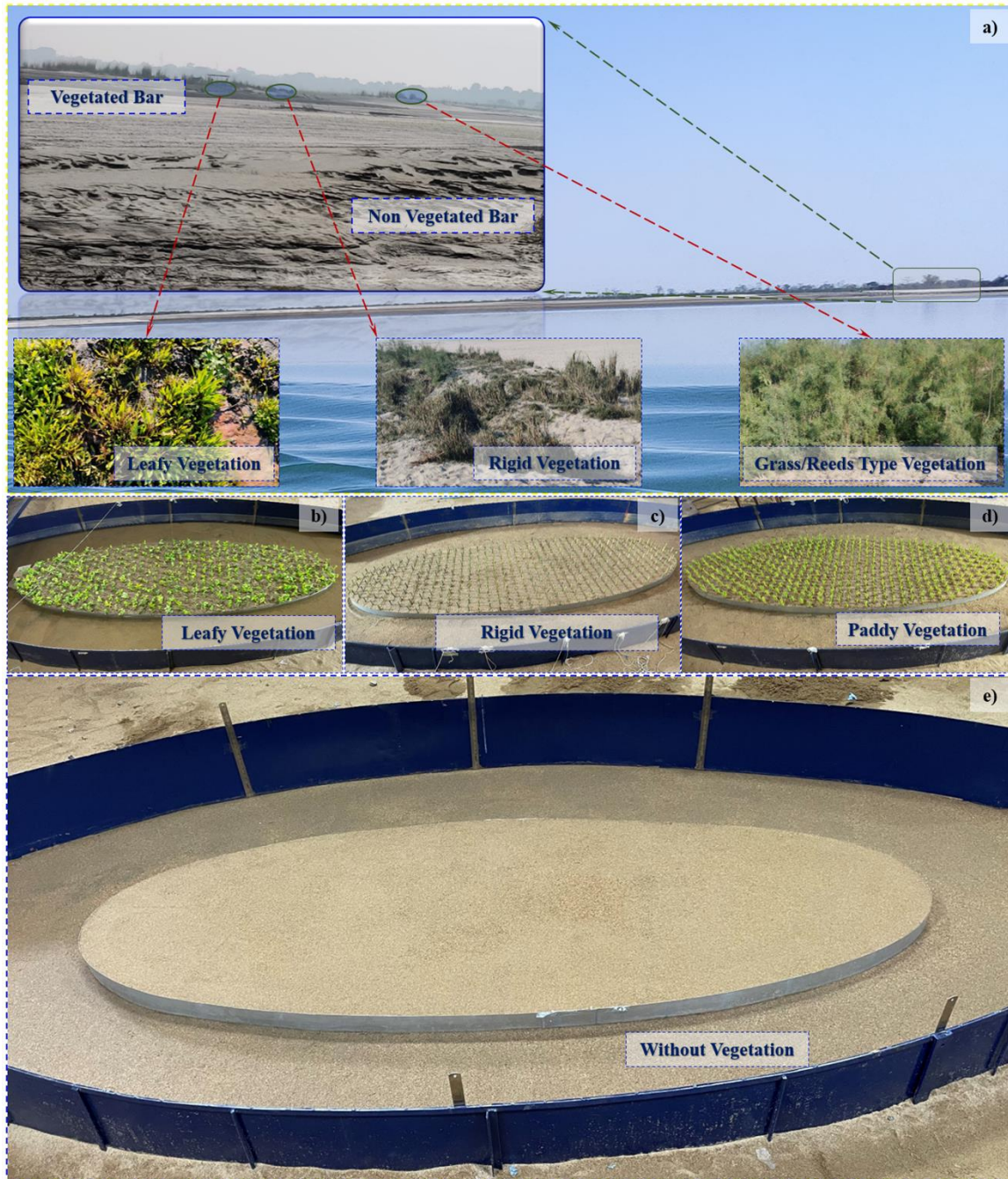
**Figure 5.2** Experimental flume setup showing the symmetric mid-channel bar layout with details of test section with velocity measurement locations; a) in-channel bar arrangements with dimensions; b) detailed measuring locations.

5.3.3 In-stream vegetation arrangements

Various types of vegetation, including young rice plants (such as *Oryza Sativa*), leafy plants (such as *Duranta*), and cylindrical stems (such as *Sphagneticola Trilobata*), have been used in the experiment. The prime objective was to simulate the biomechanical properties of real species found in the Brahmaputra river, such as flexible grass, leafy bushes, and reedy plants (Figure 5.3). These plants were chosen because they exhibit heterogeneity in structural configuration, swaying motion, and drag effect. There was flexible movement in the bladed (young rice plants), semi-flexible movement in the leafy (leaves were flexible, and stems were rigid), and rigid movement in the cylindrical vegetation arrangements. All the details about the properties and characteristics of different plant type used in the experiment are listed in table 5.1. The plants were arranged in a staggered manner with a distance of 10 cm center to center (Figure 5.3).

**Table 5.1** Property and characteristics of different plant type used in this experiment for the vegetation cover arrangements over the mid-channel bar.

Plant Property Description	Plant Type		
	Rigid Plant	Paddy Plant	Leafy Plant
Plant Form Used in the Experiment			
Average Plant Height	6 cm	6 cm	6 cm
Difference in Average Deflected Height	0.1 – 0.2 cm	1.8 to 2.1 cm	1.2 – 1.8 cm
Approximate Stem Diameter	0.30 cm	-	0.12 cm
Approximate No. of Stem/Blades per Plant	-	6 - 7	10 - 12
Average Width of Stem/Blades	-	0.15 – 0.2 cm	1.5 – 2 cm
Relative Canopy Porosity	High	Moderate	Low
Approximate Projected Area	1.5 - 1.8 cm <sup>2</sup>	6.5 – 7.5 cm <sup>2</sup>	20 - 22 cm <sup>2</sup>
Approximate Plant Flexibility	≈ 1	≈ 0.6	≈ 9



**Figure 5.3** Illustration of in-stream vegetation cover arrangements in real river scenarios and flume-scale lay outs used for the experimental study, a) scenario of different vegetation cover in the Brahmaputra river (photographs collected in field survey); b) leafy vegetation arrangement; c) rigid vegetation arrangements; d) paddy vegetation arrangements; e) without vegetation (bare mid-bar condition).

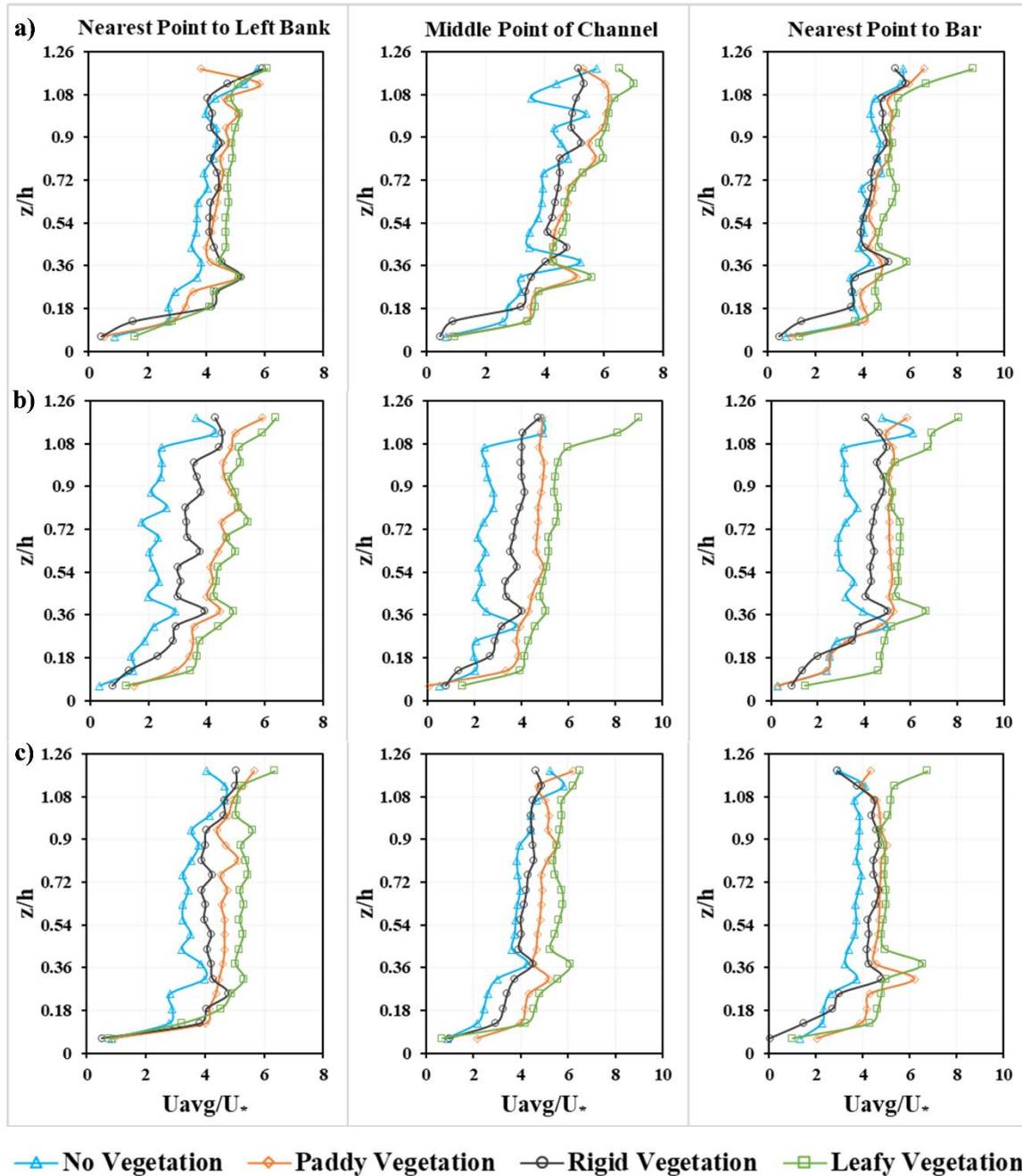
## 5.4 RESULTS

### 5.4.1 Streamwise velocity

The stream-wise (vertical distribution) velocity variations has been analysed to understand the flow behaviour in the proximity of the bar. The time-averaged velocity has been normalized by using the shear velocity ( $U_*$ ) for the channel. Figure 5.4 illustrates the vertical distribution of the normalized stream-wise velocity in the bifurcated channel considering the effect of vegetation on the mid channel bar. It has been observed that the vertical distribution of the velocity profiles exhibited the logarithmic nature for all the conditions. The canopy top and above region was the zone where the profile did not follow a logarithmic pattern. Due to the shallow submerged flow conditions (ratio of flow depth to vegetation height  $< 5$ ) during the experiments, this result is expected (Nepf, 2012). Further, the magnitude of the velocity observed to be higher for the observations collected at the point near to left bank (farthest point from mid channel bar) and subsequently decreasing towards the bar location. Also, interestingly, the velocity showed slightly increased value at/near the bar level ( $0.3 > z/h > 0.5$ ) for all cases, as visible in the plot. There might be some minor interaction between the bar top flow and the channel flow at this location. Again, at the level of  $z/h$  from 0.5 to 1, the change in the slope for the velocity gradient become steep. According to Chembolu et al. (2019), the different types of vegetation affect the velocity distribution in the channel.

In this present experiment, the magnitude of the velocity was found to be in the order of leafy  $>$  paddy  $>$  rigid  $>$  no vegetation. A similar kind of observation has been reported previously for compound meandering channel with different flood plain vegetation conditions (Modalavalasa et al., 2022). The percentage variations for leafy, paddy, rigid stem was observed to be about 32%, 28%, and 17% respectively, compared to non-vegetated condition. The velocity ranges mostly between 0.07 m/s to 0.18 m/s for no vegetation condition, 0.11 m/s to 0.21 m/s for rigid vegetation, 0.12 m/s to 0.22 m/s for paddy vegetation, and 0.18 to 0.26 m/s for leafy vegetation with an exception from some erratic observations. In this experiment, it was observed that at the canopy top ( $z/h \geq 1$ ), there was a disrupt behavior in the velocity profile which is due to the resistance offered by the vegetation canopy structure to the flow. Further, it resulted in increased velocity at the channel by enhancing the flow obstruction over

the vegetated bar and diverting the flow towards the branch/side channel. Mainly the leafy type vegetation offered comparatively more resistance to the flow than other type of vegetation. The result reported by Wilson et al. (2003) who carried out the experiment using flexible stipes with and without foliage showed a similar kind of velocity distribution.

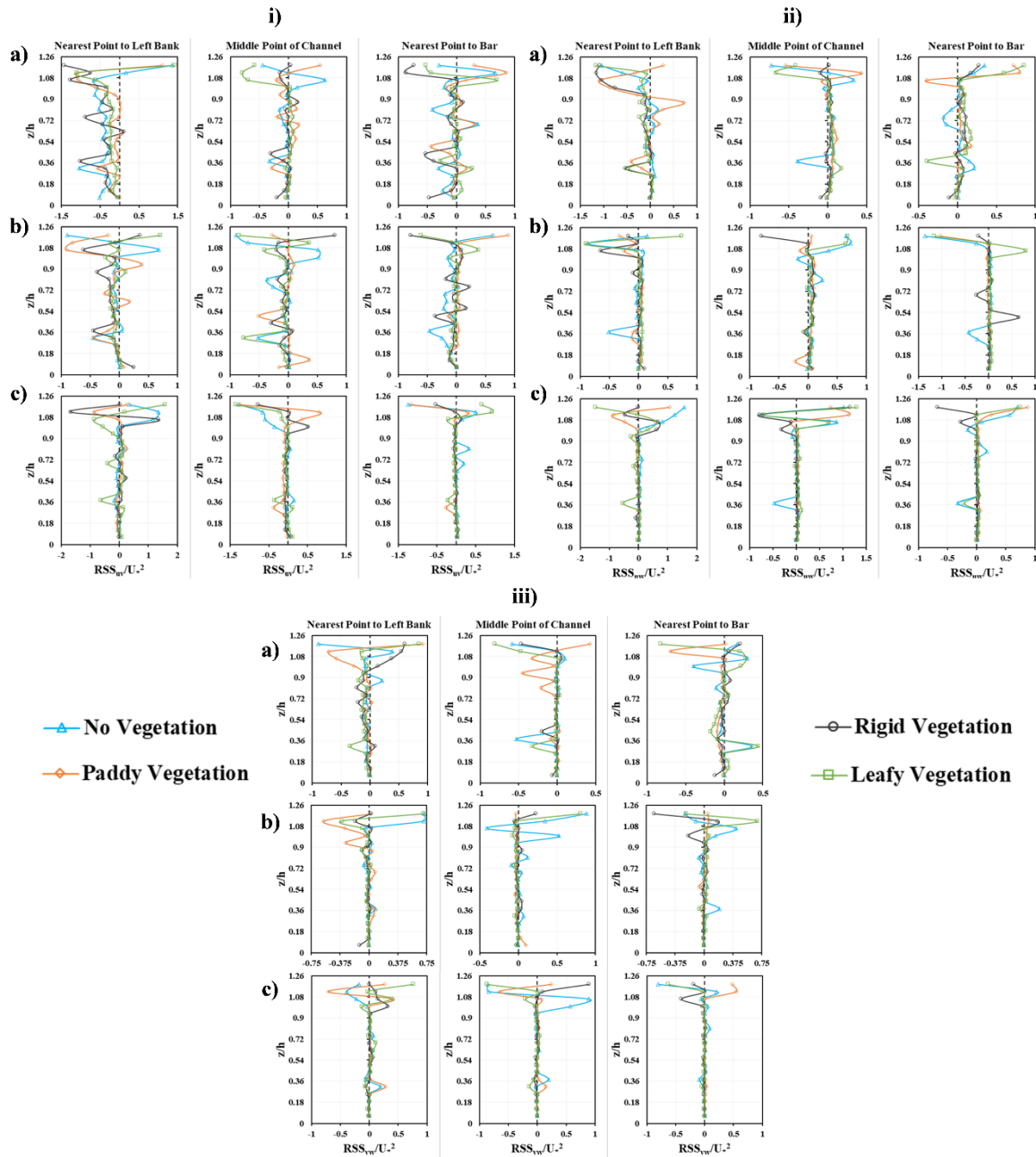


**Figure 5.4** Vertical profile for normalized stream-wise velocity distribution for with and without vegetated mid channel bar with different vegetation arrangements; a) for cross-section 1; b) for cross-section 2; c) for cross-section 3.

#### 5.4.2 Reynold's shear stress

Reynold's shear stress provides information about flow behavior, frictional resistance to flow, and stability of the flow, which can be used to predict flow patterns and sediment transport within the channel. Figure 5.5 shows the vertical distribution of normalized Reynold's shear stress in lateral ( $RSS_{uv}$ ), depth-wise ( $RSS_{uw}$ ), and stream-wise ( $RSS_{vw}$ ) directions measured in different vegetation cover arrangements. The Reynold's shear has been normalized by using the square of shear velocity ( $U_*^2$ ). Increasing positive depth-wise RSS strengthen the vertical coherence vortex; however, decreasing lateral RSS minimizes the horizontal coherence vortex's effect (Tang et al., 2023). It has been observed that the Reynolds stress value peaks just beneath the canopy's top and starts to decrease downward into the canopy. The peak has been observed at the canopy top ( $z/h \geq 0.75$ ) for various vegetation types, indicating a significant amount of mixing activity in that zone. Wilson et al., (2003) and Devi, (2016) reported similar findings while experimenting with flow through flexible submerged vegetation. The intensity of peak RSS values is dependent on the type of vegetation through which the flow passes.

In the present experiment, the normalized absolute peak RSS values were ranging between 0.5 to 1.4 for leafy, 0.2 to 1.1 for paddy, 0.15 to 1.0 for rigid and 0.1 to 0.7 for no-vegetation condition. Further, all cross sections showed a reduction in RSS values from the bar to the left bank. It is also important to note that canopy form impacts RSS distribution since irregular canopy porosity and swaying induced by different plant forms generate higher turbulent stress in the region, resulting in higher momentum exchange (Chembolu et al., 2019). This can be clearly visible in the RSS plots as flexible grass and leafy vegetation type showed higher values as compared to rigid stem type vegetation arrangements. Observation of RSS distributions in the lower canopy region reveals an approximately uniform distribution with slight fluctuations at the bar level. Further, the absolute RSS values varied in similar manner for lateral and stream-wise directions in the lower canopy region.



**Figure 5.5** Vertical distribution of normalized Reynolds shear stress; i) lateral RSS; ii) depth-wise RSS; iii) stream-wise RSS; a) variation at CS1; b) variation at CS2; c) variation at CS3.

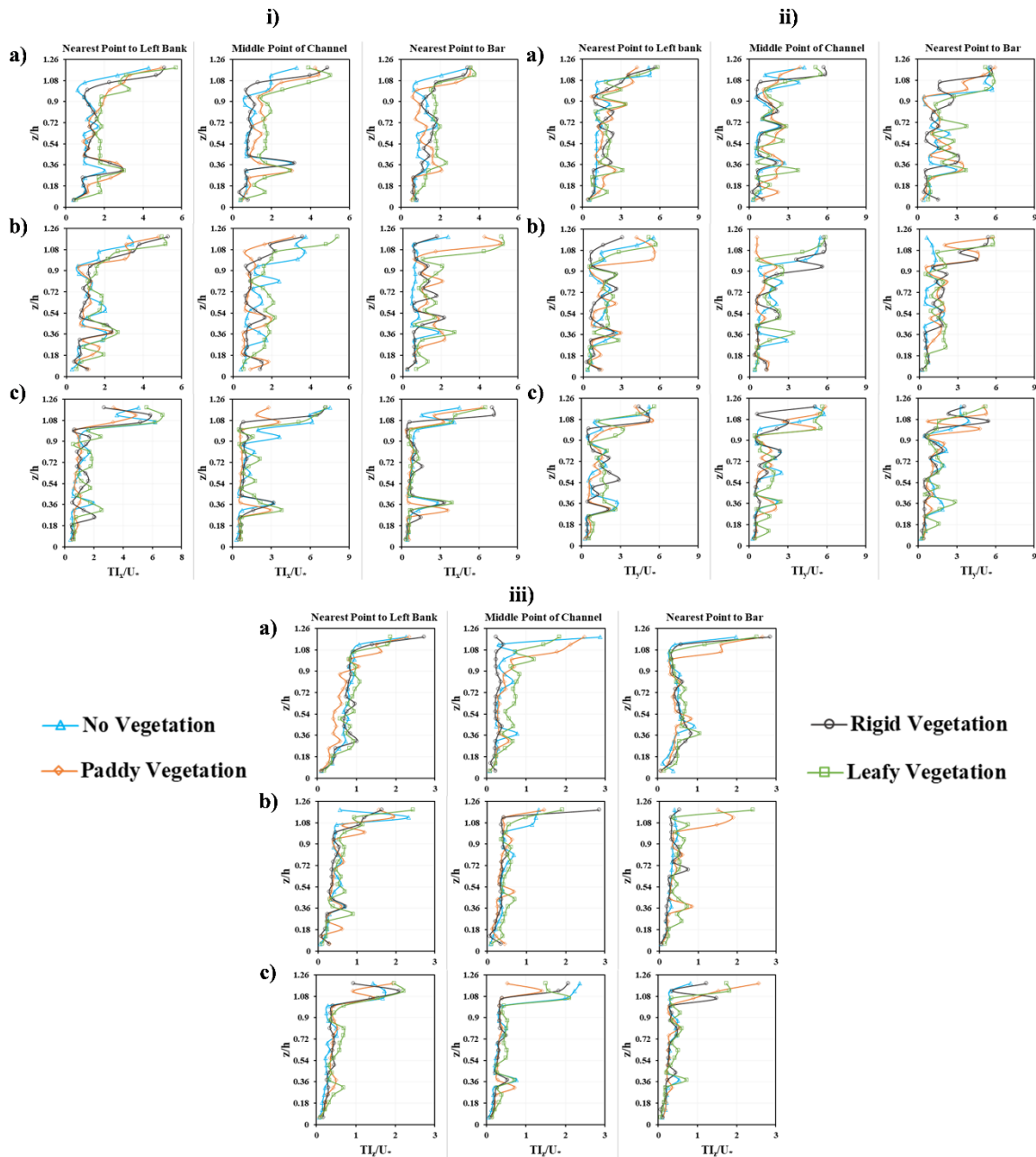
In comparison with non-vegetated flow conditions, leafy, paddy, and rigid stem arrangements showed an overall increase in peak values of around 50%, 35% and 15%, respectively. The leafy type offers additional drag due to its increased frond surface area as compare to other vegetation type resulted in amplified shear generated turbulence. In addition to increasing the drag and turbulence, this further can also alter the flow patterns within a fluid by creating vortices and other flow

structures. These effects can result in an increase in the Reynolds stress and a corresponding increase in the viscous dissipation in the fluid. It was found that the peak absolute values of normalized RSS range between 0.8 and 1.2, predominantly observed at the CS1 and relatively lower in the other two cross-sections. These variations were most likely produced by the accelerated flow in the bifurcated channel and the increased momentum exchange activity near CS1, as well as gradual turbulent dissipation towards the confluence.

#### **5.4.3 Turbulent intensity**

Turbulent intensity (TI) is one of the major parameters that helps to understand the degree of mixing and energy dissipation in a flow, which can then provide insights into the channel's morphological activity. The TI has been measured using the root mean square of the fluctuating velocities in each direction i.e stream-wise ( $TI_x$ ), lateral ( $TI_y$ ) and vertical ( $TI_z$ ) directions. The TI values were further normalized using shear velocity ( $U_*$ ), and the distribution of these parameters is shown in Figure 5.6. It was found that stream-wise and lateral turbulence intensities were of comparable magnitude and nearly doubled the value of the vertical component. It provides the information about the existence of a significant mixing in the horizontal direction. A similar result has been reported by Maji et al., (2017) regarding the turbulence intensity variation. The magnitude of normalized peak TI was found to be in the range of 5 to 6 in the stream-wise and lateral directions, and 2 to 3 in the vertical direction.

Furthermore, stream-wise and lateral TI values were observed to be highest near the water surface, where the gradient of longitudinal velocity also showed an increasing trend. Even though the variation in vertical TI was not as pronounced as in the other two components, it still indicated the transfer of energy near the surface in the depth-wise direction. It was observed that the vertical component of TI increased at the canopy top and water surface, which indicates a significant vortex rotation. Furthermore, increasing TI values at the top of the canopy vegetation were indicative of shear-induced turbulence. It was also found that the magnitude of TI was higher at the upstream cross-section (CS1) of the bifurcated channel, and gradually decreased towards the downstream cross-section (CS3). The average percentage reduction was in the range about 8 to 10 % in the CS2 and 3 as compared to CS1.



**Figure 5.6** Vertical distribution of normalized Turbulence Intensity; i) stream-wise TI; ii) lateral TI; iii) vertical TI; a) variation at CS1; b) variation at CS2; c) variation at CS3.

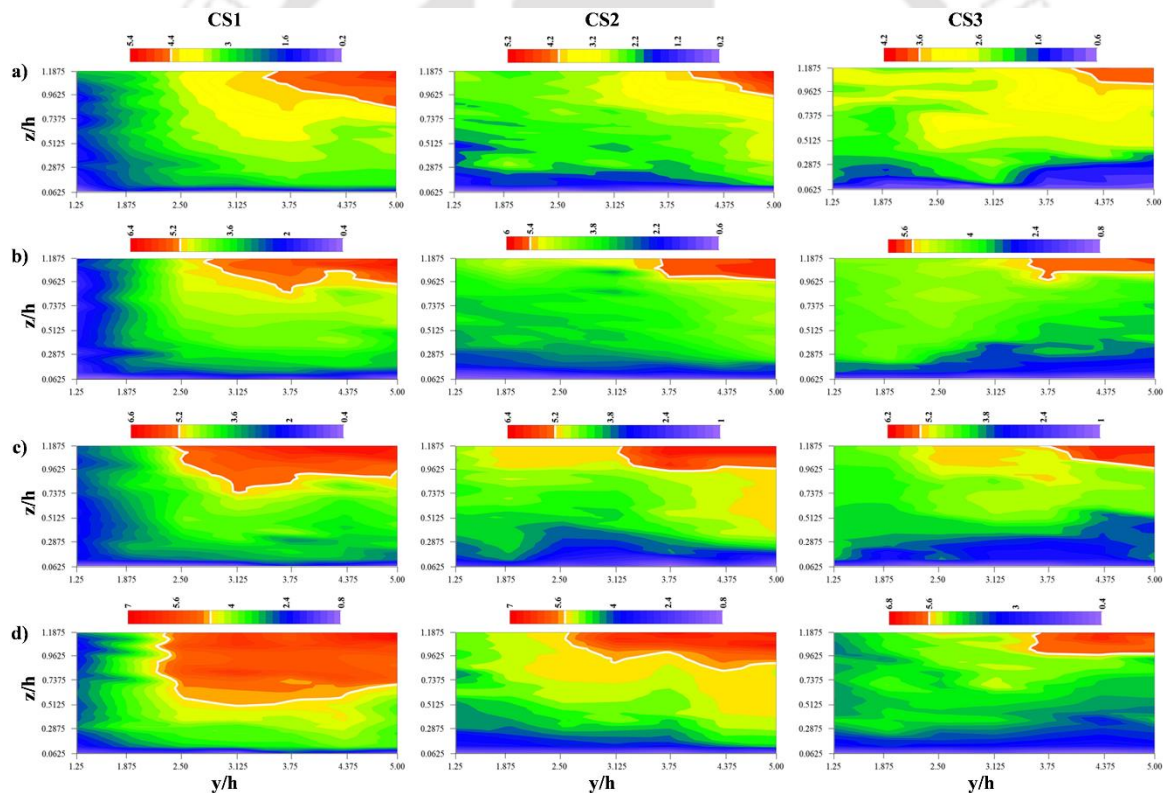
Further, the TI was observed to be higher in case of leafy vegetation cover as compared to other arrangements. On average, the turbulence intensities increased by 11%, 8% and 3% for leafy, paddy, and rigid stems as compared to non-vegetated cases. This indicates leafy vegetation covers appear to produce the extreme turbulence mixing when compared to paddy and rigid vegetation arrangements. Furthermore, the TI variation was observed to be much significant near the vegetated

bar due to the higher interaction of flow-vegetation and it became less significant towards the outer bank. This is due to the active shear layer near the zone of vegetated bar and the TI distribution becoming more uniform towards the channel (far from the bar). Boyer et al. (2006) made a similar observation while conducting a field study on the Bayonne and Berthier rivers. But the behavior was opposite at the downstream cross-section near the confluence (CS3). Vortex pairing may facilitate the mixing activity and resulted in turbulence intensity reduction towards downstream (Rhoads and Sukhodolov, 2004; Boyer et al., 2006). Results show that turbulence-induced flow mixing is significantly reduced when different vegetation covers are present.

## **5.5 DISCUSSION**

This section discusses the process-based understanding of turbulent behavior caused by the interaction of flow and vegetation in a braided loop. The turbulence characteristics of the flow are influenced by different vegetation cover arrangements and their biomechanical properties (Nepf, 2012; Chembolu et al., 2019; Vargas-Luna et al., 2019). As observed in the experiments, the distributions of velocity and other turbulence parameters showed different characteristics for leafy, paddy, and rigid vegetation cover arrangements. For example, the velocity distribution in case of leafy vegetation cover showed comparatively higher magnitude. A rigid vegetation cover, on the other hand, can produce a larger and faster rotating vortex near the top of the canopy when compared to one with a swaying canopy. A study by Nepf and Ghisalberti (2008) found that the momentum exchange is less effective in flexible vegetation canopy than in rigid vegetation. Figure 5.7 shows the normalized stream-wise velocity contour for the three measured cross-sections along the bifurcated channel. It has been observed that the velocity core region occurred at the top of the channel-bar interface. The mean velocity was observed to be in the order of  $8U_*$  for leafy vegetation which is relatively higher than flexible grass ( $5U_*$ ) and cylindrical ( $4.5U_*$ ) layouts. Interestingly, the velocity core region enlarges gradually when the vegetation cover has been changed from non-vegetated condition to rigid, paddy and leafy plants. The core region at the vicinity of the bar indicates more activity such as momentum exchange. On the other hand, the core region shrinks towards the confluence section. Due to the substantial effect of the upstream flow division, the velocity contour at the upstream section (CS1) became denser, indicating a steep

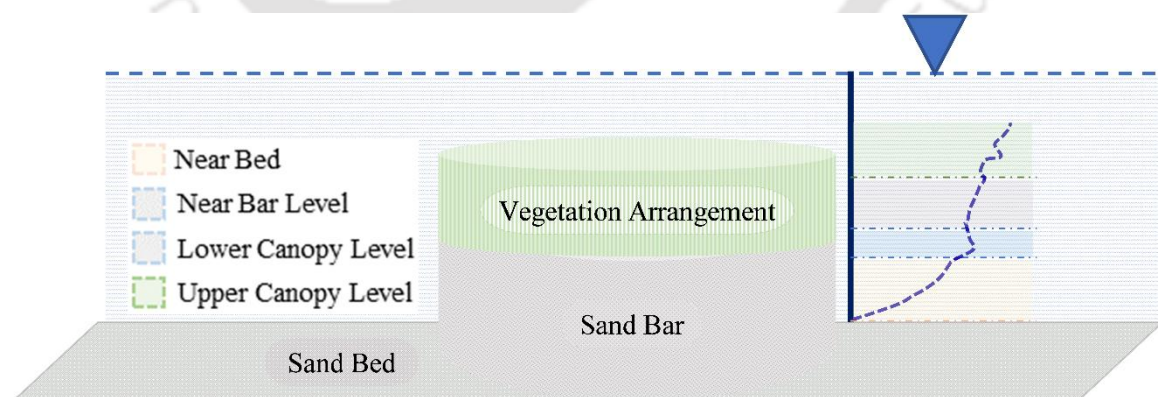
vertical velocity gradient. Several researchers reported similar observations using experimental studies (Shiono and Muto, 1998) as well as numerical model studies (Stoesser et al., 2010). Additionally, the low velocity region was observed near the bar end at the confluence section (CS3), which indicates the activity of deposition in the channel. This region gradually increases with different vegetation cover arrangements as shown in Figure 5.7. Also, the variation of shear layer has been observed to be different in different vegetation cover conditions. It appears that the shear layer increased from mid-bar toward the banks. It has been clearly observed that the presence of vegetation cover over the bar pushes the shear layer towards the bifurcated channel. The shear zone starts at  $y/h \sim 3.5$  for no vegetation condition and it gradually enters inside the channel as the vegetation cover changes as shown in Figure 5.7 and the for highly resistant leafy vegetation cover, it was at  $y/h \sim 2.0$ .



**Figure 5.7** Normalized streamwise velocity contour for different mid-bar vegetation cover arrangements; a) no-vegetation b) rigid c) paddy d) leafy.

Earlier studies have shown that the profile behaves differently in the canopy zone, as well as in the lower and upper canopy zones (Huai et al., 2009; Chen et al., 2011). The velocity distribution in the present chapter showed a nearly uniform

distribution in the lower canopy region and an accelerating profile in the upper canopy region. The profile alteration is triggered by shear layer interaction between flow and vegetation canopy, which results in accelerating velocity in the upper canopy region. Furthermore, due to the deflection of lateral flows around the canopy top, higher turbulence has been observed at the frond canopy level in comparison with rigid cylindrical vegetation, as fronds produce strong shear layers in the wake of their leaves. A significant difference in velocity distribution will form the shear layer, and active momentum exchange will occur, resulting in sediment and mineral trapping. Further, the formation of large-scale coherent vortices at the vegetation-water interface is a measure of flow instability because it is the source of momentum transfer from the non-vegetated zone to the vegetated zone in both horizontal and vertical directions. Therefore, sediment material/mineral transport/deposition near the channel-bar interface is largely controlled by flow-vegetation boundary momentum exchange. Moreover, the vegetation cover over a sand bar can be related to its formation and stabilization. Anabranching or channel widening initially causes alternate bars to become the central bar with smaller dimensions; over time, this central bar elongates as periodic deposition events occur. Further, vegetation over this bar can increase bar accretion by reducing velocity (Rominger et al., 2010; Vargas-Luna et al., 2019) towards the lower vegetated zone, as demonstrated in this chapter. Eventually, the deposition of sediment tends to secure the soil strata and further, vegetation colonization can stabilize the sand-bar.

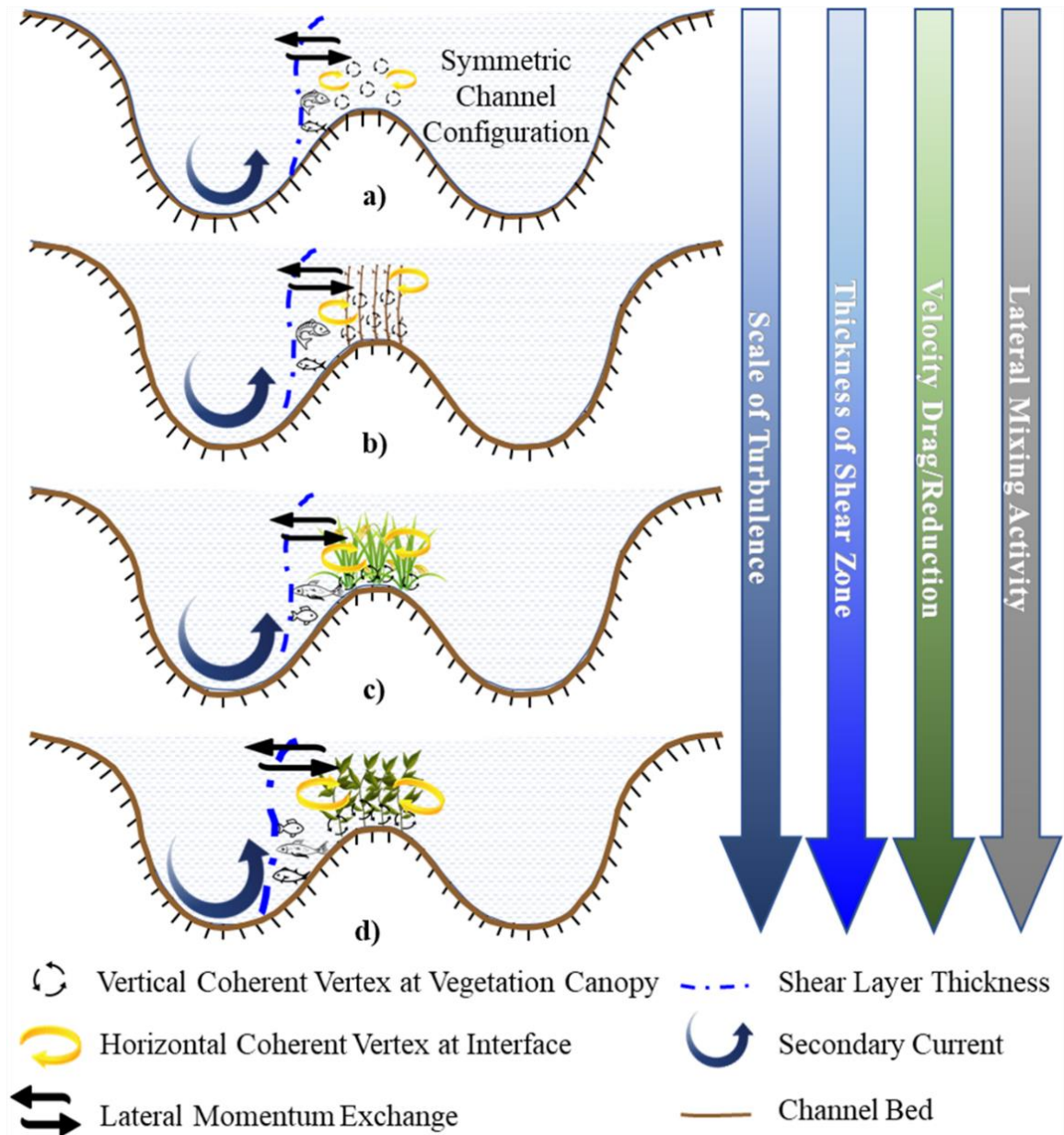


**Figure 5.8** Conceptual illustration of vertical velocity profile at different zones due to the flow-vegetation interaction.

The present study's findings align with previous research on the impact of vegetation on flow behavior in channels. Nepf (2012) reported that shallow submerged flow conditions disrupt the logarithmic pattern of velocity profiles observed in deeper flow conditions. This is because the presence of vegetation influences boundary layer development, reducing turbulence intensity and increasing flow resistance. Figure 5.8 illustrates the four distinct regions observed in this study: near the bottom of the channel, the area around the bar level, the lower canopy, and the upper canopy region. A nearly linear profile was observed at the bottom of the channel, and a slight increase in velocity near the bar level suggests minor interaction between the bar top flow and the channel flow (Figure 5.4). Xu et al. (2020) also reported that the presence of bars in the channel can alter flow patterns and velocity distribution. The change in the slope for the velocity gradient observed in the lower canopy region may be due to the presence of secondary currents in the channel. Secondary currents arise from the interaction between primary flow and flow through vegetation, and can have significant impacts on sediment transport and channel morphology (Diplas and Parker, 1992). Lastly, the upper canopy region does not follow the logarithmic law of velocity, consistent with previous observations by Nepf (2012) and Chembolu et al. (2019).

Figure 5.9 illustrates the conceptualization of turbulence effect on the bifurcated channel due to the interaction of flow and different vegetation cover over the mid-bar. The stream-wise velocity and RSS distributions near the canopy top of submerged flexible vegetation arrangements were significantly weaker and more abrupt than those under non-vegetated conditions (Banerjee et al., 2015; Zhu et al., 2015). This is due to the drag produced by the canopy structure and the increased resistance formed by the complex turbulence generated by the vegetation cover (Tang et al., 2020). Additionally, it reduces the energy transfer rate, as well as the mixing and trapping of sediment particles as large-scale vortices are formed (Murphy et al., 2006). It should be noted that the coherent vortices in both the vertical and lateral directions generate simultaneously, resulting in a decrease in total energy and flow velocity (Tang et al., 2023). This has also been observed inside the canopy structure for different vegetation scenario. Additionally, the severity of gradual swaying and local depression in the canopy accelerates turbulence and momentum flux exchange. Vegetation cover over the bar reduces peak turbulent flux penetration, preventing

erosion of the bed (Chembolu et al., 2019). In particular, the presence of different type of vegetation cover create low velocity zones that protect bar material from erosion and encourage mineral and sediment deposition. Furthermore, this eventually creates the favorable ecological zones for aquatic species by regulating the flow of nutrients and maintain a healthy ecological habitat environment.



**Figure 5.9** Conceptualization of the effects of different vegetation form on the turbulence parameter (momentum exchange, shear layer thickness, horizontal and vertical coherent vertex, secondary current etc.) of bifurcated channel of symmetric configuration. The vegetation configuration considered here is: a) No-vegetation; b) rigid vegetation; c) paddy/grass vegetation; d) leafy vegetation.

Since vegetation is difficult to upscale at the scale of natural rivers, interpreting our experimental findings are particularly challenging. Again, in a real river scenario, the non-uniform nature and heterogeneity of vegetation cover is practically impossible to maintain at the flume scale. In the context of natural river systems, the observations highlighted in this chapter cannot be directly extrapolated. Nonetheless, some aspects from the real river system environment were used in this chapter to better investigate the system's behavior. Furthermore, this research can shed light on some important aspects of flow-vegetation interaction and flow-sediment behaviour during flood scenarios. In order to better understand the actual system, it is important to consider the relative effect of vegetation cover arrangements based on river scaling.

## **5.6 CONCLUSIONS**

To simulate the braided loop mechanism, a series of experiments were carried out in a laboratory scale. Three different types of natural vegetation were used on the mid-channel bar, including paddy, leafy, and rigid plants. A detailed flow-turbulence structure of the bifurcated channel was observed to understand how vegetation affected the flow hydrodynamics. Some of the major finding of this chapter are discussed in this section. The percentage variations for leafy, paddy, rigid stem was observed to be about 32%, 28%, and 17% respectively, compared to non-vegetated condition. The leafy vegetation cover showed the higher variation due to its increased drag/resistance to the flow due to its canopy structure. Moreover, the large surface area of leafy fronds in comparison with other vegetation resulted in amplified shear generated turbulence. Consequently, the Reynolds stress can increase, leading to an increase in the fluid's viscous dissipation. When leafy, paddy, and rigid stems are present on the bar, the turbulence intensity variation in the bifurcated channel increases by 11%, 8%, and 3%, respectively, compared with non-vegetated bar. This indicates that there was a significant amount of turbulence mixing in the channel due to leafy vegetation covers. The velocity and Reynold's stress were observed to be weaker and more abrupt in case of flexible vegetation case when compared to non-vegetated condition. Furthermore, the vegetation cover on the bar protects the bar strata from erosion while also regulating sediment and mineral deposition, including the flow of nutrients, and eventually maintaining a healthy ecological habitat environment. This work can be further carried out by considering more real river

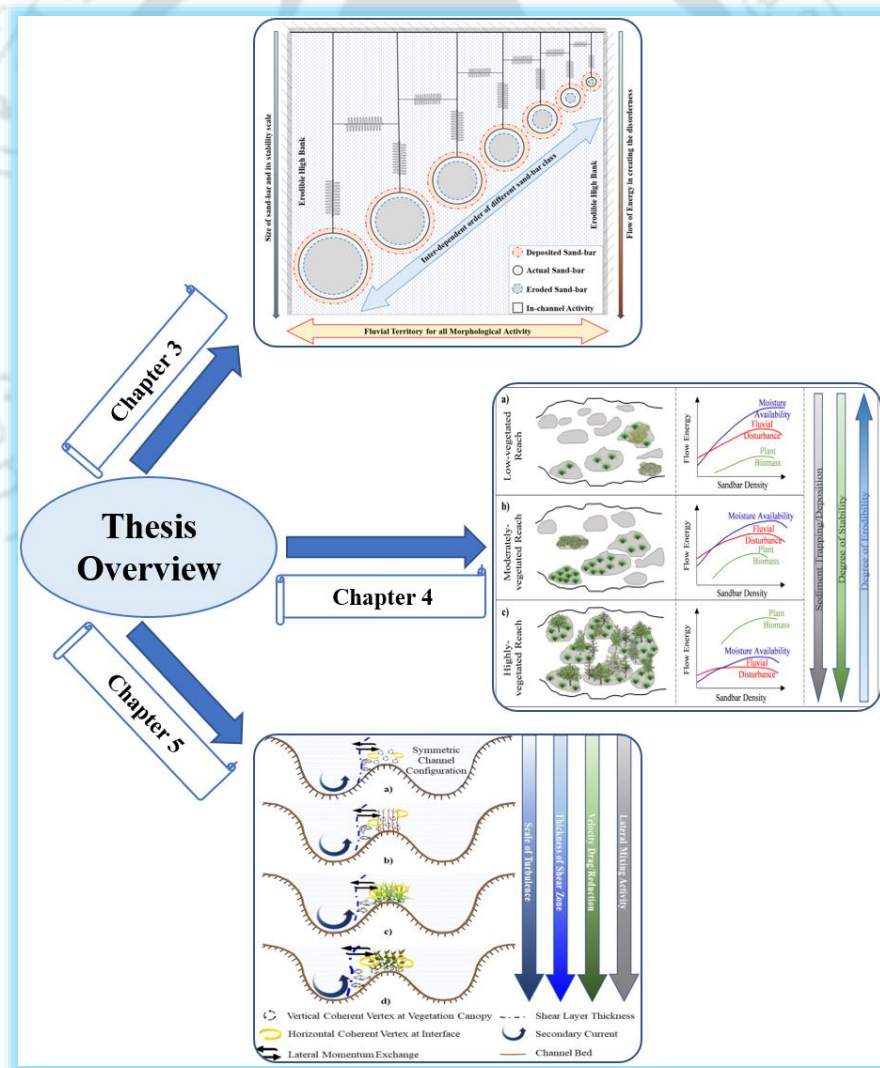
scenario with different bar model setups. It will assist in better comprehending the process-form-interaction of flow-vegetation and may be employed to design proper river ecology and river health management policy. Further research is needed to better understand the complex interplay between vegetation, flow behavior, and channel morphology. Future studies could explore the effects of different vegetation types and configurations on flow patterns and velocity distribution, and investigate the impacts of these factors on sediment transport and channel stability. Overall, this understanding can be instrumental in developing nature-inspired solutions for river restoration and management.





## CONCLUSIONS AND RECOMENDATIONS

(Summary and Future Scope)





## **6.1 CONCLUSIONS**

This research aimed to comprehend the eco-morphodynamics of large braided river systems. The middle reach of Brahmaputra river has been considered for this study. A new methodology based on entropy was developed to understand bar morphology, and the relationship between morphodynamics patterns and in-stream vegetation dynamics was established. The stability trajectory of the braided reach was also identified. Additionally, a loop-scale braided morphodynamics was accessed through laboratory scale experiments using a vegetated mid-channel bar model. The following sub-sections provide a summary of the research, the proposed approaches, and the observations.

### **6.1.1 System disorderness and energy expenditure mechanism in a large braided river**

In this objective, the concept of entropy was introduced to assess the variability of the sand bar over the selected braided planform of the Brahmaputra river. The disorderness of the system has been accessed through the intensity disorder index (IDI). Some of the major findings drawn from the analysis-

- The variations of IDI showed a decreasing trend in 2000-2010, followed by an increasing trend up to 2019, which further signals a decadal shift in morphological stability in the Brahmaputra.
- The frequency of smaller (mobile) bars is high as compared to the medium and larger bars (immobile) in the second time period and controls the IDI variability. The inter-comparison of the two braided sub-reaches showed that the downstream reach had a higher IDI attributed to the prevalence of smaller-sized bars.
- According to different stream power comparison, peak flood stream power was better correlated to IDI variation than monsoon and post-monsoon stream power. This may be credited to the dissection of the larger bars into smaller bars and increased the IDI values in the second period. In addition, the large bars increased their surface area due to the accumulation of sculpted sediment materials from the washed-out smaller bars and eroded cohesive banks for some period.

## *CONCLUSIONS AND RECOMENDATIONS*

- The disorderliness of the braided reach does not fully expend the incoming stream power, but also the additional available fluvial energy may be dissipated by geomorphological activities such as sinuosity alteration, erosion-deposition mechanism, thalweg shifting etc.

### **6.1.2 Vegetation and its impact on stability criteria of a braided reach**

In this objective, an attempted has been made to demonstrate the relationship between morphodynamic patterns and in-stream vegetation dynamics, as well as their impact on the braided reach stabilization processes. This can be effectively applied to the evaluation of the recovery trajectory in weakly or moderately braided systems. The major findings are given below:

- In the last thirty years (1990-2019), the vegetation cover assessment revealed four distinct time periods, with the last decade (2000-2019) displaying no significant change in vegetation cover and erosion or deposition activities compared to the other three time slices.
- The vegetation cover was classified as light, moderate, or dense to understand its importance in the braided river morphodynamics. It was noticed that the combination of moderate and dense vegetation has a higher rate of succession than the light vegetation cover. This owes to the fact that light vegetation is less resilient than moderate and dense vegetation type and gets eroded during higher floods.
- The detailed statistical trend analysis (improved ITA) was performed to understand the succession/reduction patterns of these three types of vegetation covers. The analysis revealed that the light vegetation cover showed a significant decreasing trend, whereas the moderate and dense vegetation cover had a positive increasing trend. The destruction of light vegetation cover increased as the peak discharge increased, and other types may have survived during this period.
- In a large braided river like the Brahmaputra, the transitional behavior of the stability trajectory is related to the combined effect of non-linear hydro-geomorphic constraints like variable climatic conditions, moisture availability, degree of fluvial disturbances and anthropogenic stresses.

### **6.1.3 Morphodynamics of vegetated mid-channel bar**

To simulate the braided loop mechanism, a series of experiments were carried out in a laboratory scale. The purpose is to obtain a better understanding of the process-form-interaction of flow-vegetation, which can then be further utilized to design appropriate river ecology and river health management policies. Some of the major finding of this study are discussed in the following points:

- The percentage variations for leafy, paddy, rigid stem was observed to be about 32%, 28%, and 17% respectively, compared to non-vegetated condition. The leafy vegetation cover showed the higher variation due to its increased drag/resistance to the flow due to its canopy structure.
- Moreover, the large surface area of leafy fronds in comparison with other vegetation resulted in amplified shear generated turbulence. Consequently, the Reynolds stress can increase, leading to an increase in the fluid's viscous dissipation.
- When leafy, paddy, and rigid stems are present on the bar, the turbulence intensity variation in the bifurcated channel increases by 11%, 8%, and 3%, respectively, compared with non-vegetated bar. This indicates that there was a significant amount of turbulence mixing in the channel due to leafy vegetation covers.
- The velocity and Reynold's stress were observed to be weaker and more abrupt in case of flexible vegetation case when compared to non-vegetated condition. Furthermore, the vegetation cover on the bar protects the bar strata from erosion while also regulating sediment and mineral deposition, including the flow of nutrients, and eventually maintaining a healthy ecological habitat environment.

### **6.2 FUTURE RECOMMENDATIONS**

The present research developed and demonstrated the insights into the process-form-vegetation interaction for a large braided Brahmaputra river system. However, still there are some aspects which has to be looked into for better understanding and proper management of large braided river systems. The present research can be extended further with a prime focus on the following aspects and improvements.

## *CONCLUSIONS AND RECOMENDATIONS*

- The proposed entropy-based methodology can be applied to other braided rivers to compare and contrast the findings and to gain a better understanding of the mechanisms that govern the morphodynamics of braided rivers. It can be helpful in quantifying the energy expenditure utilized by different geomorphological activities.
- This study can be extended by exploring impact of anthropogenic activity on braided river morphodynamics that offers insights into morphological shifts, as it has the potential to shape effective management strategies, accounting for both current human interventions and future scenarios.
- In addition, investigate the potential of using artificial intelligence and machine learning techniques to analyze and predict the behavior of braided rivers. Develop and validate models that can accurately simulate the complex interactions between flow, sediment transport, vegetation, and channel morphology.
- Utilization of high-resolution DEM and integration of SWOT satellite mission can provide a better insight to different braiding problems. Furthermore, a thorough reach-scale drone-based survey can be done to access the detailed vegetation dynamics, and proper ecological modelling can be designed which gives the better idea to maintain the river health.
- To gain a more detailed understanding of the interaction between flow and vegetation, future experiments should incorporate heterogeneous patches and variations in density that are similar to natural conditions. Additionally, it is recommended to develop and validate numerical models that are capable of simulating the complex interplay between flow dynamics, sediment transport, vegetation, and channel morphology in braided rivers.

# REFERENCES

- Abbe, T.B. and Montgomery, D.R., 2003. Patterns and processes of wood debris accumulation in the Queets river basin, Washington. *Geomorphology*, 51(1-3), pp.81-107. [https://doi.org/10.1016/S0169-555X\(02\)00326-4](https://doi.org/10.1016/S0169-555X(02)00326-4)
- Akhtar, M.P., Sharma, N.A.Y.A.N. and Ojha, C.S.P., 2011. Braiding process and bank erosion in the Brahmaputra River. *International Journal of Sediment Research*, 26(4), pp.431-444. [https://doi.org/10.1016/S1001-6279\(12\)60003-1](https://doi.org/10.1016/S1001-6279(12)60003-1)
- Alam, J.B., Uddin, M., Ahmed, J.U., Cacovean, H., Rahman, H.M., Banik, B.K. and Yesmin, N., 2007. Study of morphological change of river old Brahmaputra and its social impacts by remote sensing. *Geographia Technica*, 2, pp.1-11.
- Allmendinger, N.E., Pizzuto, J.E., Potter Jr, N., Johnson, T.E. and Hession, W.C., 2005. The influence of riparian vegetation on stream width, eastern Pennsylvania, USA. *Geological Society of America Bulletin*, 117(1-2), pp.229-243. <https://doi.org/10.1130/B25447.1>
- An, H.P., Chen, S.C., Chan, H.C. and Yi, H.S.U., 2013. Dimension and frequency of bar formation in a braided river. *International Journal of Sediment Research*, 28(3), pp.358-367. [https://doi.org/10.1016/S1001-6279\(13\)60046-3](https://doi.org/10.1016/S1001-6279(13)60046-3)
- Archana, S., RD, G. and Nayan, S., 2012. RS-GIS based assessment of river dynamics of Brahmaputra River in India. *Journal of Water Resource and Protection*, 2012. <http://dx.doi.org/10.4236/jwarp.2012.42008>
- Asahi, K., Shimizu, Y., Nelson, J., and Parker, G., 2013. Numerical simulation of river meandering with self-evolving banks. *Journal of Geophysical Research: Earth Surface*, 118(4), 2208-2229. <https://doi.org/10.1002/jgrf.20150>
- Ashmore, P., 1991b. Channel morphology and bed load pulses in braided, gravel-bed streams. *Geografiska Annaler: Series A, Physical Geography*, 73(1), 37-52. <https://doi.org/10.1080/04353676.1991.11880331>
- Ashmore, P., 1993. Anabranch confluence kinetics and sedimentation processes in gravel-braided streams. *Geological Society, London, Special Publications*, 75(1), 129-146. <https://doi.org/10.1144/GSL.SP.1993.075.01.08>
- Ashmore, P.E., 1982. Laboratory modelling of gravel braided stream morphology. *Earth Surface Processes and Landforms*, 7(3), 201-225. <https://doi.org/10.1002/esp.3290070301>
- Ashmore, P.E., 1988. Bed load transport in braided gravel-bed stream models. *Earth Surface Processes and Landforms*, 13(8), 677-695. <https://doi.org/10.1002/esp.3290130803>
- Ashmore, P.E., 1991a. How do gravel-bed rivers braid? *Canadian journal of earth sciences*, 28(3), 326-341. <https://doi.org/10.1139/e91-030>
- Ashmore, P.E., 2013. *Treatise on Geomorphology*, chap. Morphology and Dynamics of Braided Rivers, 289-312. <https://doi.org/10.1016/B978-0-12-374739-6.00242-6>
- Ashmore, P.E., Ferguson, R.I., Prestegard, K.L., Ashworth, P.J., and Paola, C., 1992. Secondary flow in anabranch confluences of a braided, gravel-bed stream. *Earth Surface Processes and Landforms*, 17(3), 299-311. <https://doi.org/10.1002/esp.3290170308>
- Ashmore, P., and Gardner, J.T., 2008. Unconfined confluences in braided rivers. *River confluences, tributaries and the fluvial network*, 119-147. <https://doi.org/10.1002/9780470760383.ch7>
- Ashmore, P., and Parker, G., 1983. Confluence scour in coarse braided streams. *Water Resources Research*, 19(2), 392-402. <https://doi.org/10.1029/WR019i002p00392>
- Ashmore, P., 1993. Anabranch confluence kinetics and sedimentation processes in gravel-braided streams. *Geological Society, London, Special Publications*, 75(1), pp.129-146. <https://doi.org/10.1144/GSL.SP.1993.075.01.08>

- Ashmore, P., 2013. Treatise on Geomorphology, chap. Morphology and Dynamics of Braided Rivers, 289–312. <https://doi.org/10.1016/B978-0-12-374739-6.00242-6>
- Ashmore, P.E., 1982. Laboratory modelling of gravel braided stream morphology. *Earth Surface Processes and Landforms*, 7(3), pp.201–225. <https://doi.org/10.1002/esp.3290070301>
- Ashworth, P.J., Best, J.L., Roden, J.E., Bristow, C.S., and Klaassen, G.J., 2000. Morphological evolution and dynamics of a large, sand braid-bar, Jamuna River, Bangladesh. *Sedimentology*, 47(3), 533–555. <https://doi.org/10.1046/j.1365-3091.2000.00305.x>
- Ashworth, P.J., Ferguson, R.I., Ashmore, P.E., Paola, C., Powell, D.M., and Prestegards, K.L., 1992. Measurements in a braided river chute and lobe: 2. Sorting of bed load during entrainment, transport, and deposition. *Water Resources Research*, 28(7), 1887–1896. <https://doi.org/10.1029/92WRO0702>
- Ashworth, P.J. and Lewin, J., 2012. How do big rivers come to be different? *Earth–Science Reviews*, 114(1–2), pp.84–107. <https://doi.org/10.1016/j.earscirev.2012.05.003>
- Ayman, A.A., and Ahmed, F., 2009. Meandering and bank erosion of the River Nile and its environmental impact on the area between Sohag and El-Minia, Egypt. *Arab. J. Geosci*, 4(1), 1–11. <https://doi.org/10.1007/s12517-009-0048-y>
- Bagnold, R.A., 1966. An approach to the sediment transport problem from general physics. US government printing office. pp. 231–291.
- Bagnold, R.A., 1977. Bed load transport by natural rivers. *Water resources research*, 13(2), pp.303–312. <https://doi.org/10.1029/WR013i002p00303>
- Baki, A.B.M. and Gan, T.Y., 2012. Riverbank migration and island dynamics of the braided Jamuna River of the Ganges–Brahmaputra basin using multi-temporal Landsat images. *Quaternary International*, 263, pp.148–161. <https://doi.org/10.1016/j.quaint.2012.03.016>
- Bandyopadhyay, S., Sinha, S., Jana, N.C. and Ghosh, D., 2014. Entropy application to evaluate the stability of landscape in Kunur River Basin, West Bengal, India. *Current Science*, pp.1842–1853. <https://www.jstor.org/stable/24107829>
- Banerjee, T., Muste, M., and Katul, G., 2015. Flume experiments on wind induced flow in static water bodies in the presence of protruding vegetation. *Advances in Water Resources*, 76, 11–28. <https://doi.org/10.1016/j.advwatres.2014.11.010>
- Baptist, M.J., 2003, February. A flume experiment on sediment transport with flexible, submerged vegetation. In *International workshop on riparian forest vegetated channels: hydraulic, morphological and ecological aspects*, RIPFOR, Trento, Italy. <https://doi.org/10.1016/j.quaint.2012.03.016>
- Barbhuiya, F., 2015. Natural disaster, especially flood and its management in India: with special reference to Assam. *International Journal of Humanities and Social Science Studies*, 2(3): 289, 299.
- Basumatary, H., Sah, R.K. and Das, A.K., 2021. Bankline dynamics and their effects on protected areas along the Brahmaputra river. *CATENA*, 197, p.104947. <https://doi.org/10.1016/j.catena.2020.104947>
- Bawa, N., Jain, V., Shekhar, S., Kumar, N. and Jyani, V., 2014. Controls on morphological variability and role of stream power distribution pattern, Yamuna River, western India. *Geomorphology*, 227, pp.60–72. <https://doi.org/10.1016/j.geomorph.2014.05.016>
- Belletti, B., Dufour, S., and Piégay, H., 2014. Regional assessment of the multi-decadal changes in braided riverscapes following large floods (Example of 12 reaches in South East of France). *Advances in Geosciences*, 37, 57–71. <https://doi.org/10.5194/adgeo-37-57-2014>
- Belletti, B., Dufour, S., and Piégay, H., 2015. What is the relative effect of space and time to explain the braided river width and island patterns at a regional scale? *River Research and Applications*, 31(1), 1–15. <https://doi.org/10.1002/rra.2714>
- Bennett, S.J., and Simon, A., 2004. *Riparian vegetation and fluvial geomorphology* (Vol. 8). American Geophysical Union.

- Bennett, S.J., Pirim, T., and Barkdoll, B. D., 2002. Using simulated emergent vegetation to alter stream flow direction within a straight experimental channel. *Geomorphology*, 44(1–2), 115–126. [https://doi.org/10.1016/S0169-555X\(01\)00148-9](https://doi.org/10.1016/S0169-555X(01)00148-9)
- Bertagni, M.B., Perona, P., and Camporeale, C., 2018. Parametric transitions between bare and vegetated states in water-driven patterns. *Proceedings of the National Academy of Sciences*, 115(32), 8125–8130. <https://doi.org/10.1073/pnas.1721765115>
- Bertoldi, W., and Gurnell, A.M., 2020. Physical engineering of an island-braided river by two riparian tree species: Evidence from aerial images and airborne lidar. *River Research and Applications*, 36(7), 1183–1201. <https://doi.org/10.1002/rra.3657>
- Bertoldi, W., and Tubino, M., 2007. River bifurcations: Experimental observations on equilibrium configurations. *Water Resources Research*, 43(10). <https://doi.org/10.1029/2007WR005907>
- Bertoldi, W., Drake, N.A., and Gurnell, A.M., 2011. Interactions between river flows and colonizing vegetation on a braided river: exploring spatial and temporal dynamics in riparian vegetation cover using satellite data. *Earth Surface Processes and Landforms*, 36(11), 1474–1486. <https://doi.org/10.1002/esp.2166>
- Bertoldi, W., Gurnell, A., Surian, N., Tockner, K., Zanoni, L., Ziliani, L., and Zolezzi, G., 2009a. Understanding reference processes: linkages between river flows, sediment dynamics and vegetated landforms along the Tagliamento River, Italy. *River Research and Applications*, 25(5), 501–516. <https://doi.org/10.1002/rra.1233>
- Bertoldi, W., Siviglia, A., Tettamanti, S., Toffolon, M., Vetsch, D., and Francalanci, S., 2014. Modeling vegetation controls on fluvial morphological trajectories. *Geophysical Research Letters*, 41(20), 7167–7175. <https://doi.org/10.1002/2014GL061666>
- Bertoldi, W., Zanoni, L., and Tubino, M., 2009b. Planform dynamics of braided streams. *Earth Surface Processes and Landforms*, 34(4), 547–557. <https://doi.org/10.1002/esp.1755>
- Best, J.L., 1986. The morphology of river channel confluences. *Progress in Physical Geography*, 10(2), 157–174. <https://doi.org/10.1177/027030913338601000201>
- Best, J.L., Ashworth, P.J., Sarker, M.H. and Roden, J.E., 2007. The Brahmaputra–Jamuna River, Bangladesh. *Large rivers: geomorphology and management*, pp.395–430.
- Biron, P.M., Buffin-Bélanger, T., Larocque, M., Choné, G., Cloutier, C.A., Ouellet, M.A., Demers, S., Olsen, T., Desjarlais, C. and Eyquem, J., 2014. Freedom space for rivers: a sustainable management approach to enhance river resilience. *Environmental management*, 54(5), pp.1056–1073. <https://doi.org/10.1007/s00267-014-0366-z>
- Biswas, R.K., Yorozuya, A., and Egashira, S., 2016. Numerical model for bank erosion in the brahmaputra river. *Journal of Disaster Research*, 11(6), 1073–1081. <https://doi.org/10.20965/jdr.2016.p1073>
- Bizzi, S., and Lerner, D.N., 2012. Characterizing physical habitats in rivers using map-derived drivers of fluvial geomorphic processes. *Geomorphology*, 169, 64–73. <https://doi.org/10.1016/j.geomorph.2012.04.009>
- Bolla Pittaluga, M., Repetto, R., and Tubino, M., 2001, September. Channel bifurcation in one-dimensional models: a physically based nodal point condition. In *Proc. IAHR Symp. River, Coastal and Estuarine Morphodynamics* (pp. 10–14).
- Bolla Pittaluga, M., Repetto, R., and Tubino, M., 2003. Channel bifurcation in braided rivers: Equilibrium configurations and stability. *Water Resources Research*, 39(3). <https://doi.org/10.1029/2001WR001112>
- Booth, E.G. and Loheide, S.P., 2012. Comparing surface effective saturation and depth-to-water-level as predictors of plant composition in a restored riparian wetland. *Ecohydrology*, 5(5), pp.637–647. <https://doi.org/10.1002/eco.250>
- Boothroyd, R.J., Williams, R.D., Hoey, T.B., Tolentino, P.L. and Yang, X., 2021. National-scale assessment of decadal river migration at critical bridge infrastructure in the Philippines.

Science of the Total Environment, 768, p.144460.  
<https://doi.org/10.1016/j.scitotenv.2020.144460>

- Borah, M., Das, D., Kalita, J., Boruah, H.P.D., Phukan, B. and Neog, B., 2015. Tree species composition, biomass and carbon stocks in two tropical forest of Assam. *biomass and bioenergy*, 78, pp.25–35. <https://doi.org/10.1016/j.biombioe.2015.04.007>
- Borghain, S., Das, J., Saraf, A.K., Singh, G. and Baral, S.S., 2017. Structural controls on topography and river morphodynamics in Upper Assam Valley, India. *Geodinamica acta*, 29(1), pp.62–69. <https://doi.org/10.1080/09853111.2017.1313090>
- Bornette, G., and Puijalon, S., 2011. Response of aquatic plants to abiotic factors: a review. *Aquatic sciences*, 73(1), 1–14. <https://doi.org/10.1007/s00027-010-0162-7>
- Borogayary, B., Das, A.K. and Nath, A.J., 2018. Tree species composition and population structure of a secondary tropical evergreen forest in Cachar district, Assam. *Journal of Environmental Biology*, 39(1), pp.67–71.
- Boruah, S., Gilvear, D., Hunter, P., and Sharma, N., 2008. Quantifying channel planform and physical habitat dynamics on a large braided river using satellite data—The Brahmaputra, India. *River research and applications*, 24(5), 650–660. <https://doi.org/10.1002/rra.1132>
- Boyer, C., Roy, A.G., and Best, J.L., 2006. Dynamics of a river channel confluence with discordant beds: Flow turbulence, bed load sediment transport, and bed morphology. *Journal of Geophysical Research: Earth Surface*, 111(F4). <https://doi.org/10.1029/2005JF000458>
- Brachet, C., 2015. *The Handbook for Management and Restoration of Aquatic Ecosystems in river and lake basins*.
- Brasington, J., and Richards, K., 2007. Reduced-complexity, physically-based geomorphological modelling for catchment and river management. <https://doi.org/10.1016/j.geomorph.2006.10.028>
- Brebner, A. and Wilson, K.C., 1967. Derivation of the regime equations from relationships for pressurized flow by use of the principle of minimum energy-degradation rate. *Proceedings of the Institution of Civil Engineers*, 36(1), pp.47–62. <https://doi.org/10.1680/iicep.1967.8590>
- Bridge, J.S., 1993. The interaction between channel geometry, water flow, sediment transport and deposition in braided rivers. *Geological Society, London, Special Publications*, 75(1), 13–71. <https://doi.org/10.1144/GSL.SP.1993.075.01.02>
- Bridge, J.S., 2003. *Rivers and floodplains. Forms, Processes and Sedimentary Record* Blackwell Science. New York, 491.
- Bridge, J.S., 2009. *Rivers and floodplains: forms, processes, and sedimentary record*. John Wiley and Sons.
- Bridge, J.S., and Lunt, I. A., 2006. Depositional models of braided rivers. In *Braided rivers: Process, deposits, ecology and management* (Vol. 36, pp. 11–50). Special Publication 36: International Association of Sedimentologists. <https://doi.org/10.1002/9781444304374.ch2>
- Bristow, C.S., and Best, J.L., 1993. Braided rivers: perspectives and problems. *Geological society, London, special publications*, 75(1), 1–11. <https://doi.org/10.1144/GSL.SP.1993.075.01.01>
- Brunsdon, D., 2001. A critical assessment of the sensitivity concept in geomorphology. *Catena*, 42(2–4), pp.99–123. [https://doi.org/10.1016/S0341-8162\(00\)00134-X](https://doi.org/10.1016/S0341-8162(00)00134-X)
- Bull, W.B., 1979. Threshold of critical power in streams. *Geological Society of America Bulletin*, 90(5), pp.453–464. [https://doi.org/10.1130/0016-7606\(1979\)90%3C453:TOCPIS%3E2.0.CO;2](https://doi.org/10.1130/0016-7606(1979)90%3C453:TOCPIS%3E2.0.CO;2)
- Bywater-Reyes, S., Diehl, R.M., and Wilcox, A.C., 2018. The influence of avegetated bar on channel-bend flow dynamics. *Earth Surface Dynamics*, 6(2), 487–503. <https://doi.org/10.5194/esurf-6-487-2018>

- Camporeale, C. and Ridolfi, L., 2006. Riparian vegetation distribution induced by river flow variability: A stochastic approach. *Water resources research*, 42(10). <https://doi.org/10.1029/2006WR004933>
- Camporeale, C., Perona, P., and Ridolfi, L., 2019. Hydrological and geomorphological significance of riparian vegetation in drylands, (2nd ed.). In D'Odorico, P., Porporato, A., and Wilkinson, C. R. (Eds.), *Dryland hydrology*: Springer International Publishing, pp. 239–275. [https://doi.org/10.1007/978-3-030-23269-6\\_10](https://doi.org/10.1007/978-3-030-23269-6_10)
- Camporeale, C., Perucca, E., Ridolfi, L. and Gurnell, A.M., 2013. Modeling the interactions between river morphodynamics and riparian vegetation. *Reviews of Geophysics*, 51(3), pp.379–414. <https://doi.org/10.1002/rog.20014>
- Chang, H.H., 1979. Minimum stream power and river channel patterns. *Journal of Hydrology*, 41(3–4), pp.303–327. [https://doi.org/10.1016/0022-1694\(79\)90068-4](https://doi.org/10.1016/0022-1694(79)90068-4)
- Charlton, R., 2007. *Fundamentals of fluvial geomorphology*. Routledge. <https://doi.org/10.4324/9780203371084>
- Chembolu, V. and Dutta, S., 2018. An entropy based morphological variability assessment of a large braided river. *Earth Surface Processes and Landforms*, 43(14), pp.2889–2896. <https://doi.org/10.1002/esp.4441>
- Chembolu, V., and Dutta, S., 2016. Entropy and energy dissipation of a braided river system. *Procedia Engineering*, 144, 1175–1179. <https://doi.org/10.1016/j.proeng.2016.05.094>
- Chembolu, V., and Dutta, S., 2020. Hydrodynamics of heterogeneous vegetation patches. In *River Flow 2020* (pp. 1523–1526). CRC Press.
- Chembolu, V., Kakati, R., and Dutta, S., 2019. A laboratory study of flow characteristics in natural heterogeneous vegetation patches under submerged conditions. *Advances in Water Resources*, 133, 103418. <https://doi.org/10.1016/j.advwatres.2019.103418>
- Chen, S.C., Kuo, Y.M., and Li, Y.H., 2011. Flow characteristics within different configurations of submerged flexible vegetation. *Journal of Hydrology*, 398(1–2), 124–134. <https://doi.org/10.1016/j.jhydrol.2010.12.018>
- Chen, Z., Jiang, C., and Nepf, H., 2013. Flow adjustment at the leading edge of a submerged aquatic canopy. *Water Resources Research*, 49(9), 5537–5551. <https://doi.org/10.1002/wrcr.20403>
- Chorley, R.J., 1962. *Geomorphology and general systems theory*. U. S Geol. Survey Prof. Paper 500-B.
- Claps, P., Fiorentino, M. and Oliveto, G., 1996. Informational entropy of fractal river networks. *Journal of Hydrology*, 187(1–2), pp.145–156. [https://doi.org/10.1016/S0022-1694\(96\)03092-2](https://doi.org/10.1016/S0022-1694(96)03092-2)
- Coleman, J.M., 1969. Brahmaputra River: channel processes and sedimentation. *Sedimentary geology*, 3(2–3), pp.129–239. [https://doi.org/10.1016/0037-0738\(69\)90010-4](https://doi.org/10.1016/0037-0738(69)90010-4)
- Corenblit, D., and Steiger, J., 2009. Vegetation as a major conductor of geomorphic changes on the Earth surface: toward evolutionary geomorphology. *Earth Surface Processes and Landforms*, 34(6), 891–896. <https://doi.org/10.1002/esp.1788>
- Corenblit, D., Steiger, J., Gurnell, A.M., Tabacchi, E. and Roques, L., 2009. Control of sediment dynamics by vegetation as a key function driving biogeomorphic succession within fluvial corridors. *Earth Surface Processes and Landforms: The Journal of the British Geomorphological Research Group*, 34(13), pp.1790–1810. <https://doi.org/10.1002/esp.1876>
- Corenblit, D., Tabacchi, E., Steiger, J. and Gurnell, A.M., 2007. Reciprocal interactions and adjustments between fluvial landforms and vegetation dynamics in river corridors: a review of complementary approaches. *Earth-Science Reviews*, 84(1–2), pp.56–86. <https://doi.org/10.1016/j.earscirev.2007.05.004>
- Cotton, J.A., Wharton, G., Bass, J.A.B., Heppell, C.M., and Wotton, R.S., 2006. The effects of seasonal changes to in-stream vegetation cover on patterns of flow and accumulation of

- sediment. *Geomorphology*, 77 (3–4), 320–334.  
<https://doi.org/10.1016/j.geomorph.2006.01.010>
- Coulthard, T.J., 2005. Effects of vegetation on braided stream pattern and dynamics. *Water Resources Research*, 41(4). <https://doi.org/10.1029/2004WR003201>
- Crosato, A. and Saleh, M.S., 2011. Numerical study on the effects of floodplain vegetation on river planform style. *Earth Surface Processes and Landforms*, 36(6), pp.711–720.  
<https://doi.org/10.1002/esp.2088>
- Crouzy, B., Wüthrich, D., Perona, P. and D'Odorico, P., 2014. Ecomorphodynamic conditions for the emergence of river anabranching patterns. In 7th International Conference on Fluvial Hydraulics, RIVER FLOW 2014 (pp. 1119–1125). CRC Press/Balkema.
- Curran, J.C., and Hession, W.C., 2013. Vegetative impacts on hydraulics and sediment processes across the fluvial system. *Journal of Hydrology*, 505, 364–376.  
<https://doi.org/10.1016/j.jhydrol.2013.10.013>
- Davoren, A., and Mosley, M.P., 1986. Observations of bedload movement, bar development and sediment supply in the braided Ohau River. *Earth Surface Processes and Landforms*, 11(6), 643–652. <https://doi.org/10.1002/esp.3290110607>
- Deng, S., Xia, J., and Zhou, M., 2019. Coupled two-dimensional modeling of bed evolution and bank erosion in the Upper JingJiang Reach of Middle Yangtze River. *Geomorphology*, 344, 10–24. <https://doi.org/10.1016/j.geomorph.2019.07.010>
- Devi, T.B., 2016. Hydrodynamics of vegetative channel with downward seepage (Doctoral dissertation).
- Devi, T.B., and Kumar, B., 2016. Experimentation on submerged flow over flexible vegetation patches with downward seepage. *Ecological Engineering*, 91, 158–168.  
<https://doi.org/10.1016/j.ecoleng.2016.02.045>
- Devi, T.B., Daga, R., Mahto, S.K., and Kumar, B., 2016. Drag and turbulent characteristics of mobile bed channel with mixed vegetation densities under downward seepage. *Journal of Fluids Engineering*, 138(7). <https://doi.org/10.1115/1.4032753>
- DeVries, B., Huang, C., Armston, J., Huang, W., Jones, J.W. and Lang, M.W., 2020. Rapid and robust monitoring of flood events using Sentinel-1 and Landsat data on the Google Earth Engine. *Remote Sensing of Environment*, 240, p.111664.  
<https://doi.org/10.1016/j.rse.2020.111664>
- Dey, S., Das, R., Gaudio, R., and Bose, S.K., 2012. Turbulence in mobile-bed streams. *Acta Geophysica*, 60(6), 1547–1588. <https://doi.org/10.2478/s11600-012-0055-3>
- Dietrich, W.E. and Smith, J.D., 1984. Bed load transport in a river meander. *Water Resources Research*, 20(10), pp.1355–1380. <https://doi.org/10.1029/WR020i010p01355>
- Dikshit, K.R. and Dikshit, J.K., 2014. Natural vegetation: forests and grasslands of North-East India. In *North-East India: Land, People and Economy* (pp. 213–255). Springer, Dordrecht.  
[https://doi.org/10.1007/978-94-007-7055-3\\_9](https://doi.org/10.1007/978-94-007-7055-3_9)
- Diplas, P. and Parker, G., 1992. Deposition and removal of fines in gravel-bed streams. *Dynamics of gravel-bed rivers*, pp.313–329.
- Dosskey, M. G., Vidon, P., Gurwick, N.P., Allan, C.J., Duval, T.P., and Lowrance, R., 2010. The role of riparian vegetation in protecting and improving chemical water quality in streams 1. *JAWRA Journal of the American Water Resources Association*, 46(2), 261–277.  
<https://doi.org/10.1111/j.1752-1688.2010.00419.x>
- Dubey, A.K., Chembolu, V., and Dutta, S., 2020. Utilization of satellite altimetry retrieved river roughness properties in hydraulic flow modelling of braided river system. *International Journal of River Basin Management*, 1–14. <https://doi.org/10.1080/15715124.2020.1830785>
- Dubey, A.K., Gupta, P., Dutta, S., and Kumar, B., 2014. Evaluation of satellite-altimetry-derived river stage variation for the braided Brahmaputra River. *International journal of remote sensing*, 35(23), 7815–7827. <https://doi.org/10.1080/01431161.2014.978033>

- Dubey, A.K., Kumar, P., Chembolu, V., Dutta, S., Singh, R.P., and Rajawat, A.S., 2021. Flood modeling of a large transboundary river using WRF–Hydro and microwave remote sensing. *Journal of Hydrology*, 598, 126391. <https://doi.org/10.1016/j.jhydrol.2021.126391>
- Dutta, S., Medhi, H., Karmaker, T., Singh, Y., Prabu, I. and Dutta, U., 2010. Probabilistic flood hazard mapping for embankment breaching. *ISH Journal of Hydraulic Engineering*, 16(sup1), pp.15–25. <https://doi.org/10.1080/09715010.2010.10515012>
- Eaton, B.C., 2006. Bank stability analysis for regime models of vegetated gravel bed rivers. *Earth Surface Processes and Landforms: The Journal of the British Geomorphological Research Group*, 31(11), pp.1438–1444. <https://doi.org/10.1002/esp.1364>
- Evette, A., Balique, C., Lavaine, C., Rey, F. and Prunier, P., 2012. Using ecological and biogeographical features to produce a typology of the plant species used in bioengineering for riverbank protection in Europe. *River Research and Applications*, 28(10), pp.1830–1842. <https://doi.org/10.1002/rra.1560>
- Federici, B., and Paola, C., 2003. Dynamics of channel bifurcations in noncohesive sediments. *Water Resources Research*, 39(6). <https://doi.org/10.1029/2002WR001434>
- Ferguson, R.I., 1993. Understanding braiding processes in gravel–bed rivers: progress and unsolved problems. Geological Society, London, Special Publications, 75(1), 73–87. <https://doi.org/10.1144/GSL.SP.1993.075.01.03>
- Ferguson, R.I., Ashmore, P.E., Ashworth, P.J., Paola, C., and Prestegard, K.L., 1992. Measurements in a braided river chute and lobe: 1. Flow pattern, sediment transport, and channel change. *Water Resources Research*, 28(7), 1877–1886. <https://doi.org/10.1029/92WR00700>
- Ferguson, R.I., 1987. Hydraulic and sedimentary controls of channel pattern. *River channels: Environments and processes*, pp.129–158.
- Fielding, C.R., Alexander, J. and Newman–Sutherland, E., 1997. Preservation of in situ, arborescent vegetation and fluvial bar construction in the Burdekin River of north Queensland, Australia. *Palaeogeography, Palaeoclimatology, Palaeoecology*, 135(1–4), pp.123–144. [https://doi.org/10.1016/S0031-0182\(97\)00022-9](https://doi.org/10.1016/S0031-0182(97)00022-9)
- Fiorentino, M., Claps, P. and Singh, V.P., 1993. An entropy-based morphological analysis of river basin networks. *Water Resources Research*, 29(4), pp.1215–1224. <https://doi.org/10.1029/92WR02332>
- Fischer, S., Pietroń, J., Bring, A., Thorslund, J., and Jarsjö, J., 2017. Present to future sediment transport of the Brahmaputra River: reducing uncertainty in predictions and management. *Regional Environmental Change*, 17(2), 515–526. <https://doi.org/10.1007/s10113-016-1039-7>
- Fotherby, L.M., 2009. Valley confinement as a factor of braided river pattern for the Platte River. *Geomorphology*, 103(4), pp.562–576. <https://doi.org/10.1016/j.geomorph.2008.08.001>
- Fryirs, K.A., and Brierley, G.J., 2012. *Geomorphic analysis of river systems: an approach to reading the landscape*. John Wiley and Sons.
- Fryirs, K., Lisenby, P. and Croke, J., 2015. Morphological and historical resilience to catastrophic flooding: the case of Lockyer Creek, SE Queensland, Australia. *Geomorphology*, 241, pp.55–71. <https://doi.org/10.1016/j.geomorph.2015.04.008>
- Fu, B. and Burgher, I., 2015. Riparian vegetation NDVI dynamics and its relationship with climate, surface water and groundwater. *Journal of Arid Environments*, 113, pp.59–68. <https://doi.org/10.1016/j.jaridenv.2014.09.010>
- Gao, P., Li, Z., You, Y., Zhou, Y. and Piégay, H., 2022. Assessing functional characteristics of a braided river in the Qinghai–Tibet Plateau, China. *Geomorphology*, 403, p.108180. <https://doi.org/10.1016/j.geomorph.2022.108180>
- Gautier, E., Piégay, H. and Bertaina, P., 2000. A methodological approach of fluvial dynamics oriented towards hydrosystem management: case study of the Loire and Allier rivers. *Geodinamica Acta*, 13(1), pp.29–43. <https://doi.org/10.1080/09853111.2000.11105360>

- Gibling, M.R., Davies, N.S., Falcon-Lang, H.J., Bashforth, A.R., DiMichele, W.A., Rygel, M.C. and Ielpi, A., 2014. Palaeozoic co-evolution of rivers and vegetation: a synthesis of current knowledge. *Proceedings of the Geologists' Association*, 125(5–6), pp.524–533. <https://doi.org/10.1016/j.pgeola.2013.12.003>
- Gibson, L.J., 2012. The hierarchical structure and mechanics of plant materials. *Journal of the royal society interface*, 9(76), 2749–2766. <https://doi.org/10.1098/rsif.2012.0341>
- Gillfellow, G.B., Sarma, J.N. and Gohain, K., 2003. Channel and bed morphology of a part of the Brahmaputra River in Assam. *Journal-Geological Society of India*, 62(2), pp.227–236.
- Goff, J.R., and Ashmore, P., 1994. Gravel transport and morphological change in braided Sunwapta River, Alberta, Canada. *Earth Surface Processes and Landforms*, 19(3), 195–212. <https://doi.org/10.1002/esp.3290190302>
- González, E., Martínez-Fernández, V., Shafroth, P.B., Sher, A.A., Henry, A.L., Garófano-Gómez, V., and Corenblit, D., 2018. Regeneration of Salicaceae riparian forests in the Northern Hemisphere: A new framework and management tool. *Journal of environmental management*, 218, 374–387. <https://doi.org/10.1016/j.jenvman.2018.04.069>
- Gonzalez, E., Shafroth, P.B., Lee, S.R., Leverich, G.T., Real De Asua, R., Sherry, R.A., Ostoja, S.M. and Orr, B.K., 2019. Short-term geomorphological and riparian vegetation responses to a 40-year flood on a braided, dryland river. *Ecohydrology*, 12(8), p.e2152. <https://doi.org/10.1002/eco.2152>
- Gorelick, N., Hancher, M., Dixon, M., Ilyushchenko, S., Thau, D. and Moore, R., 2017. Google Earth Engine: Planetary-scale geospatial analysis for everyone. *Remote sensing of Environment*, 202, pp.18–27. <https://doi.org/10.1016/j.rse.2017.06.031>
- Goring, D.G., and Nikora, V.I., 2002. Despiking acoustic Doppler velocimeter data. *Journal of hydraulic engineering*, 128(1), 117–126. [https://doi.org/10.1061/\(ASCE\)0733-9429\(2002\)128:1\(117\)](https://doi.org/10.1061/(ASCE)0733-9429(2002)128:1(117))
- Goswami, D.C., 1985. Brahmaputra River, Assam, India: Physiography, basin denudation, and channel aggradation. *Water Resources Research*, 21(7), 959–978. <https://doi.org/10.1029/WR021i007p00959>
- Gran, K., and Paola, C., 2001. Riparian vegetation controls on braided stream dynamics. *Water Resources Research*, 37(12), 3275–3283. <https://doi.org/10.1029/2000WR000203>
- Green, J.C., 2005. Further comment on drag and reconfiguration of macrophytes. *Freshwater Biology*, 50(12), 2162–2166. <https://doi.org/10.1111/j.1365-2427.2005.01470.x>
- Güçlü, Y.S., 2020. Improved visualization for trend analysis by comparing with classical Mann-Kendall test and ITA. *Journal of Hydrology*, 584, p.124674. <https://doi.org/10.1016/j.jhydrol.2020.124674>
- Gul, A. A., Yorozyua, A., Koseki, H., Egashira, S., and Okada, S., 2018. Analysis of bedform and boil based on observations in Brahmaputra river. *Journal of Japan Society of Civil Engineers, Ser. B1 (Hydraulic Engineering)*, 74(5), 1\_925–1\_930. [https://doi.org/10.2208/jscejhe.74.5\\_1\\_925](https://doi.org/10.2208/jscejhe.74.5_1_925)
- Gurbisz, C., Kemp, W.M., Cornwell, J.C., Sanford, L.P., Owens, M.S., and Hinkle, D.C., 2017. Interactive effects of physical and biogeochemical feedback processes in a large submersed plant bed. *Estuaries and Coasts*, 40(6), 1626–1641. <https://doi.org/10.1007/s12237-017-0249-7>
- Gurbisz, C., Kemp, W.M., Sanford, L.P., and Orth, R.J., 2016. Mechanisms of storm-related loss and resilience in a large submersed plant bed. *Estuaries and Coasts*, 39(4), 951–966. <https://doi.org/10.1007/s12237-016-0074-4>
- Gurnell, A., 2014. Plants as river system engineers. *Earth Surface Processes and Landforms*, 39(1), 4–25. <https://doi.org/10.1002/esp.3397>
- Gurnell, A.M., and Petts, G.E., 2002. Island-dominated landscapes of large floodplain rivers: A European perspective. *Freshwater Biology*, 47(4), 581–600. <https://doi.org/10.1046/j.1365-2427.2002.00923.x>

- Gurnell, A.M., Bertoldi, W., and Corenblit, D., 2012. Changing river channels: The roles of hydrological processes, plants and pioneer fluvial landforms in humid temperate, mixed load, gravel bed rivers. *Earth-Science Reviews*, 111(1-2), 129-141. <https://doi.org/10.1016/j.earscirev.2011.11.005>
- Gurnell, A.M., Petts, G.E., Harris, N., Ward, J.V., Tockner, K., Edwards, P.J., and Kollmann, J., 2000. Large wood retention in river channels: the case of the Fiume Tagliamento, Italy. *Earth Surface Processes and Landforms*, 25(3), 255-275. [https://doi.org/10.1002/\(SICI\)1096-9837\(200003\)25:3%3C255::AID-ESP56%3E3.0.CO;2-H](https://doi.org/10.1002/(SICI)1096-9837(200003)25:3%3C255::AID-ESP56%3E3.0.CO;2-H)
- Gurnell, A., and Petts, G., 2006. Trees as riparian engineers: the Tagliamento River, Italy. *Earth Surface Processes and Landforms: The Journal of the British Geomorphological Research Group*, 31(12), 1558-1574. <https://doi.org/10.1002/esp.1342>
- Gurnell, A., Tockner, K., Edwards, P. and Petts, G., 2005. Effects of deposited wood on biocomplexity of river corridors. *Frontiers in Ecology and the Environment*, 3(7), pp.377-382. [https://doi.org/10.1890/1540-9295\(2005\)003\[0377:EODWOB\]2.0.CO;2](https://doi.org/10.1890/1540-9295(2005)003[0377:EODWOB]2.0.CO;2)
- Gurnell, A.M., Petts, G.E., Hannah, D.M., Smith, B.P., Edwards, P.J., Kollmann, J., Ward, J.V. and Tockner, K., 2000. Wood storage within the active zone of a large European gravel-bed river. *Geomorphology*, 34(1-2), pp.55-72. [https://doi.org/10.1016/S0169-555X\(99\)00131-2](https://doi.org/10.1016/S0169-555X(99)00131-2)
- Gurnell, A.M., Petts, G.E., Hannah, D.M., Smith, B.P., Edwards, P.J., Kollmann, J., Ward, J.V. and Tockner, K., 2001. Riparian vegetation and island formation along the gravel-bed Fiume Tagliamento, Italy. *Earth Surface Processes and Landforms: The Journal of the British Geomorphological Research Group*, 26(1), pp.31-62. [https://doi.org/10.1002/1096-9837\(200101\)26:1%3C31::AID-ESP155%3E3.0.CO;2-Y](https://doi.org/10.1002/1096-9837(200101)26:1%3C31::AID-ESP155%3E3.0.CO;2-Y)
- Han, M., Brierley, G., Li, B., Li, Z. and Li, X., 2020. Impacts of flow regulation on geomorphic adjustment and riparian vegetation succession along an anabranching reach of the Upper Yellow River. *Catena*, 190, p.104561. <https://doi.org/10.1016/j.catena.2020.104561>
- Han-Qiu XU., 2005. A study on information extraction of water body with the modified normalized difference water index (MNDWI). *Journal of remote sensing*, 5, 589-595.
- Hardy, R.J., 2013. Process-based sediment transport modeling. In J. F. Shroder and A. Baas (Eds.), *Quantitative modeling of geomorphology* (pp. 147-159). Academic Press. <https://doi.org/10.1016/B978-0-12-374739-6.00036-1>
- Harvey, J. and Gooseff, M., 2015. River corridor science: Hydrologic exchange and ecological consequences from bedforms to basins. *Water Resources Research*, 51(9), pp.6893-6922. <https://doi.org/10.1002/2015WR017617>
- Hassan, M.A., Church, M. and Ashworth, P.J., 1992. Virtual rate and mean distance of travel of individual clasts in gravel-bed channels. *Earth Surface Processes and Landforms*, 17(6), pp.617-627. <https://doi.org/10.1002/esp.3290170607>
- Henriques, M., McVicar, T.R., Holland, K.L. and Daly, E., 2022. Riparian vegetation and geomorphological interactions in anabranching rivers: A global review. *Ecohydrology*, 15(2), p.e2370. <https://doi.org/10.1002/eco.2370>
- Henshaw, A.J., Gurnell, A.M., Bertoldi, W. and Drake, N.A., 2013. An assessment of the degree to which Landsat TM data can support the assessment of fluvial dynamics, as revealed by changes in vegetation extent and channel position, along a large river. *Geomorphology*, 202, pp.74-85. <https://doi.org/10.1016/j.geomorph.2013.01.011>
- Hicks, D.M., Baynes, E.R.C., Measures, R., Stecca, G., Tunnicliffe, J. and Friedrich, H., 2021. Morphodynamic research challenges for braided river environments: Lessons from the iconic case of New Zealand. *Earth Surface Processes and Landforms*, 46(1), pp.188-204. <https://doi.org/10.1002/esp.5014>

- Hoey, T.B., and Sutherland, A.J., 1991. Channel morphology and bedload pulses in braided rivers: a laboratory study. *Earth Surface Processes and Landforms*, 16(5), 447–462. <https://doi.org/10.1002/esp.3290160506>
- Huai, W.X., Zeng, Y.H., Xu, Z.G., and Yang, Z.H. (2009). Three-layer model for vertical velocity distribution in open channel flow with submerged rigid vegetation. *Advances in Water Resources*, 32(4), 487–492. <https://doi.org/10.1016/j.advwatres.2008.11.014>
- Jagers, B., 2003. Modelling planform changes of braided rivers. Universiteit Twente.
- Javernick, L., Brasington, J., and Caruso, B., 2014. Modeling the topography of shallow braided rivers using Structure-from-Motion photogrammetry. *Geomorphology*, 213, 166–182. <https://doi.org/10.1016/j.geomorph.2014.01.006>
- Javernick, L., Hicks, D.M., Measures, R., Caruso, B., and Brasington, J., 2016. Numerical modelling of braided rivers with structure-from-motion-derived terrain models. *River Research and Applications*, 32(5), 1071–1081. <https://doi.org/10.1002/rra.2918>
- Ji, L., Zhang, L. and Wylie, B., 2009. Analysis of dynamic thresholds for the normalized difference water index. *Photogrammetric Engineering and Remote Sensing*, 75(11), pp.1307–1317. <https://doi.org/10.14358/PERS.75.11.1307>
- Johnson, S.L., and Jones, J.A., 2000. Stream temperature responses to forest harvest and debris flows in western Cascades, Oregon. *Canadian Journal of Fisheries and Aquatic Sciences*, 57(S2), 30–39. <https://doi.org/10.1139/f00-109>
- Jordanova, A.A., and James, C.S., 2003. Experimental study of bed load transport through emergent vegetation. *Journal of Hydraulic Engineering*, 129(6), 474–478. [https://doi.org/10.1061/\(ASCE\)0733-9429\(2003\)129:6\(474\)](https://doi.org/10.1061/(ASCE)0733-9429(2003)129:6(474))
- Kale, V.S., 2008. A half-a-century record of annual energy expenditure and geomorphic effectiveness of the monsoon-fed Narmada River, central India. *Catena*, 75(2), pp.154–163. <https://doi.org/10.1016/j.catena.2008.05.004>
- Karmaker, T. and Dutta, S., 2010. Generation of synthetic seasonal hydrographs for a large river basin. *Journal of hydrology*, 381(3–4), pp.287–296. <https://doi.org/10.1016/j.jhydrol.2009.12.001>
- Karmaker, T. and Dutta, S., 2011. Erodibility of fine soil from the composite river bank of Brahmaputra in India. *Hydrological Processes*, 25(1), pp.104–111. <https://doi.org/10.1002/hyp.7826>
- Karmaker, T., and Dutta, S., 2013. Modeling seepage erosion and bank retreat in a composite river bank. *Journal of hydrology*, 476, 178–187. <https://doi.org/10.1016/j.jhydrol.2012.10.032>
- Karmaker, T., and Dutta, S., 2015. Stochastic erosion of composite banks in alluvial river bends. *Hydrological Processes*, 29(6), 1324–1339. <https://doi.org/10.1002/hyp.10266>
- Karmaker, T., and Dutta, S., 2016. Prediction of short-term morphological change in large braided river using 2D numerical model. *Journal of Hydraulic Engineering*, 142(10), 04016039. [https://doi.org/10.1061/\(ASCE\)HY.1943-7900.0001167](https://doi.org/10.1061/(ASCE)HY.1943-7900.0001167)
- Karmaker, T., Medhi, H., and Dutta, S., 2017. Study of channel instability in the braided Brahmaputra river using satellite imagery. *Current Science*, 1533–1543. <http://www.jstor.org/stable/24912701>
- Karrenberg, S., Edwards, P.J., and Kollmann, J., 2002. The life history of Salicaceae living in the active zone of floodplains. *Freshwater Biology*, 47(4), 733–748. <https://doi.org/10.1046/j.1365-2427.2002.00894.x>
- Kasvi, E., Vaaja, M., Alho, P., Hyppä, H., Hyppä, J., Kaartinen, H. and Kukko, A., 2013. Morphological changes on meander point bars associated with flow structure at different discharges. *Earth Surface Processes and Landforms*, 38(6), pp.577–590. <https://doi.org/10.1002/esp.3303>
- Kath, J., Reardon-Smith, K., Le Brocq, A.F., Dyer, F.J., Dafny, E., Fritz, L. and Batterham, M., 2014. Groundwater decline and tree change in floodplain landscapes: Identifying non-

- linear threshold responses in canopy condition. *Global Ecology and Conservation*, 2, pp.148–160. <https://doi.org/10.1016/j.gecco.2014.09.002>
- Kaushal, R.K., Sarkar, A., Mishra, K., Sinha, R., Nepal, S. and Jain, V., 2020. Spatio-temporal variability in stream power distribution in the Upper Kosi River basin, Central Himalaya: Controls and geomorphic implications. *Geomorphology*, 350, p.106888. <https://doi.org/10.1016/j.geomorph.2019.106888>
- Khan, I., Ahammad, M. and Sarker, S., 2014. A study on River Bank erosion of Jamuna River using GIS and remote sensing technology.
- Khan, M. A., Sharma, N., and Singhal, G. D., 2017. Experimental study on bursting events around a bar in physical model of a braided channel. *ISH Journal of Hydraulic Engineering*, 23(1), 63–70. <https://doi.org/10.1080/09715010.2016.1239554>
- Khan, M. A., Sharma, N., Pu, J.H., Pandey, M., and Azamathulla, H., 2022. Experimental observation of turbulent structure at region surrounding the mid-channel braid bar. *Marine Georesources and Geotechnology*, 40(4), 448–461. <https://doi.org/10.1080/1064119X.2021.1906366>
- Khan, M.A., Sharma, N., Pu, J., Alfaisal, F.M., Alam, S., and Khan, W.A., 2021. Analysis of Turbulent Flow Structure with Its Fluvial Processes Around Mid-Channel Bar. *Sustainability*, 14(1), 392. <https://doi.org/10.3390/su14010392>
- Khan, N.I. and Islam, A., 2003. Quantification of erosion patterns in the Brahmaputra–Jamuna River using geographical information system and remote sensing techniques. *Hydrological Processes*, 17(5), pp.959–966. <https://doi.org/10.1002/hyp.1173>
- Kim, J.Y., Rastogi, G., Do, Y., Kim, D.K., Muduli, P.R., Samal, R.N., Pattnaik, A.K. and Joo, G.J., 2015. Trends in a satellite-derived vegetation index and environmental variables in a restored brackish lagoon. *Global Ecology and Conservation*, 4, pp.614–624. <https://doi.org/10.1016/j.gecco.2015.10.010>
- King, A.T., Tinoco, R.O., and Cowen, E.A., 2012. A  $k-\epsilon$  turbulence model based on the scales of vertical shear and stem wakes valid for emergent and submerged vegetated flows. *Journal of Fluid Mechanics*, 701, 1–39. <https://doi.org/10.1017/jfm.2012.113>
- Kirilova, A., Likhacheva, E. and Kokin, O., 2022. Assessment of the eco-geomorphological conditions of Udmurtia, European Russia. *Environmental Earth Sciences*, 81(7), pp.1–14. <https://doi.org/10.1007/s12665-022-10323-x>
- Klaassen, G.J., Mosselman, E. and Bruehl, H., 1993. On the Prediction of Planform Changes in Braided Sand-and-Ed Rivers. *Delft Hydraulics*.
- Kondolf, G.M., Podolak, K., and Grantham, T.E., 2013. Restoring mediterranean-climate rivers. *Hydrobiologia*, 719(1), 527–545. <https://doi.org/10.1007/s10750-012-1363-y>
- Kothiyari, U.C., Hashimoto, H., and Hayashi, K., 2009. Effect of tall vegetation on sediment transport by channel flows. *Journal of Hydraulic Research*, 47(6), 700–710. <https://doi.org/10.3826/jhr.2009.3317>
- Kui, L., Stella, J.C., Shafroth, P.B., House, P.K., and Wilcox, A.C., 2017. The long-term legacy of geomorphic and riparian vegetation feedbacks on the dammed Bill Williams River, Arizona, USA. *Ecohydrology*, 10(4), e1839. <https://doi.org/10.1002/eco.1839>
- Lallias-Tacon, S., Liébault, F., and Piégay, H., 2014. Step by step error assessment in braided river sediment budget using airborne LiDAR data. *Geomorphology*, 214, 307–323. <https://doi.org/10.1016/j.geomorph.2014.02.014>
- Lane, S.N., Westaway, R.M. and Murray Hicks, D., 2003. Estimation of erosion and deposition volumes in a large, gravel-bed, braided river using synoptic remote sensing. *Earth surface processes and landforms: the journal of the British Geomorphological Research Group*, 28(3), pp.249–271. <https://doi.org/10.1002/esp.483>
- Larsen, E.W., Premier, A.K., and Greco, S.E., 2006. CUMULATIVE EFFECTIVE STREAM POWER AND BANK EROSION ON THE SACRAMENTO RIVER, CALIFORNIA, USA 1.

- JAWRA Journal of the American Water Resources Association, 42(4), 1077–1097.  
<https://doi.org/10.1111/j.1752-1688.2006.tb04515.x>
- Latrubesse, E.M., 2015. Large rivers, megafans and other Quaternary avulsive fluvial systems: A potential “who's who” in the geological record. *Earth-Science Reviews*, 146, 1–30.  
<https://doi.org/10.1016/j.earscirev.2015.03.004>
- Lawler, D.M., 1995. The impact of scale on the processes of channel-side sediment supply: a conceptual model. *IAHS Publications-Series of Proceedings and Reports-Intern Assoc Hydrological Sciences*, 226, 175–186.
- Lawler, D.M., Grove, J.R., Couperthwaite, J.S. and Leeks, G.J.L., 1999. Downstream change in river bank erosion rates in the Swale-Ouse system, northern England. *Hydrological processes*, 13(7), pp.977–992.  
[https://doi.org/10.1002/\(SICI\)1099-1085\(199905\)13:7%3C977::AID-HYP785%3E3.0.CO;2-5](https://doi.org/10.1002/(SICI)1099-1085(199905)13:7%3C977::AID-HYP785%3E3.0.CO;2-5)
- Leopold, L.B., and Wolman, M. G., 1957. *River channel patterns: braided, meandering, and straight*. US Government Printing Office.
- Leopold, L.B. and Langbein, W.B., 1962. *The concept of entropy in landscape evolution (Vol. 500)*. US Government Printing Office.
- Lera, S., Nardin, W., Sanford, L., Palinkas, C., and Guercio, R., 2019. The impact of submersed aquatic vegetation on the development of river mouth bars. *Earth Surface Processes and Landforms*, 44(7), 1494–1506. <https://doi.org/10.1002/esp.4585>
- Li, Y., Wang, Y., Anim, D.O., Tang, C., Du, W., Ni, L., Yu, Z. and Acharya, K., 2014. Flow characteristics in different densities of submerged flexible vegetation from an open-channel flume study of artificial plants. *Geomorphology*, 204, pp.314–324.  
<https://doi.org/10.1016/j.geomorph.2013.08.015>
- Li, Z., Lu, H., Gao, P., You, Y. and Hu, X., 2020. Characterizing braided rivers in two nested watersheds in the Source Region of the Yangtze River on the Qinghai-Tibet Plateau. *Geomorphology*, 351, p.106945. <https://doi.org/10.1016/j.geomorph.2019.106945>
- Lira, J., 2006. Segmentation and morphology of open water bodies from multispectral images. *International Journal of Remote Sensing*, 27(18), pp.4015–4038.  
<https://doi.org/10.1080/01431160600702384>
- Liu, D., Diplas, P., Fairbanks, J.D., and Hodges, C.C., 2008. An experimental study of flow through rigid vegetation. *Journal of Geophysical Research: Earth Surface*, 113(F4).  
<https://doi.org/10.1029/2008JF001042>
- López, F., and García, M., 1998. Open-channel flow through simulated vegetation: Suspended sediment transport modeling. *Water resources research*, 34(9), 2341–2352.  
<https://doi.org/10.1029/98WR01922>
- Lu, H., Li, Z., Hu, X., Chen, B. and You, Y., 2022. Morphodynamic processes in a large gravel-bed braided channel in response to runoff change: a case study in the Source Region of Yangtze River. *Arabian Journal of Geosciences*, 15(5), pp.1–16.  
<https://doi.org/10.1007/s12517-022-09641-y>
- Lytle, D.A. and Merritt, D.M., 2004. Hydrologic regimes and riparian forests: a structured population model for cottonwood. *Ecology*, 85(9), pp.2493–2503.  
<https://doi.org/10.1890/04-0282>
- Magilligan, F. J., Buraas, E. M., and Renshaw, C. E., 2015. The efficacy of stream power and flow duration on geomorphic responses to catastrophic flooding. *Geomorphology*, 228, 175–188. <https://doi.org/10.1016/j.geomorph.2014.08.016>
- Maji, S., Pal, D., Hanmaiahgari, P.R., and Gupta, U.P., 2017. Hydrodynamics and turbulence in emergent and sparsely vegetated open channel flow. *Environmental Fluid Mechanics*, 17(4), 853–877. <https://doi.org/10.1007/s10652-017-9531-2>
- Majumdar, S. and Mandal, S., 2020. Assessment of relationship of braiding intensities with stream power and bank erosion rate through Plan Form Index (PFI) method: a study on selected reaches of the upstream of Ganga river near Malda district, West Bengal, India. *Sustainable*

- Water Resources Management, 6(6), pp.1–18. <https://doi.org/10.1007/s40899-020-00462-z>
- Malavasi, M., Bazzichetto, M., Komárek, J., Moudrý, V., Rocchini, D., Bagella, S., Acosta, A.T. and Carranza, M.L., 2021. Unmanned aerial systems-based monitoring of the eco-geomorphology of coastal dunes through spectral Rao's Q. *Applied Vegetation Science*, 24(1), p.e12567. <https://doi.org/10.1111/avsc.12567>
- Maruyama, T., Kawachi, T. and Singh, V.P., 2005. Entropy-based assessment and clustering of potential water resources availability. *Journal of hydrology*, 309(1–4), pp.104–113. <https://doi.org/10.1016/j.jhydrol.2004.11.020>
- McFeeters, S.K., 1996. The use of the Normalized Difference Water Index (NDWI) in the delineation of open water features. *International journal of remote sensing*, 17(7), pp.1425–1432. <https://doi.org/10.1080/01431169608948714>
- McLelland, S.J., Ashworth, P., and Best, J.L., 1996. The origin and downstream development of coherent flow structures at channel junctions. In *Coherent flow structures in open channels* (pp. 459–490). John Wiley and Sons.
- McShane, R.R., Auerbach, D.A., Friedman, J.M., Auble, G.T., Shafroth, P.B., Merigliano, M.F., Scott, M.L. and Poff, N.L., 2015. Distribution of invasive and native riparian woody plants across the western USA in relation to climate, river flow, floodplain geometry and patterns of introduction. *Ecography*, 38(12), pp.1254–1265. <https://doi.org/10.1111/ecog.01285>
- Meier, C.I., Reid, B.L., and Sandoval, O., 2013. Effects of the invasive plant *Lupinus polyphyllus* on vertical accretion of fine sediment and nutrient availability in bars of the gravel-bed Paloma River. *Limnologia*, 43(5), 381–387. <https://doi.org/10.1016/j.limno.2013.05.004>
- Millar, R.G., 2005. Theoretical regime equations for mobile gravel-bed rivers with stable banks. *Geomorphology*, 64(3–4), pp.207–220. <https://doi.org/10.1016/j.geomorph.2004.07.001>
- Mishra, A.K., Özger, M. and Singh, V.P., 2009. An entropy-based investigation into the variability of precipitation. *Journal of Hydrology*, 370(1–4), pp.139–154. <https://doi.org/10.1016/j.jhydrol.2009.03.006>
- Modalavalasa, S., Chembolu, V., Dutta, S., and Kulkarni, V., 2022. Combined effect of bridge piers and floodplain vegetation on main channel hydraulics. *Experimental Thermal and Fluid Science*, 136, 110669. <https://doi.org/10.1016/j.expthermflusci.2022.110669>
- Moody, J.A., 2019. Dynamic relations for the deposition of sediment on floodplains and point bars of a freely-meandering river. *Geomorphology*, 327, pp.585–597. <https://doi.org/10.1016/j.geomorph.2018.11.032>
- Mosley, M. P., 1976. An experimental study of channel confluences. *The journal of geology*, 84(5), 535–562. <https://doi.org/10.1086/628230>
- Mosselman, E., 2006. Bank protection and river training along the braided Brahmaputra–Jamuna River, Bangladesh. *Braided rivers: Process, deposits, ecology and management*, 36, 279–287.
- Mosselman, E., Huisink, M., Koomen, E. and Seijmonsbergen, A.C., 1995. Morphological changes in a large braided sand-bed river. In *River geomorphology* (No. 2, pp. 235–247). <http://pascal-francis.inist.fr/vibad/index.php?action=getRecordDetail&did=6312378>
- Mount, N.J., Tate, N.J., Sarker, M.H., and Thorne, C.R., 2013. Evolutionary, multi-scale analysis of river bank line retreat using continuous wavelet transforms: Jamuna River, Bangladesh. *Geomorphology*, 183, 82–95. <https://doi.org/10.1016/j.geomorph.2012.07.017>
- Murhy, E., Ghisalberti, M., and Nepf, H.M., 2006. Longitudinal dispersion in vegetated channels. In *Longitudinal dispersion in vegetated channels* (pp. 613–621). Taylor and Francis. <https://doi.org/10.1201/9781439833865.ch63>
- Murray, A.B. and Paola, C., 1994. A cellular model of braided rivers. *Nature*, 371(6492), pp.54–57. <https://doi.org/10.1038/371054a0>
- Murray, A.B. and Paola, C., 1997. Properties of a cellular braided-stream model. *Earth Surface Processes and Landforms: The Journal of the British Geomorphological Group*, 22(11),

- pp.1001–1025. [https://doi.org/10.1002/\(SICI\)1096-9837\(199711\)22:11%3C1001::AID-ESP798%3E3.0.CO;2-O](https://doi.org/10.1002/(SICI)1096-9837(199711)22:11%3C1001::AID-ESP798%3E3.0.CO;2-O)
- Naiman, R.J. and Decamps, H., 1997. The ecology of interfaces: riparian zones. *Annual review of Ecology and Systematics*, pp.621–658. <https://www.jstor.org/stable/2952507>
- Nandi, K.K., Pradhan, C., Padhee, S.K., Dutta, S., and Khatua, K.K., 2022b. Understanding the Entropy-based Morphological Variability and Energy Expenditure Mechanism of a large Braided River System. *Journal of Hydrology*, 128662. <https://doi.org/10.1016/j.jhydrol.2022.128662>
- Nandi, K.K., Akkimi, A., Pradhan, C., Dutta, S. and Khatua, K., 2021, December. Entropy Based Relation Between In-stream Green Corridor and Channel Stability of a Large Braided Brahmaputra River. In *AGU Fall Meeting Abstracts* (Vol. 2021, pp. EP25C-1329).
- Nandi, K.K., Pradhan, C., Dutta, S. and Khatua, K.K., 2022. How dynamic is the Brahmaputra? Understanding the process–form–vegetation interactions for hierarchies of energy dissipation. *Ecohydrology*, 15(3), p. e2416. <https://doi.org/10.1002/eco.2416>
- Nanson, G.C. and Knighton, A.D., 1996. Anabranching rivers: their cause, character and classification. *Earth surface processes and landforms*, 21(3), pp.217–239. [https://doi.org/10.1002/\(SICI\)1096-9837\(199603\)21:3%3C217::AID-ESP611%3E3.0.CO;2-U](https://doi.org/10.1002/(SICI)1096-9837(199603)21:3%3C217::AID-ESP611%3E3.0.CO;2-U)
- Nayak, P. and Panda, B., 2016. Brahmaputra and the socio-economic life of people of Assam. *The Mahabahu Brahmaputra*, Published by Flood and River Management Agency of Assam, Guwahati, Assam, pp.77–85. <https://dx.doi.org/10.2139/ssrn.2790210>
- Nepf, H.M., 1999. Drag, turbulence, and diffusion in flow through emergent vegetation. *Water resources research*, 35(2), 479–489. <https://doi.org/10.1029/1998WR900069>
- Nepf, H., and Ghisalberti, M., 2008. Flow and transport in channels with submerged vegetation. *Acta Geophysica*, 56(3), 753–777. <https://doi.org/10.2478/s11600-008-0017-y>
- Nepf, H., 2012. Flow and transport in regions with aquatic vegetation. *Annual Rev. Fluid Mech.* 44, 123–142. <https://doi.org/10.1146/annurev-fluid-120710-101048>
- Nepf, H., White, B., Lightbody, A. and Ghisalberti, M., 2007. Transport in aquatic canopies. In *Flow and transport processes with complex obstructions* (pp. 221–250). Springer, Dordrecht. [https://doi.org/10.1007/978-1-4020-5385-6\\_6](https://doi.org/10.1007/978-1-4020-5385-6_6)
- Nicholas, A.P., 2013. Modelling the continuum of river channel patterns. *Earth Surface Processes and Landforms*, 38(10), 1187–1196. <https://doi.org/10.1002/esp.3431>
- Nield, J.M., 2006. Equilibrium morphological modelling in coastal and river environments: the development and application of self-organisation-and entropy-based techniques (Doctoral dissertation)., The University of Adelaide. <https://hdl.handle.net/2440/37843>
- Nykanen, D.K., Fofoula-Georgiou, E. and Sapozhnikov, V.B., 1998. Study of spatial scaling in braided river patterns using synthetic aperture radar imagery. *Water resources research*, 34(7), pp.1795–1807. <https://doi.org/10.1029/98WR00940>
- Ollero, A., 2010. Channel changes and floodplain management in the meandering middle Ebro River, Spain. *Geomorphology*, 117(3–4), pp.247–260. <https://doi.org/10.1016/j.geomorph.2009.01.015>
- Orton, G.J., and Reading, H.G., 1993. Variability of deltaic processes in terms of sediment supply, with particular emphasis on grain size. *Sedimentology*, 40(3), 475–512. <https://doi.org/10.1111/j.1365-3091.1993.tb01347.x>
- Osterkamp, W.R., Hupp, C.R. and Stoffel, M., 2012. The interactions between vegetation and erosion: new directions for research at the interface of ecology and geomorphology. *Earth Surface Processes and Landforms*, 37(1), pp.23–36. <https://doi.org/10.1002/esp.2173>
- Ouma, Y.O. and Tateishi, R., 2006. A water index for rapid mapping of shoreline changes of five East African Rift Valley lakes: an empirical analysis using Landsat TM and ETM+ data. *International Journal of Remote Sensing*, 27(15), pp.3153–3181. <https://doi.org/10.1080/01431160500309934>

- Pangare, G., Nishat, B., Liao, X. and Qaddumi, H.M., 2021. The Restless River. <https://openknowledge.worldbank.org/handle/10986/36258> License: CC BY 3.0 IGO.
- Paola, Chris., 2001. Modelling Stream Braiding Over a Range of Scales. New Zealand Hydrological Society. Retrieved from the University of Minnesota Digital Conservancy, <https://hdl.handle.net/11299/164368>
- Pekel, J. F., Cottam, A., Gorelick, N., and Belward, A.S., 2016. High-resolution mapping of global surface water and its long-term changes. *Nature*, 540(7633), 418–422. <https://doi.org/10.1038/nature20584>
- Perucca, E., Camporeale, C., and Ridolfi, L., 2009. Estimation of the dispersion coefficient in rivers with riparian vegetation. *Advances in Water Resources*, 32(1), 78–87. <https://doi.org/10.1016/j.advwatres.2008.10.007>
- Pettit, N.E. and Naiman, R.J., 2006. Flood-deposited wood creates regeneration niches for riparian vegetation on a semi-arid South African river. *Journal of Vegetation Science*, 17(5), pp.615–624. <https://doi.org/10.1111/j.1654-1103.2006.tb02485.x>
- Phillips, J.D. and Van Dyke, C., 2016. Principles of geomorphic disturbance and recovery in response to storms. *Earth Surface Processes and Landforms*, 41(7), pp.971–979. <https://doi.org/10.1002/esp.3912>
- Phillips, J.D., 1995. Biogeomorphology and landscape evolution: the problem of scale. *Geomorphology*, 13(1–4), pp.337–347. [https://doi.org/10.1016/0169-555X\(95\)00023-X](https://doi.org/10.1016/0169-555X(95)00023-X)
- Phillips, J.D., 2009. Changes, perturbations, and responses in geomorphic systems. *Progress in Physical Geography*, 33(1), pp.17–30. <https://doi.org/10.1177/0309133309103889>
- Phongsapan, K., Chishtie, F., Poortinga, A., Bhandari, B., Meechaiya, C., Kunlamai, T., Aung, K.S., Saah, D., Anderson, E., Markert, K. and Markert, A., 2019. Operational flood risk index mapping for disaster risk reduction using Earth Observations and cloud computing technologies: a case study on Myanmar. *Frontiers in Environmental Science*, 7, p.191. <https://doi.org/10.3389/fenvs.2019.00191>
- Piegay, H., Alber, A., Slater, L., and Bourdin, L., 2009. Census and typology of braided rivers in the French Alps. *Aquatic Sciences*, 71(3), 371–388. <https://doi.org/10.1007/s00027-009-9220-4>
- Piégay, H., Darby, S.E., Mosselman, E. and Surian, N., 2005. A review of techniques available for delimiting the erodible river corridor: a sustainable approach to managing bank erosion. *River research and applications*, 21(7), pp.773–789. <https://doi.org/10.1002/rra.881>
- Piégay, H., Grant, G., Nakamura, F., and Trustrum, N., 2006. Braided river management: from assessment of river behaviour to improved sustainable development. *Braided rivers: process, deposits, ecology and management*, 36, 257–275.
- Pitchford, J.O.N.A.T.H.A.N., Strager, M.I.C.H.A.E.L., Riley, A.D.A.M., Lin, L. and Anderson, J., 2015. Modelling streambank erosion potential using maximum entropy in a central Appalachian watershed. *Proceedings of the International Association of Hydrological Sciences*, 367, pp.122–127. <https://doi.org/10.5194/piahs-367-122-2015>
- Pizarro, A., Samela, C., Fiorentino, M., Link, O. and Manfreda, S., 2017. BRISSENT: an entropy-based model for bridge-pier scour estimation under complex hydraulic scenarios. *Water*, 9(11), p.889. <https://doi.org/10.3390/w9110889>
- Pollen, N., Simon, A. and Collison, A., 2004. Advances in assessing the mechanical and hydrologic effects of riparian vegetation on streambank stability. *Riparian vegetation and fluvial geomorphology*, 8, pp.125–139.
- Polvi, L.E., Wohl, E., and Merritt, D.M., 2014. Modeling the functional influence of vegetation type on streambank cohesion. *Earth Surface Processes and Landforms*, 39(9), 1245–1258. <https://doi.org/10.1002/esp.3577>
- Pradhan, C., Bharti, R. and Dutta, S., 2017, July. Assessment of post-impoundment geomorphic variations along Brahmani River using remote sensing. In 2017 IEEE International Geoscience

- and Remote Sensing Symposium (IGARSS) (pp. 5598–5601). IEEE.  
<https://doi.org/10.1109/IGARSS.2017.8128274>
- Pradhan, C., Chembolu, V., and Dutta, S., 2019. Impact of river interventions on alluvial channel morphology. *ISH Journal of Hydraulic Engineering*, 25(1), 87–93.  
<https://doi.org/10.1080/09715010.2018.1453878>
- Pradhan, C., Chembolu, V., Bharti, R. and Dutta, S., 2021a. Regulated rivers in India: research progress and future directions. *ISH Journal of Hydraulic Engineering*, pp.1–13.  
<https://doi.org/10.1080/09715010.2021.1975319>
- Pradhan, C., Chembolu, V., Dutta, S., and Bharti, R., 2021. Role of effective discharge on morphological changes for a regulated macrochannel river system. *Geomorphology*, 385, 107718. <https://doi.org/10.1016/j.geomorph.2021.107718>
- Pradhan, C., Dutta, S., and Bharti, R., 2021d. Understanding River Freedom Space and Seasonal Variation of Surface Water Dynamics in Large Fluvial Landscapes: Implications for Floods and Anthropogenic Stress. In AGU Fall Meeting 2021. AGU.
- Pradhan, C., Modalavalasa, S., Dutta, S., and Bharti, R., 2020. A geomorphic approach to evaluate river recovery potential for regulated river basin. In *River Flow 2020* (pp. 1805–1809). CRC Press.
- Pradhan, C., Padhee, S.K., Bharti, R., and Dutta, S., 2022. A process-based recovery indicator for anthropogenically disturbed river system. *Scientific Reports*, 12(1), 1–14.  
<https://doi.org/10.1038/s41598-022-14542-x>
- Pradhan, C., Padhee, S., Dutta, S. and Bharti, R., 2021c, April. An entropy-based investigation on the river recovery potential in a regulated river basin. In EGU General Assembly Conference Abstracts (pp. EGU21–9362).
- Pu, J.H., Tait, S., Guo, Y., Huang, Y., and Hanmaiahgari, P.R., 2018. Dominant features in three-dimensional turbulence structure: comparison of non-uniform accelerating and decelerating flows. *Environmental Fluid Mechanics*, 18(2), 395–416.  
<https://doi.org/10.1007/s10652-017-9557-5>
- Rapp, C.F. and Abbe, T.B., 2003. A framework for delineating channel migration zones (No. Ecology Publication# 30–06–027).
- Reid, I. and Frostick, L.E., 1986. Dynamics of bedload transport in Turkey Brook, a coarse-grained alluvial channel. *Earth Surface Processes and Landforms*, 11(2), pp.143–155.  
<https://doi.org/10.1002/esp.3290110205>
- Repetto, R., Tubino, M. and Paola, C., 2002. Planimetric instability of channels with variable width. *Journal of Fluid Mechanics*, 457, pp.79–109.  
<https://doi.org/10.1017/S0022112001007595>
- Rhoads, B.L., and Sukhodolov, A.N., 2004. Spatial and temporal structure of shear layer turbulence at a stream confluence. *Water Resources Research*, 40(6).  
<https://doi.org/10.1029/2003WR002811>
- Rice, S., Stoffel, M., Turowski, J.M. and Wolf, A., 2012. Disturbance regimes at the interface of geomorphology and ecology. *Earth Surface Processes and Landforms*, 37(15), pp.1678–1682. <https://doi.org/10.1002/esp.3326>
- Richardson, W.R., and Thorne, C.R., 2001. Multiple thread flow and channel bifurcation in a braided river: Brahmaputra–Jamuna River, Bangladesh. *Geomorphology*, 38(3–4), 185–196.  
[https://doi.org/10.1016/S0169-555X\(00\)00080-5](https://doi.org/10.1016/S0169-555X(00)00080-5)
- Richardson, W.R., Thorne, C.R. and Mahmood, S., 1996. Secondary flow and channel changes around a bar in the Brahmaputra River, Bangladesh. *Coherent flow structures in open channels*, pp.519–543.
- Richardson, W.R.R., 1997. Secondary flow and channel change in braided rivers (Doctoral dissertation, University of Nottingham).

- Rogers, K.G., and Goodbred, S.L., 2014. The Sundarbans and Bengal Delta: the world's largest tidal mangrove and delta system. In *Landscapes and landforms of India* (pp. 181–187). Springer, Dordrecht. [https://doi.org/10.1007/978-94-017-8029-2\\_18](https://doi.org/10.1007/978-94-017-8029-2_18)
- Rouse Jr, J.W., Haas, R.H., Deering, D.W., Schell, J.A. and Harlan, J.C., 1974. Monitoring the vernal advancement and retrogradation (green wave effect) of natural vegetation (No. E75–10354).
- Rozo, M.G., Nogueira, A.C. and Truckenbrodt, W., 2012. The anastomosing pattern and the extensively distributed scroll bars in the middle Amazon River. *Earth Surface Processes and Landforms*, 37(14), pp.1471–1488. <https://doi.org/10.1002/esp.3249>
- Sambrook Smith, G.H., Ashworth, P.J., Best, J.L., Woodward, J. and Simpson, C.J., 2005. The morphology and facies of sandy braided rivers: some considerations of scale invariance. *Fluvial sedimentology VII*, pp.145–158. <https://doi.org/10.1002/9781444304350.ch9>
- Sapozhnikov, V.B. and Foufoula-Georgiou, E., 1996. Do the current landscape evolution models show self-organized criticality? *Water Resources Research*, 32(4), pp.1109–1112. <https://doi.org/10.1029/96WR00161>
- Sapozhnikov, V.B. and Foufoula-Georgiou, E., 1997. Experimental evidence of dynamic scaling and indications of self-organized criticality in braided rivers. *Water Resources Research*, 33(8), pp.1983–1991. <https://doi.org/10.1029/97WR01233>
- Sarker, M.H., Thorne, C.R., Aktar, M.N., and Ferdous, M.R., 2014. Morpho-dynamics of the Brahmaputra–Jamuna River, Bangladesh. *Geomorphology*, 215, 45–59. <https://doi.org/10.1016/j.geomorph.2013.07.025>
- Sarker, M.H. and Thorne, C.R., 2006. Morphological response of the Brahmaputra–Padma–Lower Meghna river system to the Assam earthquake of 1950. *Braided rivers: process, deposits, ecology and management*, 21, pp.289–310. <https://doi.org/10.1002/9781444304374.ch14>
- Sarker, S., 2021. *Investigating Topologic and Geometric Properties of Synthetic and Natural River Networks under Changing Climate*. University of Central Florida. <https://stars.library.ucf.edu/etd2020/965>
- Sarker, S., 2021a. *Understanding the Complexity and Dynamics of Anastomosing River Planform: A Case Study of Brahmaputra River in Bangladesh*. <https://doi.org/10.1002/essoar.10508926.2>
- Sarker, S., Veremyev, A., Boginski, V. and Singh, A., 2019. Critical nodes in river networks. *Scientific reports*, 9(1), pp.1–11. <https://doi.org/10.1038/s41598-019-47292-4>
- Sarma, J.N., 2005. Fluvial process and morphology of the Brahmaputra River in Assam, India. *Geomorphology*, 70(3–4), 226–256. <https://doi.org/10.1016/j.geomorph.2005.02.007>
- Sarma, J.N., and Acharjee, S., 2018. A study on variation in channel width and braiding intensity of the Brahmaputra River in Assam, India. *Geosciences*, 8(9), 343. <https://doi.org/10.3390/geosciences8090343>
- Sarma, J.N. and Phukan, M.K., 2006. Bank erosion and bankline migration of the Brahmaputra River in Assam during the twentieth century. *Journal–Geological Society of India*, 68(6), pp.1023–1036.
- Sarma, J.N., 2004. An overview of the Brahmaputra river system. *The Brahmaputra basin water resources*, pp.72–87. [https://doi.org/10.1007/978-94-017-0540-0\\_5](https://doi.org/10.1007/978-94-017-0540-0_5)
- Sarma, J.N., 2005. Fluvial process and morphology of the Brahmaputra River in Assam, India. *Geomorphology*, 70(3–4), pp.226–256. <https://doi.org/10.1016/j.geomorph.2005.02.007>
- Schneider, J., Hegglin, R., Meier, S., Turowski, J.M., Nitsche, M. and Rickenmann, D., 2010. Studying sediment transport in mountain rivers by mobile and stationary RFID antennas. *River flow 2010*, pp.1723–1730.
- Schnitzler, A., Hale, B.W., and Alsum, E.M., 2007. Examining native and exotic species diversity in European riparian forests. *Biological conservation*, 138(1–2), 146–156. <https://doi.org/10.1016/j.biocon.2007.04.010>

- Schumm, S.A., 1985. Patterns of alluvial rivers. *Annual Review of Earth and Planetary Sciences*, 13, p.5.
- Shannon, C.E., 1948. A mathematical theory of communication. *The Bell system technical journal*, 27(3), pp.379–423. <https://doi.org/10.1002/j.1538-7305.1948.tb01338.x>
- Sharma, A., and Kumar, B., 2019. Boundary layer development over non-uniform sand rough bed channel. *ISH Journal of Hydraulic Engineering*, 25(2), 162–169. <https://doi.org/10.1080/09715010.2017.1391133>
- Sharma, N., 2004. Mathematical modelling and braid indicators. In the Brahmaputra basin water resources (pp. 229–260). Springer, Dordrecht. [https://doi.org/10.1007/978-94-017-0540-0\\_11](https://doi.org/10.1007/978-94-017-0540-0_11)
- Sharma, N., and Akhtar, M.P., 2017. Prospects of Modeling and Morpho-dynamic Study for Brahmaputra River. In *River System Analysis and Management* (pp. 189–209). Springer, Singapore. [https://doi.org/10.1007/978-981-10-1472-7\\_10](https://doi.org/10.1007/978-981-10-1472-7_10)
- Shiono, K., and Muto, Y., 1998. Complex flow mechanisms in compound meandering channels with overbank flow. *Journal of fluid mechanics*, 376, 221–261. <https://doi.org/10.1017/S0022112098002869>
- Shucksmith, J.D., Boxall, J.B. and Guymer, I., 2010. Effects of emergent and submerged natural vegetation on longitudinal mixing in open channel flow. *Water Resources Research*, 46(4). <https://doi.org/10.1029/2008WR007657>
- Simon, A., 1992. Energy, time, and channel evolution in catastrophically disturbed fluvial systems. *Geomorphology*, 5(3–5), 345–372. [https://doi.org/10.1016/0169-555X\(92\)90013-E](https://doi.org/10.1016/0169-555X(92)90013-E)
- Singh, V., Sharma, N., and Ojha, C.S.P. (Eds.), 2004. *The Brahmaputra basin water resources* (Vol. 47). Springer Science and Business Media.
- Siniscalchi, F., Nikora, V.I., and Aberle, J., 2012. Plant patch hydrodynamics in streams: Mean flow, turbulence, and drag forces. *Water Resources Research*, 48(1). <https://doi.org/10.1029/2011WR011050>
- Smith, N.D., 1974. Sedimentology and bar formation in the upper Kicking Horse River, a braided outwash stream. *The Journal of Geology*, 82(2), 205–223. <https://doi.org/10.1086/627959>
- Srivastava, S., Singh, T.P., Singh, H., Kushwaha, S.P.S. and Roy, P.S., 2002. Assessment of large-scale deforestation in Sonitpur district of Assam. *Current science*, pp.1479–1484. <https://www.jstor.org/stable/24106185>
- Stallins, J.A. and Corenblit, D., 2018. Interdependence of geomorphic and ecologic resilience properties in a geographic context. *Geomorphology*, 305, pp.76–93. <https://doi.org/10.1016/j.geomorph.2017.09.012>
- Stallins, J.A., 2006. Geomorphology and ecology: unifying themes for complex systems in biogeomorphology. *Geomorphology*, 77(3–4), pp.207–216. <https://doi.org/10.1016/j.geomorph.2006.01.005>
- Steiger, J., Tabacchi, E., Dufour, S., Corenblit, D. and Peiry, J.L., 2005. Hydrogeomorphic processes affecting riparian habitat within alluvial channel–floodplain river systems: a review for the temperate zone. *River Research and Applications*, 21(7), pp.719–737. <https://doi.org/10.1002/rra.879>
- Stoesser, T., Ruether, N., and Olsen, N.R.B., 2010. Calculation of primary and secondary flow and boundary shear stresses in a meandering channel. *Advances in Water Resources*, 33(2), 158–170. <https://doi.org/10.1016/j.advwatres.2009.11.001>
- Surabuddin Mondal, M., Sharma, N., Kappas, M., and Garg, P.K., 2013. Modeling of spatio-temporal dynamics of land use and land cover in a part of Brahmaputra River basin using Geoinformatic techniques. *Geocarto International*, 28(7), 632–656. <https://doi.org/10.1080/10106049.2013.776641>
- Surian, N., 1999. Channel changes due to river regulation: the case of the Piave River, Italy. *Earth Surface Processes and Landforms: The Journal of the British Geomorphological*

- Research Group, 24(12), 1135–1151. [https://doi.org/10.1002/\(SICI\)1096-9837\(199911\)24:12%3C1135::AID-ESP40%3E3.0.CO;2-F](https://doi.org/10.1002/(SICI)1096-9837(199911)24:12%3C1135::AID-ESP40%3E3.0.CO;2-F)
- Surian, N., Barban, M., Ziliani, L., Monegato, G., Bertoldi, W., and Comiti, F., 2015. Vegetation turnover in a braided river: frequency and effectiveness of floods of different magnitude. *Earth Surface Processes and Landforms*, 40(4), 542–558. <https://doi.org/10.1002/esp.3660>
- Surian, N., Mao, L., Giacomini, M., and Ziliani, L., 2009. Morphological effects of different channel-forming discharges in a gravel-bed river. *Earth Surface Processes and Landforms*, 34(8), 1093–1107. <https://doi.org/10.1002/esp.1798>
- Szupiany, R.N., Amsler, M.L., Hernandez, J., Parsons, D.R., Best, J.L., Fornari, E. and Trento, A., 2012. Flow fields, bed shear stresses, and suspended bed sediment dynamics in bifurcations of a large river. *Water resources research*, 48(11). <https://doi.org/10.1029/2011WR011677>
- Tabacchi, E., Planty-Tabacchi, A.M., Roques, L. and Nadal, E., 2005. Seed inputs in riparian zones: implications for plant invasion. *River research and applications*, 21(2-3), pp.299–313. <https://doi.org/10.1002/rra.848>
- Takagi, T., Oguchi, T., Matsumoto, J., Grossman, M.J., Sarker, M.H. and Matin, M.A., 2007. Channel braiding and stability of the Brahmaputra River, Bangladesh, since 1967: GIS and remote sensing analyses. *Geomorphology*, 85(3-4), pp.294–305. <https://doi.org/10.1016/j.geomorph.2006.03.028>
- Tal, M., and Paola, C., 2007. Dynamic single-thread channels maintained by the interaction of flow and vegetation. *Geology*, 35(4), 347–350. <https://doi.org/10.1130/G23260A.1>
- Tal, M., and Paola, C., 2010. Effects of vegetation on channel morphodynamics: results and insights from laboratory experiments. *Earth Surface Processes and Landforms*, 35(9), 1014–1028. <https://doi.org/10.1002/esp.1908>
- Talukdar, G., Sarma, A.K. and Bhattacharjya, R.K., 2020. Mapping agricultural activities and their temporal variations in the riverine ecosystem of the Brahmaputra River using geospatial techniques. *Remote Sensing Applications: Society and Environment*, 20, p.100423. <https://doi.org/10.1016/j.rsase.2020.100423>
- Talukdar, G., Sarma, A.K. and Bhattacharjya, R.K., 2021. Sediment analysis and modelling based approach for optimal allocation of riverine sandbar for socio economic benefits. *Ecological Engineering*, 173, p.106415. <https://doi.org/10.1016/j.ecoleng.2021.106415>
- Tang, C., Yi, Y., and Zhang, S., 2023. Flow and turbulence in unevenly obstructed channels with rigid and flexible vegetation. *Journal of Environmental Management*, 326, 116736. <https://doi.org/10.1016/j.jenvman.2022.116736>
- Tang, C., Yi, Y., Jia, W., and Zhang, S., 2020. Velocity and turbulence evolution in a flexible vegetation canopy in open channel flows. *Journal of Cleaner Production*, 270, 122543. <https://doi.org/10.1016/j.jclepro.2020.122543>
- Tanino, Y., and Nepf, H. M., 2008. Laboratory investigation of mean drag in a random array of rigid, emergent cylinders. *Journal of Hydraulic Engineering*, 134(1), 34–41. [https://doi.org/10.1061/\(ASCE\)0733-9429\(2008\)134:1\(34\)](https://doi.org/10.1061/(ASCE)0733-9429(2008)134:1(34))
- Tejedor, A., Longjas, A., Edmonds, D.A., Zaliapin, I., Georgiou, T.T., Rinaldo, A. and Foufoula-Georgiou, E., 2017. Entropy and optimality in river deltas. *Proceedings of the National Academy of Sciences*, 114(44), pp.11651–11656. <https://doi.org/10.1073/pnas.1708404114>
- Thomas, M.F., 2001. Landscape sensitivity in time and space—an introduction. *Catena*, 42(2-4), pp.83–98. [https://doi.org/10.1016/S0341-8162\(00\)00133-8](https://doi.org/10.1016/S0341-8162(00)00133-8)
- Thoms, M.C., Meitzen, K.M., Julian, J.P. and Butler, D.R., 2018. Bio-geomorphology and resilience thinking: Common ground and challenges. *Geomorphology*, 305, pp.1–7. <https://doi.org/10.1016/j.geomorph.2018.01.021>

- Thorne, C.R., Russell, A.P. and Alam, M.K., 1993. Planform pattern and channel evolution of the Brahmaputra River, Bangladesh. Geological Society, London, Special Publications, 75(1), pp.257–276. <https://doi.org/10.1144/GSL.SP.1993.075.01.16>
- Tobón-Marín, A. and Canon Barriga, J., 2020. Analysis of changes in rivers planforms using google earth engine. International Journal of Remote Sensing, 41(22), pp.8654–8681. <https://doi.org/10.1080/01431161.2020.1792575>
- Tooth, S. and Nanson, G.C., 2000. The role of vegetation in the formation of anabranching channels in an ephemeral river, Northern plains, arid central Australia. Hydrological processes, 14(16-17), pp.3099–3117. [https://doi.org/10.1002/1099-1085\(200011/12\)14:16/17%3C3099::AID-HYP136%3E3.0.CO;2-4](https://doi.org/10.1002/1099-1085(200011/12)14:16/17%3C3099::AID-HYP136%3E3.0.CO;2-4)
- Tooth, S., Jansen, J.D., Nanson, G.C., Coulthard, T.J. and Pietsch, T., 2008. Riparian vegetation and the late Holocene development of an anabranching river: Magela Creek, northern Australia. Geological Society of America Bulletin, 120(7–8), pp.1021–1035. <https://doi.org/10.1130/B26165.1>
- Tubino, M. and Bertoldi, W., 2007. 6 Bifurcations in gravel-bed streams. Developments in Earth Surface Processes, 11, pp.133–159. [https://doi.org/10.1016/S0928-2025\(07\)11123-8](https://doi.org/10.1016/S0928-2025(07)11123-8)
- Valdiya, K.S., 1999. Why does river Brahmaputra remain untamed? Current Science, 76(10), pp.1301–1305. <https://www.jstor.org/stable/24102168>
- van Andel, J., Bakker, J.P. and Grootjans, A.P., 1993. Mechanisms of vegetation succession: a review of concepts and perspectives. Acta botanica neerlandica, 42(4), pp.413–433.
- Van den Berg, J.H., 1995. Prediction of alluvial channel pattern of perennial rivers. Geomorphology, 12(4), pp.259–279. [https://doi.org/10.1016/0169-555X\(95\)00014-V](https://doi.org/10.1016/0169-555X(95)00014-V)
- Vargas-Luna, A., Crosato, A., Anders, N., Hoitink, A.J., Keesstra, S.D., and Uijttewaal, W.S., 2018. Morphodynamic effects of riparian vegetation growth after stream restoration. Earth Surface Processes and Landforms, 43(8), 1591–1607. <https://doi.org/10.1002/esp.4338>
- Vargas-Luna, A., Duró, G., Crosato, A., and Uijttewaal, W., 2019. Morphological adaptation of river channels to vegetation establishment: A laboratory study. Journal of Geophysical Research: Earth Surface, 124(7), 1981–1995. <https://doi.org/10.1029/2018JF004878>
- Velasco, D., Bateman, A., and Medina, V., 2008. A new integrated, hydro-mechanical model applied to flexible vegetation in riverbeds. Journal of Hydraulic Research, 46(5), 579–597. <https://doi.org/10.3826/jhr.2008.2986>
- Vorosmarty, C.J., Fekete, B.M. and Tucker, B.A., 1998. Global River Discharge, 1807–1991, V [ersion]. 1.1 (RivDIS). ORNL DAAC. <http://dx.doi.org/10.3334/ORNLDAAC/199>
- Walsh, J. and Hicks, D.M., 2002. Braided channels: Self-similar or self-affine? Water Resources Research, 38(6), pp.18–1. <https://doi.org/10.1029/2001WR000749>
- Warburton, J., 1996. Active braidplain width, bed load transport and channel morphology in a model braided river. Journal of Hydrology (New Zealand), 259–285. <http://www.jstor.org/stable/43944775>
- Westaway, R.M., Lane, S.N. and Hicks, D.M., 2000. The development of an automated correction procedure for digital photogrammetry for the study of wide, shallow, gravel-bed rivers. Earth Surface Processes and Landforms: The Journal of the British Geomorphological Research Group, 25(2), pp.209–226. [https://doi.org/10.1002/\(SICI\)1096-9837\(200002\)25:2%3C209::AID-ESP84%3E3.0.CO;2-Z](https://doi.org/10.1002/(SICI)1096-9837(200002)25:2%3C209::AID-ESP84%3E3.0.CO;2-Z)
- Westaway, R.M., Lane, S.N. and Hicks, D.M., 2001. Remote sensing of clear-water, shallow, gravel-bed rivers using digital photogrammetry. Photogrammetric Engineering and Remote Sensing, 67(11), pp.1271–1282.
- Westaway, R.M., Lane, S.N. and Hicks, D.M., 2003. Remote survey of large-scale braided, gravel-bed rivers using digital photogrammetry and image analysis. International Journal of Remote Sensing, 24(4), pp.795–815. <https://doi.org/10.1080/01431160110113070>

- Wetzel, P.R., 2002. Analysis of tree island vegetation communities. In *Tree islands of the Everglades* (pp. 357–389). Springer, Dordrecht. [https://doi.org/10.1007/978-94-009-0001-1\\_12](https://doi.org/10.1007/978-94-009-0001-1_12)
- Wheaton, J.M., Brasington, J., Darby, S.E., Kasprak, A., Sear, D. and Vericat, D., 2013. Morphodynamic signatures of braiding mechanisms as expressed through change in sediment storage in a gravel-bed river. *Journal of Geophysical Research: Earth Surface*, 118(2), pp.759–779. <https://doi.org/10.1002/jgrf.20060>
- White, P.S., 1985. Natural disturbance and patch dynamics: an introduction. *Natural disturbance and patch dynamics*, pp.3–13.
- Williams, R.D., Brasington, J., Vericat, D., and Hicks, D.M., 2014. Hyperscale terrain modelling of braided rivers: fusing mobile terrestrial laser scanning and optical bathymetric mapping. *Earth Surface Processes and Landforms*, 39(2), 167–183. <https://doi.org/10.1002/esp.3437>
- Williams, R.D., Bangen, S., Gillies, E., Kramer, N., Moir, H. and Wheaton, J., 2020. Let the river erode! Enabling lateral migration increases geomorphic unit diversity. *Science of the Total Environment*, 715, p.136817. <https://doi.org/10.1016/j.scitotenv.2020.136817>
- Wilson, C.A.M.E., Stoesser, T., Bates, P.D. and Pinzen, A.B., 2003. Open channel flow through different forms of submerged flexible vegetation. *Journal of Hydraulic Engineering*, 129(11), pp.847–853. [https://doi.org/10.1061/\(ASCE\)0733-9429\(2003\)129:11\(847\)](https://doi.org/10.1061/(ASCE)0733-9429(2003)129:11(847))
- Wintenberger, C.L., Rodrigues, S., Bréhéret, J.G. and Villar, M., 2015. Fluvial islands: First stage of development from nonmigrating (forced) bars and woody-vegetation interactions. *Geomorphology*, 246, pp.305–320. <https://doi.org/10.1016/j.geomorph.2015.06.026>
- Wright, N.G., and Hargreaves, D.M., 2013. *Environmental applications of computational fluid dynamics. Environmental modelling: finding simplicity in complexity*. Chichester: Wiley-Blackwell, 91–109.
- Wu, F.C. and Yeh, T.H., 2005. Forced bars induced by variations of channel width: Implications for incipient bifurcation. *Journal of Geophysical Research: Earth Surface*, 110(F2). <https://doi.org/10.1029/2004JF000160>
- Xu, H., 2006. Modification of normalised difference water index (NDWI) to enhance open water features in remotely sensed imagery. *International journal of remote sensing*, 27(14), pp.3025–3033. <https://doi.org/10.1080/01431160600589179>
- Xu, H., 2007. Extraction of urban built-up land features from Landsat imagery using a thematic oriented index combination technique. *Photogrammetric Engineering and Remote Sensing*, 73(12), 1381–1391. <https://doi.org/10.14358/PERS.73.12.1381>
- Xu, G. and Zhao, L., 2013. Analysis of fluvial process based on information entropy. *Journal of Tianjin University Science and Technology*, 43, pp.347–353.
- Xu, G.B. and Yang, C.T., 2012. Analysis of river bed changes based on the theories of minimum entropy production dissipative structure and chaos. *Shuili Xuebao (Journal of Hydraulic Engineering)*, 43(8), pp.948–956.
- Xu, H.Q., 2005. Extraction of water information by improved normalized difference water index (MNDWI). *Chin. J. Remote Sens*, 5, pp.589–595.
- Xu, Z.X., Ye, C., Zhang, Y.Y., Wang, X.K. and Yan, X.F., 2020. 2D numerical analysis of the influence of near-bank vegetation patches on the bed morphological adjustment. *Environmental Fluid Mechanics*, 20, pp.707–738. <https://doi.org/10.1007/s10652-019-09718-5>
- Yagci, O., Tschiesche, U., and Kabdasli, M. S., 2010. The role of different forms of natural riparian vegetation on turbulence and kinetic energy characteristics. *Advances in water Resources*, 33(5), 601–614. <https://doi.org/10.1016/j.advwatres.2010.03.008>
- Yang, C.T., 1971a. Formation of riffles and pools. *Water Resources Research*, 7(6), pp.1567–1574. <https://doi.org/10.1029/WR007i006p01567>

- Yang, C.T., 1971b. On river meanders. *Journal of hydrology*, 13, pp.231–253. [https://doi.org/10.1016/0022-1694\(71\)90226-5](https://doi.org/10.1016/0022-1694(71)90226-5)
- Yang, C.T., 1971c. Potential energy and stream morphology. *Water Resources Research*, 7(2), pp.311–322. <https://doi.org/10.1029/WR007i002p00311>
- Yang, C.T., 1972. Unit stream power and sediment transport. *Journal of the Hydraulics Division*, 98(10), pp.1805–1826. <https://doi.org/10.1061/JYCEAJ.0003439>
- Yi, Y.J., Zhou, Y., Song, J., Zhang, S., Cai, Y., Yang, W. and Yang, Z., 2019. The effects of cascade dam construction and operation on riparian vegetation. *Advances in Water Resources*, 131, p.103206. <https://doi.org/10.1016/j.advwatres.2018.09.015>
- You, Y., Li, Z., Gao, P. and Hu, T., 2022. Impacts of dams and land-use changes on hydromorphology of braided channels in the Lhasa River of the Qinghai–Tibet Plateau, China. *International Journal of Sediment Research*, 37(2), pp.214–228. <https://doi.org/10.1016/j.ijsrc.2021.07.003>
- Young, W.J. and Davies, T.R.H., 1991. Bedload transport processes in a braided gravel-bed river model. *Earth Surface Processes and Landforms*, 16(6), pp.499–511. <https://doi.org/10.1002/esp.3290160603>
- Zanoni, L., Gurnell, A., Drake, N. and Surian, N., 2008. Island dynamics in a braided river from analysis of historical maps and air photographs. *River Research and Applications*, 24(8), pp.1141–1159. <https://doi.org/10.1002/rra.1086>
- Zhang, Y., Tang, C., and Nepf, H., 2018. Turbulent kinetic energy in submerged model canopies under oscillatory flow. *Water Resources Research*, 54(3), 1734–1750. <https://doi.org/10.1002/2017WR021732>
- Zhao, H., Yan, J., Yuan, S., Liu, J., and Zheng, J., 2019. Effects of submerged vegetation density on turbulent flow characteristics in an open channel. *Water*, 11(10), 2154. <https://doi.org/10.3390/w11102154>
- Zhu, M., Zhu, G., Nurminen, L., Wu, T., Deng, J., Zhang, Y., Qin, B. and Ventelä, A.M., 2015. The influence of macrophytes on sediment resuspension and the effect of associated nutrients in a shallow and large lake (Lake Taihu, China). *PLoS One*, 10(6), p.e 0127915. <https://doi.org/10.1371/journal.pone.0127915>
- Zolezzi, G., Bertoldi, W., Tubino, M., Smith, G.H.S., Best, J.L., Bristow, C.S. and Petts, G.E., 2006. Morphological analysis and prediction of river bifurcations. *Braided rivers: process, deposits, ecology and management*, 36, pp.233–256.

# PUBLICATIONS

## JOURNALS

1. Nandi, K. K., Pradhan, C., Dutta, S., & Khatua, K. K. (2022). How dynamic is the Brahmaputra? Understanding the process–form–vegetation interactions for hierarchies of energy dissipation. *Ecohydrology*, 15(3), e2416. <https://doi.org/10.1002/eco.2416>
2. Nandi, K. K., Pradhan, C., Padhee, S. K., Dutta, S., & Khatua, K. K. (2022). Understanding the entropy-based morphological variability and energy expenditure mechanism of a large braided river system. *Journal of Hydrology*, 615, 128662. <https://doi.org/10.1016/j.jhydrol.2022.128662>
3. Nandi, K. K., Pradhan, C., Dutta, S., & Khatua, K. K. Identifying the stability trajectory of a large braided Brahmaputra River using reach-scale process-based approach. *Journal of Hydrology* (Under Review).
4. Nandi, K. K., Kakati, R., Dutta, S., & Khatua, K. K. Exploring the Influence of Vegetated Mid-Channel Bars on Flow and Turbulence in Bifurcated Channels: An Experimental Approach. *Advances in Water Resources* (Under Review).

## CONFERENCES

1. Nandi, K. K., Pradhan, C., Sultan, J., Dutta, S., & Khatua, K. K. (2020). Energy Dissipation Modeling in Highly Braided Brahmaputra River. *Hydro International Conference*.
2. Nandi, K. K., Pradhan, C., Dutta, S., & Khatua, K. K. (2021). Sediment Transport and Morphological Characterization for a Large Braided River Using Hydrodynamic Modeling. *World's Large Rivers, Moscow, Russia*.

## **PUBLICATIONS**

3. Nandi, K. K., Akkimi, A., Pradhan, C., Dutta, S., & Khatua, K. K. (2021, December). Entropy Based Relation Between In-stream Green Corridor and Channel Stability of a Large Braided Brahmaputra River. In **AGU Fall Meeting Abstracts**.
4. Nandi, K. K., Pradhan, C., Dutta, S., & Khatua, K. K. (2022, December). Assessment of braided dynamics of a large river system with respect to the energy dissipation mechanism using cloud computing technique. In **AGU Fall Meeting Abstracts**.
5. Nandi, K. K., Pradhan, C., Dutta, S., & Khatua, K. K. (2022). Morphological Characterization of Large Braided Brahmaputra River using High-resolution Satellite Imageries. **STREAM**.

